First Principles Model Hamiltonian Ensembles for Light Harvesting: Modeling Dissipative Down Conversion - Signatures of Vibronic Energy Transfer in Nonlinear 2DES Signals - CSDM+PLDM

David F. Coker

Departments of Chemistry & Physics & Center for Computational Science

Boston University

Charge and Energy Transfer Processes: Open Problems in Open Quantum Systems
Banff International Research Center Workshop, Banff, Alberta, Canada
August 18-23, 2019

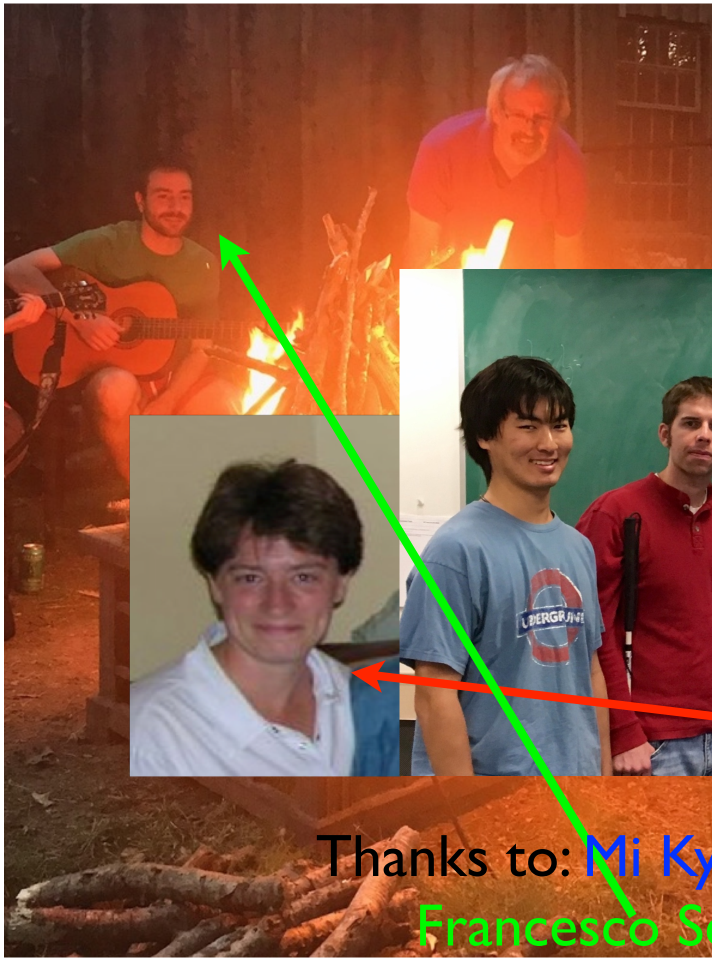

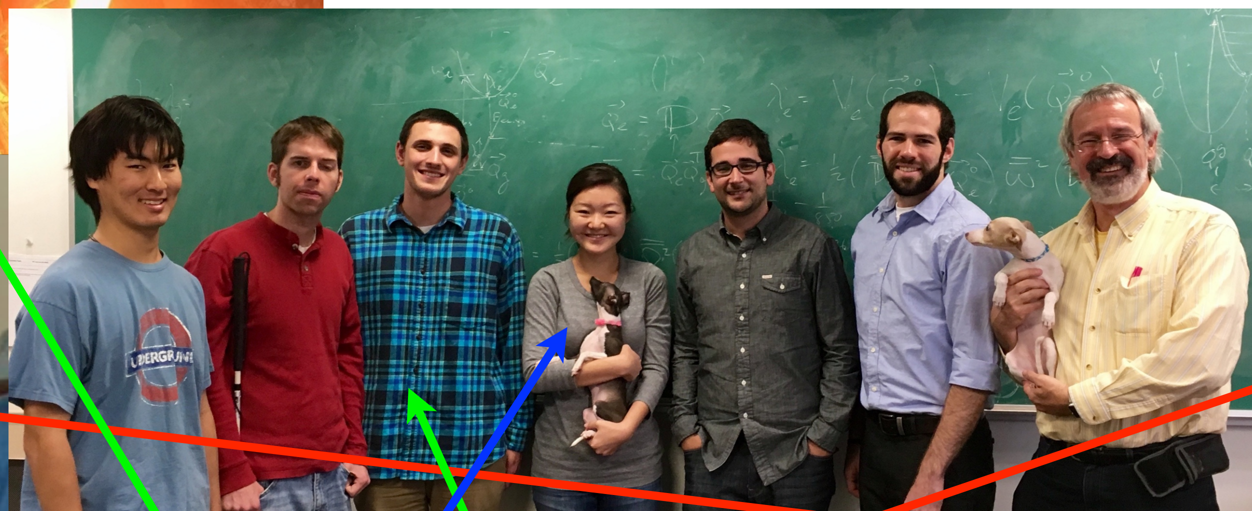

Ksenia Bravaya

Thanks to: Mi Kyung Lee, Pengfei (Frank) Huo, Sara Bonella
Francesco Segatta, Justin Provazza, Marco Garavelli

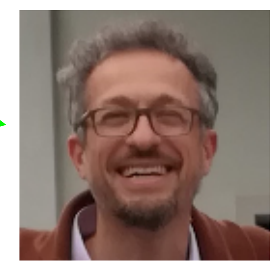

BOSTON UNIVERSITY

NSF

FONDAZIONE BRUNO KESSLER

ALMA MATER STUDIORUM UNIVERSITÀ DI BOLOGNA A.D. 1088

Time scale separation?

(1) Excitation Energy Transfer (EET) dynamics is usually explored using averaged model Hamiltonians.
(2) However, the EET dynamics can occur faster than the time scale on which these model Hamiltonians change.
So rather than looking at
The dynamics of an average Hamiltonian (fit to average experimental results)
we should be studying
The average dynamics of an ENSEMBLE of model Hamiltonians, e.g. averaging dynamics over site disorder, etc. Fluctuations, perhaps with correlations, around INHERENT STRUCTURES - F. Stillinger J. Chem. Phys. 83, 6413 (1985).

$$\{\epsilon_\alpha\} \ \{\Delta_{\alpha,\beta}\} \ \{J_\alpha(\omega)\}$$

Parameterized Frenkel Exciton Hamiltonian: local Interpolation Model

$$\hat{H} = \sum_{\alpha=1}^{N_{state}} \epsilon_\alpha |\alpha\rangle\langle\alpha| + \sum_{\alpha\neq\beta}^{N_{state}} \Delta_{\alpha,\beta}[|\alpha\rangle\langle\beta| + |\beta\rangle\langle\alpha|]$$

$$+ \sum_{\alpha=1}^{N_{state}} \sum_{i=1}^{n^{(\alpha)}} c_i^{(\alpha)} R_i^{(\alpha)} |\alpha\rangle\langle\alpha|$$

$$+ \sum_{\alpha=1}^{N_{state}} \sum_{i=1}^{n^{(\alpha)}} \frac{1}{2}[P_i^{(\alpha)2} + \omega_i^{(\alpha)2} R_i^{(\alpha)2}]$$

7 state FMO test

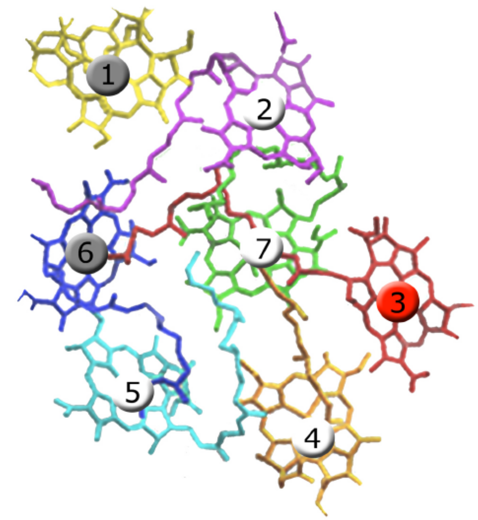

In principle Site dependent "spectral densities"

$$J^{(\alpha)}(\omega) = \frac{\pi}{2}\sum_i \frac{c_i^{(\alpha)2}}{\omega_i}\delta(\omega-\omega_i) = \quad 2\lambda\omega\tau_c/(1+\omega^2\tau_c^2) \quad \tau_c = 50 \text{ fs and } \lambda = 35 \text{ cm}^{-1}$$

Experimental fit assumes all have identical environments!

Fucoxanthin - Chlorophyll Proteins (FCP) from light harvesting antennae of diatoms
Kruger et al. PNAS 114, E11063 (2017)

Protein fluctuations drive switching of exciton delocalization

Carotenoid - Chlorophyll complexes

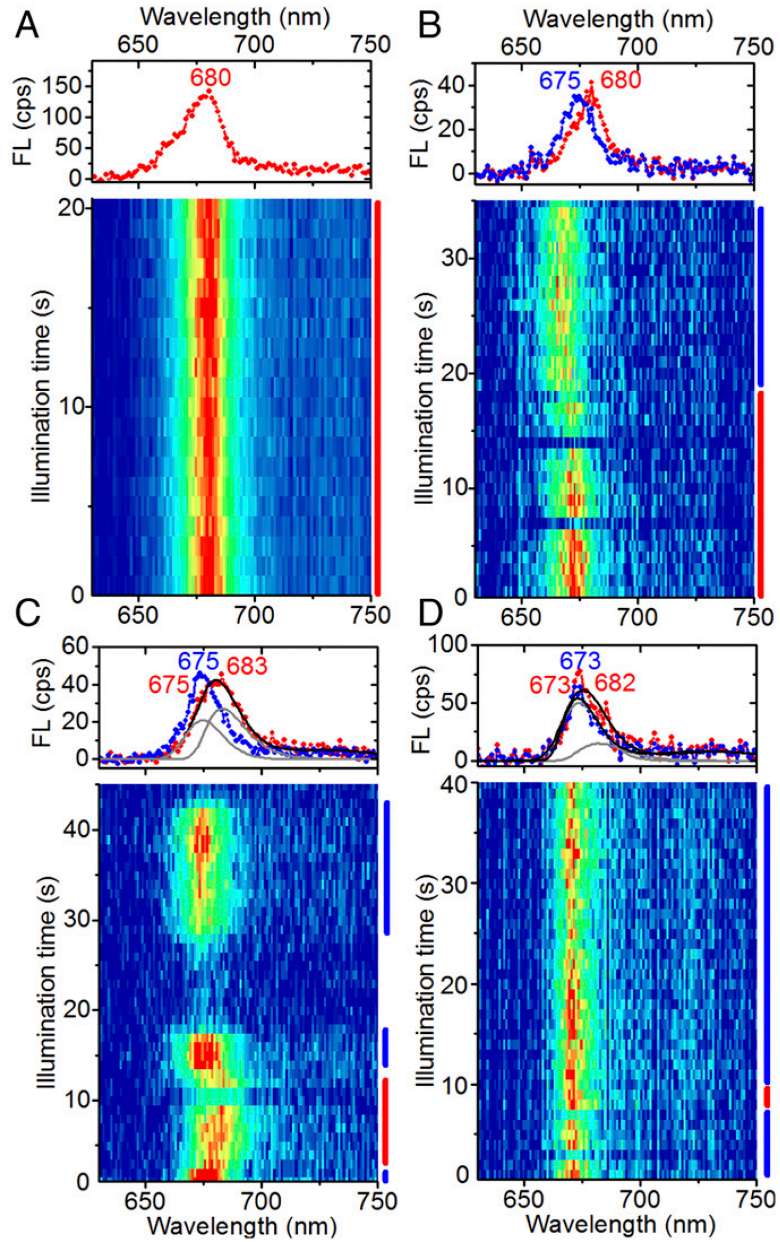

Enhanced Sampling: Replica Exchange, Parallel Tempering - Sugita (RIKEN)
Alex Hino

Down Conversion Pigment-Protein Complexes

Down-conversion molecules that enable absorbed blue light to "plug into" red functioning chlorophyll energy transport and transduction networks by using vibronic transitions and engineered environmental dissipation e.g. in Peridinin-Chlorophyll-a Protein (PCP), or phycobiliproteins like PC645

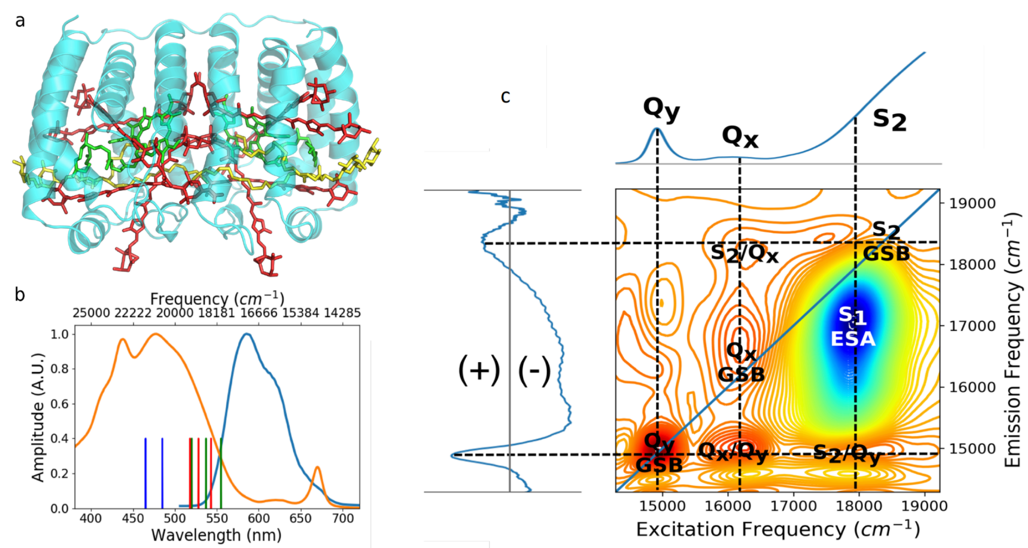

“step down transformer”

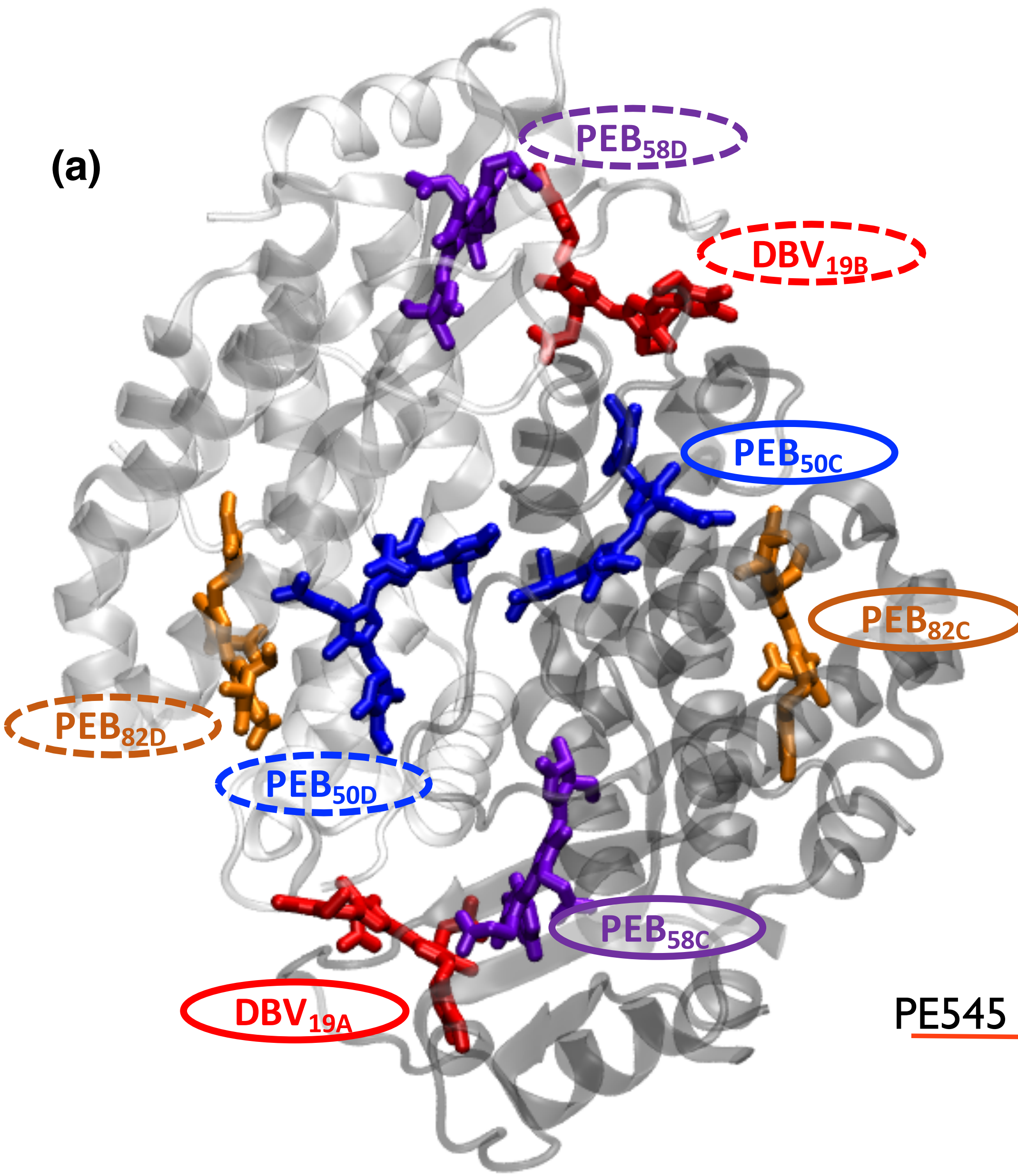

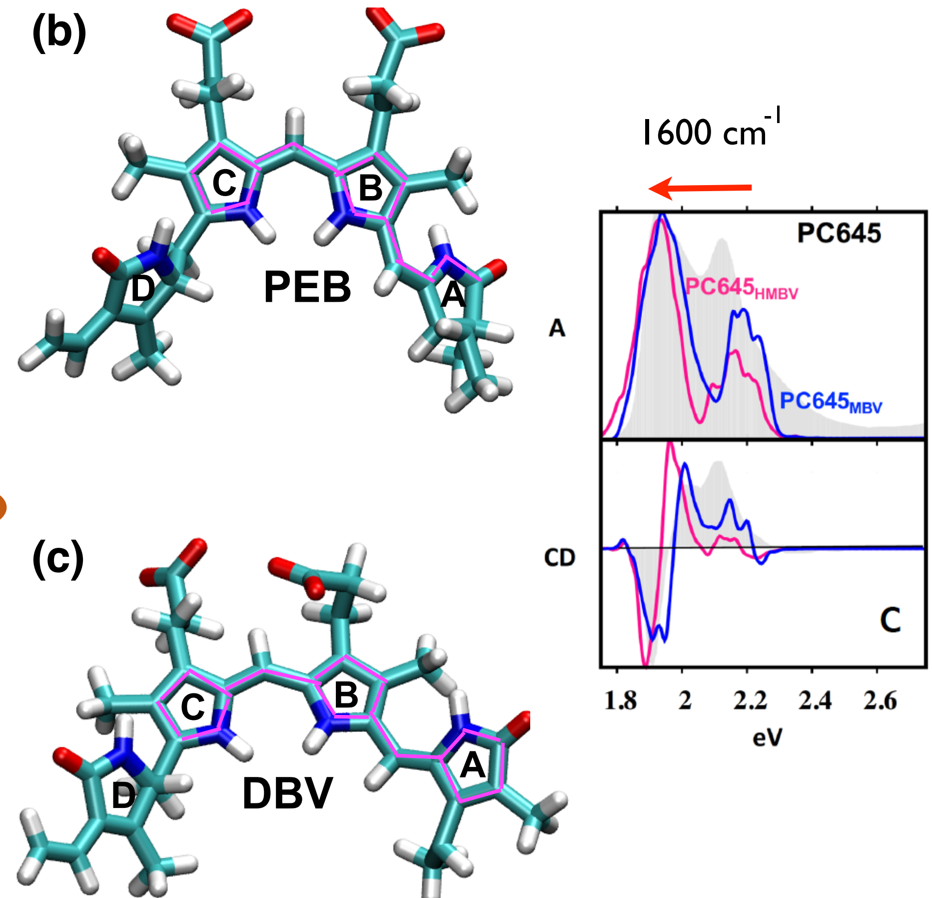

PE545 from cryptophyte algae linear tetrapyrols or “bilins” & phycobili proteins (PC645,PC577,PE555,PC612,...)

A. Chenu & G. Scholes
Annu. Rev. Phys. Chem. 66, 69-96 (2015)

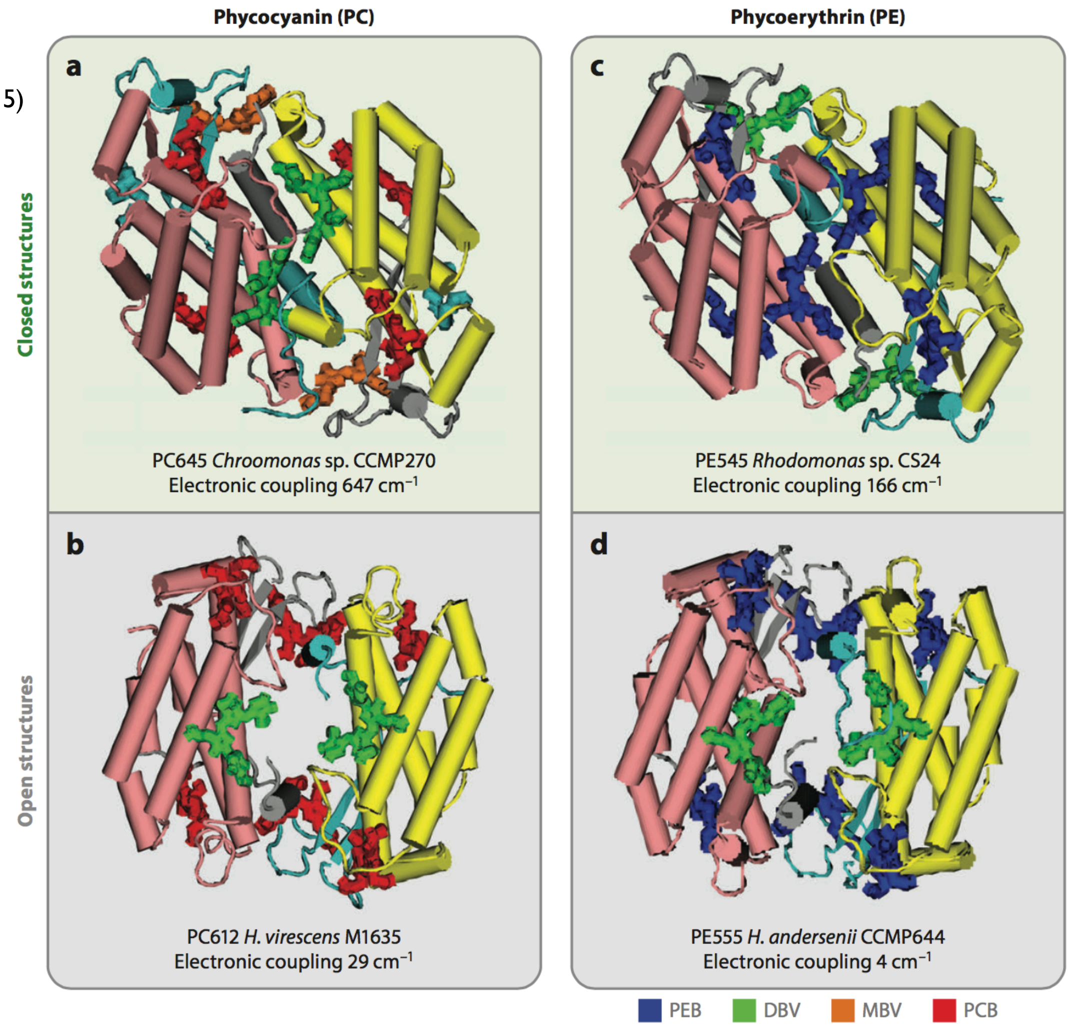

Figure 2

Structures of four representative phycobiliproteins from cryptophyte algae (40, 41): two phycocyanin light-harvesting complexes, (*a*) PC645 and (*b*) PC612, and two phycoerythrin light-harvesting complexes, (*c*) PE545 and (*d*) PE555. PC645 and PE545 (*top row*) are examples of closed structures, characterized by a large electronic coupling between the chromophores in the indicated central dimer of bilins. PC612 and PE555 (*bottom row*) are examples of open structures, in which the electronic coupling is weak. The large β-subunits are colored pink and yellow, and the small α-subunits are colored cyan and gray. Abbreviations: DBV, 15,16-dihydrobiliverdin; MBV, mesobiliverdin; PCB, phycocyanobilin; PEB, phycoerythrobilin.

Scholes, Thordarson and co-workers

Controllable Chimeras with function

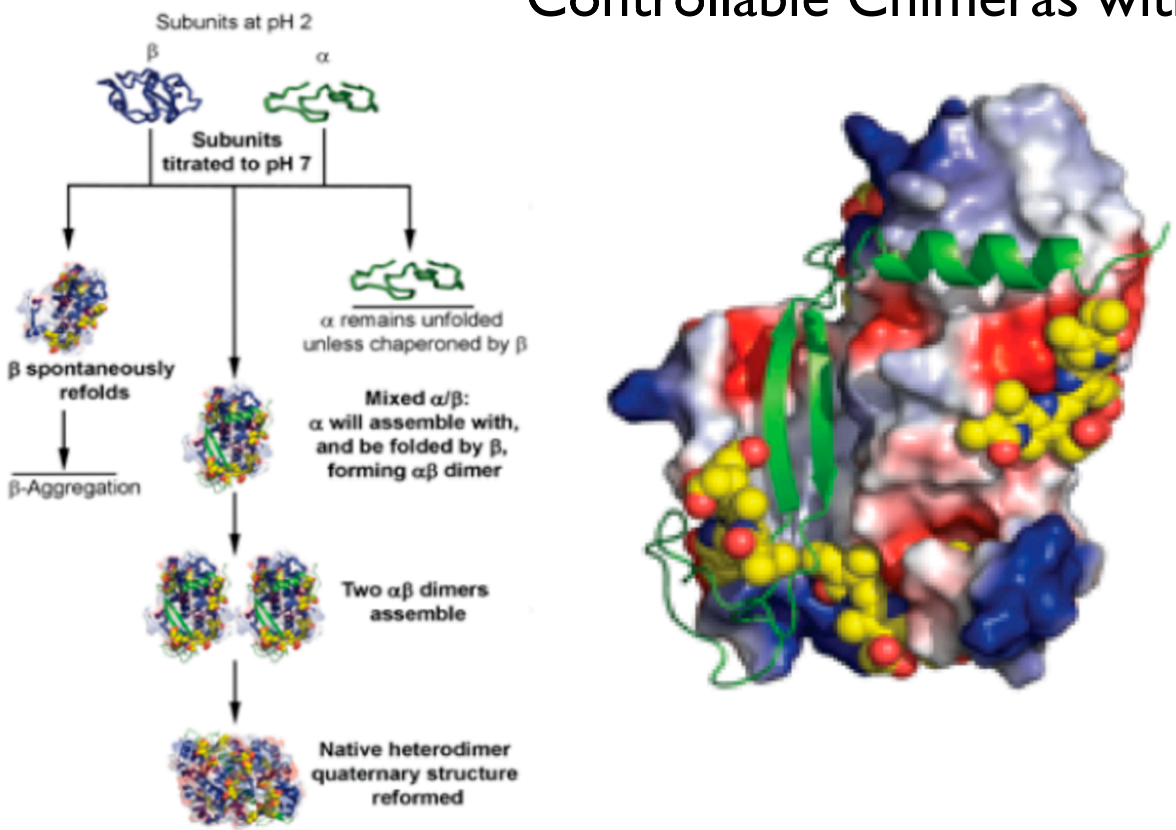

Figure 4: Schematic illustrating how we separate the light harvesting complex α and β subunits, and how we can reassemble them into a functional protein. The right figure shows a single β subunit and, in green, how the α subunit associates with it after assembly of the tetrameric light harvesting complex.

Moix, Cao, Huo, DFC JPCL (2011)

FMO bacterial LH complex

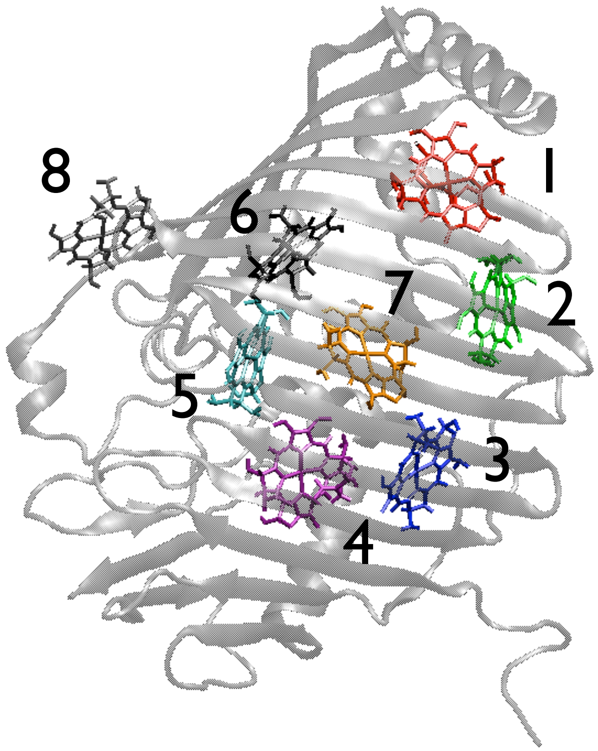

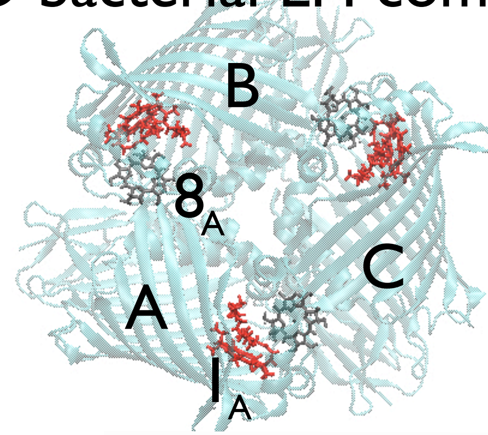

8000cm^{-1} ~ 1eV

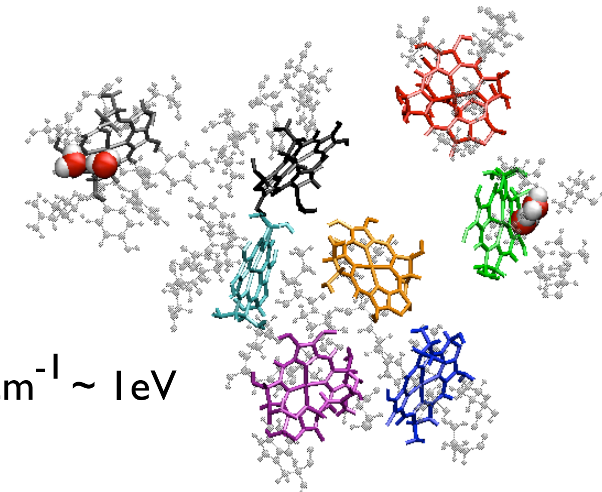

Site Dependent Spectral Density Models

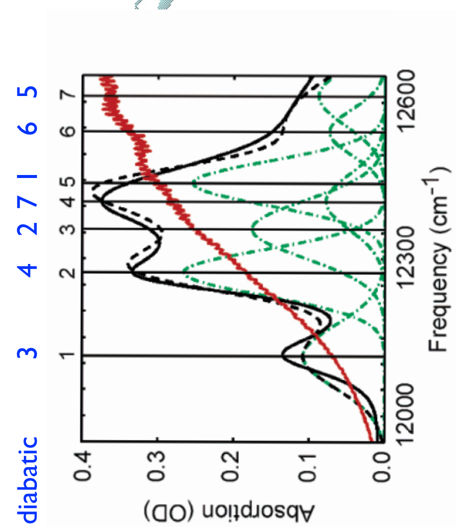

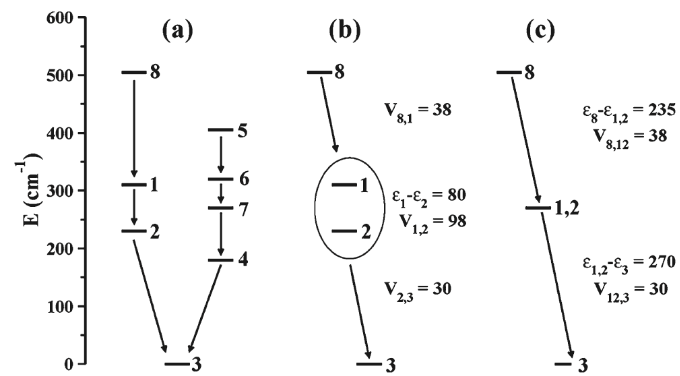

Figure 1. Energy diagrams for the eight-site model (a), the reduced four-site model (b), and the reduced three-site model (c) used in the calculations of Figure 3.

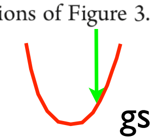

FLN

OUTLINE:

(1) Spectral Density Calculations
(2) Excitation Energy Calculations
(3) Dissipative Quantum Dynamics for General Regimes
(4) Issues with Linearized Dynamics of Higher Frequency Modes
(5) Spectra (PC645/HPC645) - Influence of Protonation and "Flickering" Pathways
(6) Quantum Dynamics and Nonlinear Spectroscopy
(7) Coherent State Density Matrix Dynamics (+PLDM)

Exciton-Phonon Coupling

$$\hat{H} = \hat{H}_{\mathrm{s}} + \hat{H}_{\mathrm{sb}}$$

$$\hat{H}_{\mathrm{sb}} = \sum_{\alpha=1}^{N} \sum_{i_\alpha=1}^{n_\alpha} \left[\frac{1}{2} \left(P_{i_\alpha}^2 + \omega_{i_\alpha}^2 Q_{i_\alpha}^2 \right) - c_{i_\alpha} Q_{i_\alpha} |\alpha\rangle\langle\alpha| \right]$$

$$\hat{H}_{\mathrm{s}} = \sum_{\alpha=1}^{N} \varepsilon_\alpha |\alpha\rangle\langle\alpha| + \sum_{\alpha\neq\gamma}^{N} \Delta_{\alpha,\gamma} |\alpha\rangle\langle\gamma|$$

$$J_\alpha(\omega) \equiv \frac{\pi}{2} \sum_{i_\alpha} \frac{c_{i_\alpha}^2}{\omega_{i_\alpha}} \delta(\omega - \omega_{i_\alpha})$$

$$\delta\varepsilon_\alpha = \sum_{i_\alpha} c_{i_\alpha} Q_{i_\alpha}$$

Standard Approach: Ground state (MM) MD averaged excitation energy fluctuation correlation function. Inconsistent MM and electronic structure!

$$C_\alpha(t) = \langle \delta\varepsilon_\alpha(0) \delta\varepsilon_\alpha(t) \rangle = \sum_{i_\alpha} c_{i_\alpha}^2 \langle Q_{i_\alpha}(0) Q_{i_\alpha}(t) \rangle$$

$$J_\alpha(\omega) = \beta\omega \int_0^\infty dt C_\alpha^{\mathrm{cl}}(t) \cos\omega t$$

Simple harmonic model of the standard approach

Kleinekathoefer & Schulten 2002

$$\delta \varepsilon_\alpha = \sum_{i_\alpha} c_{i_\alpha} Q_{i_\alpha}$$

$$V_\alpha^{g}(\mathbf{Q}_\alpha) = \frac{1}{2}\sum_{i_\alpha} \omega_{i_\alpha}^2 (Q_{i_\alpha} - Q_{i_\alpha}^{g})^2$$

$$\delta \varepsilon_\alpha(Q_{i_\alpha}) = V_\alpha^{e}(Q_{i_\alpha}) - V_\alpha^{g}(Q_{i_\alpha}) = \text{constant} - \sum_{i_\alpha} \omega_{i_\alpha}^2 (Q_{i_\alpha}^{e} - Q_{i_\alpha}^{g}) Q_{i_\alpha}$$

$$V_\alpha^{e}(\mathbf{Q}_\alpha) = \frac{1}{2}\sum_{i_\alpha} \omega_{i_\alpha}^2 (Q_{i_\alpha} - Q_{i_\alpha}^{e})^2 + E_\alpha$$

$$\lambda_{i_\alpha} = \frac{1}{2}\omega_{i_\alpha}^2 (Q_{i_\alpha}^{e} - Q_{i_\alpha}^{g})^2 = S_{i_\alpha} \hbar \omega_{i_\alpha}$$

Huang-Rhys (HR) Factors

$$V_\alpha^{\mathrm{MM}}(\mathbf{q}_\alpha) = \frac{1}{2}\sum_{i_\alpha} \Omega_{i_\alpha}^2 (q_{i_\alpha} - q_{i_\alpha}^{\mathrm{MM}})^2 + E_\alpha^{\mathrm{MM}}$$

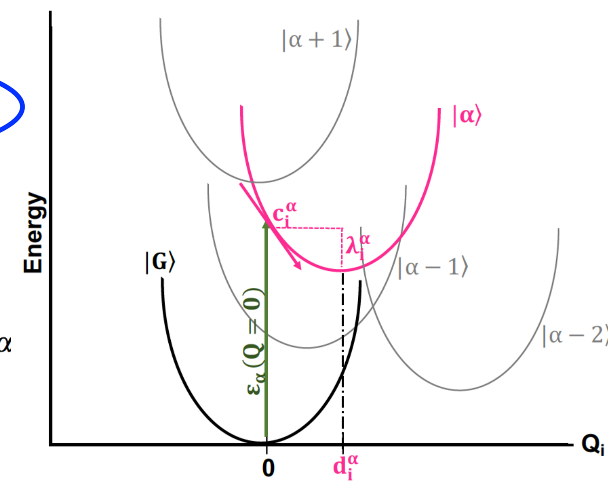

$$c_{i_\alpha} = \omega_{i_\alpha}^2 (Q_{i_\alpha}^{e} - Q_{i_\alpha}^{g}) = \sqrt{2\lambda_{i_\alpha}}\,\omega_{i_\alpha} = \sqrt{2\hbar\omega_{i_\alpha} S_{i_\alpha}}\,\omega_{i_\alpha}$$

$$\lambda_{i_\alpha} = c_{i_\alpha}^2 / 2\omega_{i_\alpha}^2$$

$$J_\alpha(\omega) = \pi \sum_{i_\alpha} \omega_{i_\alpha} \lambda_{i_\alpha} \delta(\omega - \omega_{i_\alpha})$$

What about the MD time correlation function with the MM potential??

ω_{i_α}

$$V_\alpha^{\mathrm{MM}}(\mathbf{q}_\alpha) = \frac{1}{2}\sum_{i_\alpha} \Omega_{i_\alpha}^2 (q_{i_\alpha} - q_{i_\alpha}^{\mathrm{MM}})^2 + E_\alpha^{\mathrm{MM}}$$

Duschinsky-like rotation

$$\mathbf{Q}_\alpha = \underline{\underline{D}}_\alpha \mathbf{q}_\alpha \qquad D_{k_\alpha i_\alpha} = \hat{\mathbf{q}}_{i_\alpha}^T \hat{\mathbf{Q}}_{k_\alpha}$$

$$H_{\mathrm{MM}}(\mathbf{p}^\alpha, \mathbf{q}^\alpha) = \tfrac{1}{2}\sum_{i_\alpha} p_{i_\alpha}^2 + V_{\mathrm{MM}}^\alpha(\mathbf{q}^\alpha)$$

$$q_{i\alpha}(t) = q_{i\alpha}^{\mathrm{MM}} + (q_{i\alpha}(0) - q_{i\alpha}^{\mathrm{MM}})\cos\Omega_{i_\alpha} t + \frac{p_{i\alpha}(0)}{\Omega_{i_\alpha}}\sin\Omega_{i_\alpha} t$$

$$C_\alpha^{\mathrm{MM}}(t) = \frac{1}{Z^{\mathrm{MM}}}\int d\mathbf{p}_\alpha(0)\int d\mathbf{q}_\alpha(0)\exp[-\beta H^{\mathrm{MM}}(\mathbf{p}_\alpha(0), \mathbf{q}_\alpha(0))]\delta\varepsilon_\alpha(0)\delta\varepsilon_\alpha(t)$$

$$Z^{\mathrm{MM}} = \int d\mathbf{p}_\alpha(0)\int d\mathbf{q}_\alpha(0)\exp[-\beta H^{\mathrm{MM}}(\mathbf{p}_\alpha(0), \mathbf{q}_\alpha(0))]$$

$$C_\alpha^{\mathrm{MM}}(t) = \frac{2}{\beta}\sum_{i_\alpha}\sum_{k_\alpha}\left(\frac{\omega_{k_\alpha} D_{k_\alpha i_\alpha}}{\Omega_{i_\alpha}}\right)^2 \lambda_{k_\alpha}\cos\Omega_{i_\alpha} t$$

$$J_\alpha^{\mathrm{MM}}(\omega) = \pi\omega\sum_{i_\alpha}\sum_{k_\alpha}\left(\frac{\omega_{k_\alpha} D_{k_\alpha i_\alpha}}{\Omega_{i_\alpha}}\right)^2 \lambda_{k_\alpha}\delta(\omega - \Omega_{i_\alpha})$$

$$J_\alpha(\omega) = \pi\sum_{i_\alpha}\omega_{i_\alpha}\lambda_{i_\alpha}\delta(\omega - \omega_{i_\alpha})$$

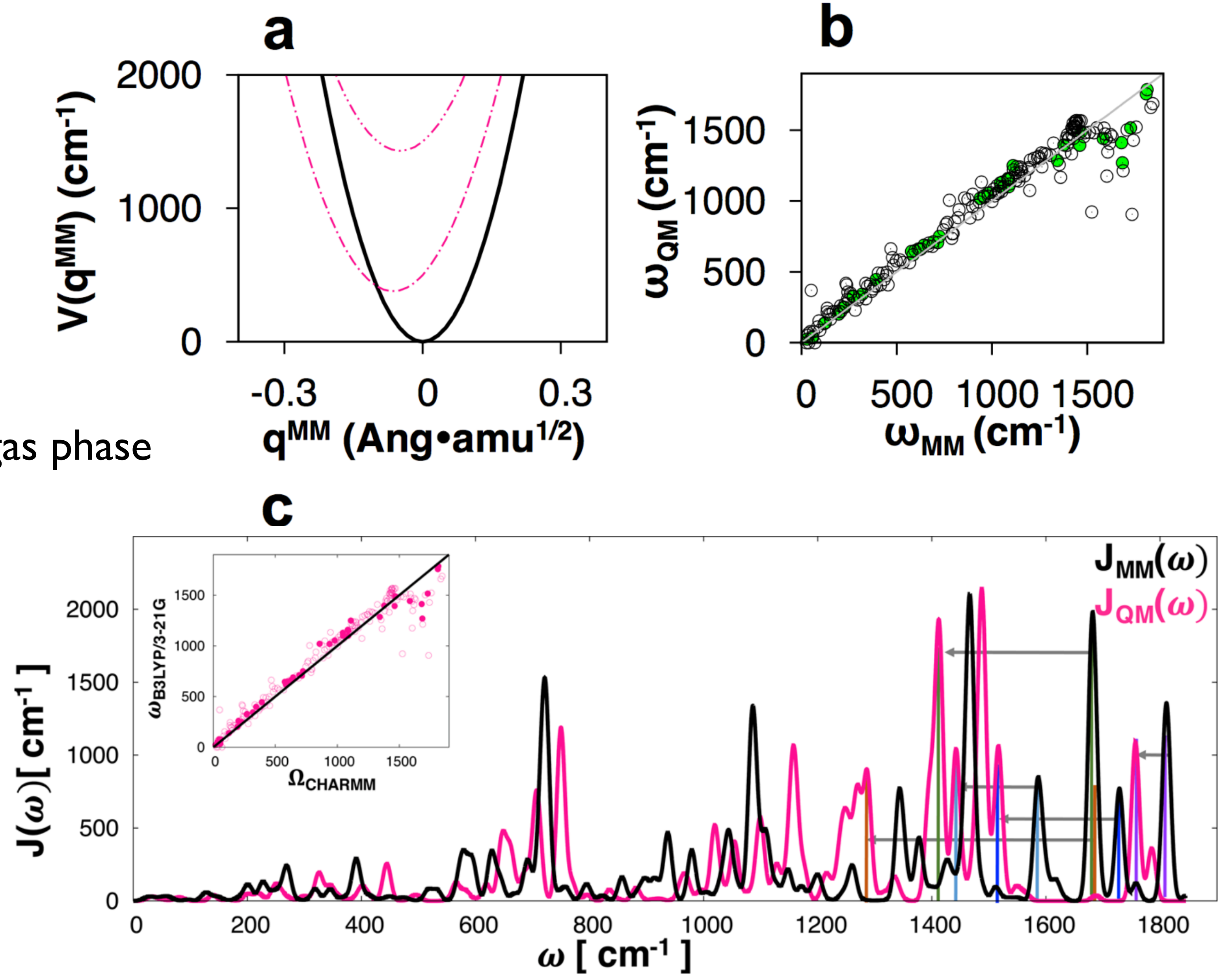

BChl - gas phase

An alternative approach

$$\delta\varepsilon_\alpha(t) = \delta\varepsilon_\alpha^{\rm sr}(t) + \delta\varepsilon_\alpha^{\rm lr}(t)$$

$$C_\alpha(t) = \langle \delta\varepsilon_\alpha(0)\delta\varepsilon_\alpha(t)\rangle$$

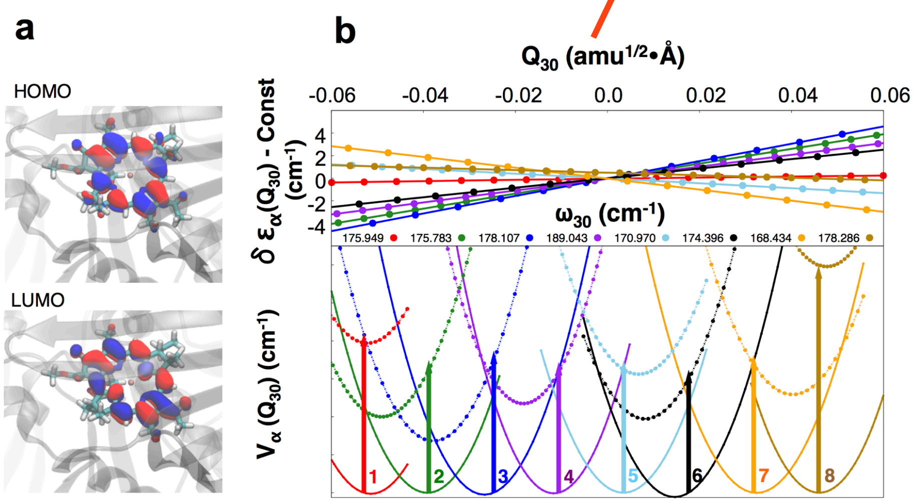

$$\delta\epsilon_\alpha^{\rm lr}(t) = \frac{1}{4\pi\epsilon_0}\sum_i\sum_K \frac{\delta z_i^\alpha Z_K^\alpha}{|r_i^\alpha(t) - R_K^\alpha(t)|}$$

Charge Density Coupling (CDC)

(1) Adolphs, J.; Muh, F.; Madjet, M. E.-A.; Renger, T. Photosynth. Res. 2008, 95, 197–209.
(2) Renger, T. Photosynth. Res. 2009, 102, 471–485.
(3) Shi and coworkers J. Phys. Chem. B 116, 1164 (2012)
(4) Rivera, Montemayor, Masia, Coker J. Phys. Chem. B 117, 5510 (2013)

Mi Kyung Lee, DFC, J. Phys. Chem. Lett. 7, 3171(2016)

$$C_\alpha(t) \sim \langle \delta\varepsilon_\alpha^{\rm sr}(0)\delta\varepsilon_\alpha^{\rm sr}(t)\rangle + \langle \delta\varepsilon_\alpha^{\rm lr}(0)\delta\varepsilon_\alpha^{\rm lr}(t)\rangle$$

$$\langle \delta\varepsilon_\alpha^{\rm sr}(0)\delta\varepsilon_\alpha^{\rm lr}(t)\rangle \sim 0$$

FMO HR factors - gray bars (expt. Freiburg and co-workers)

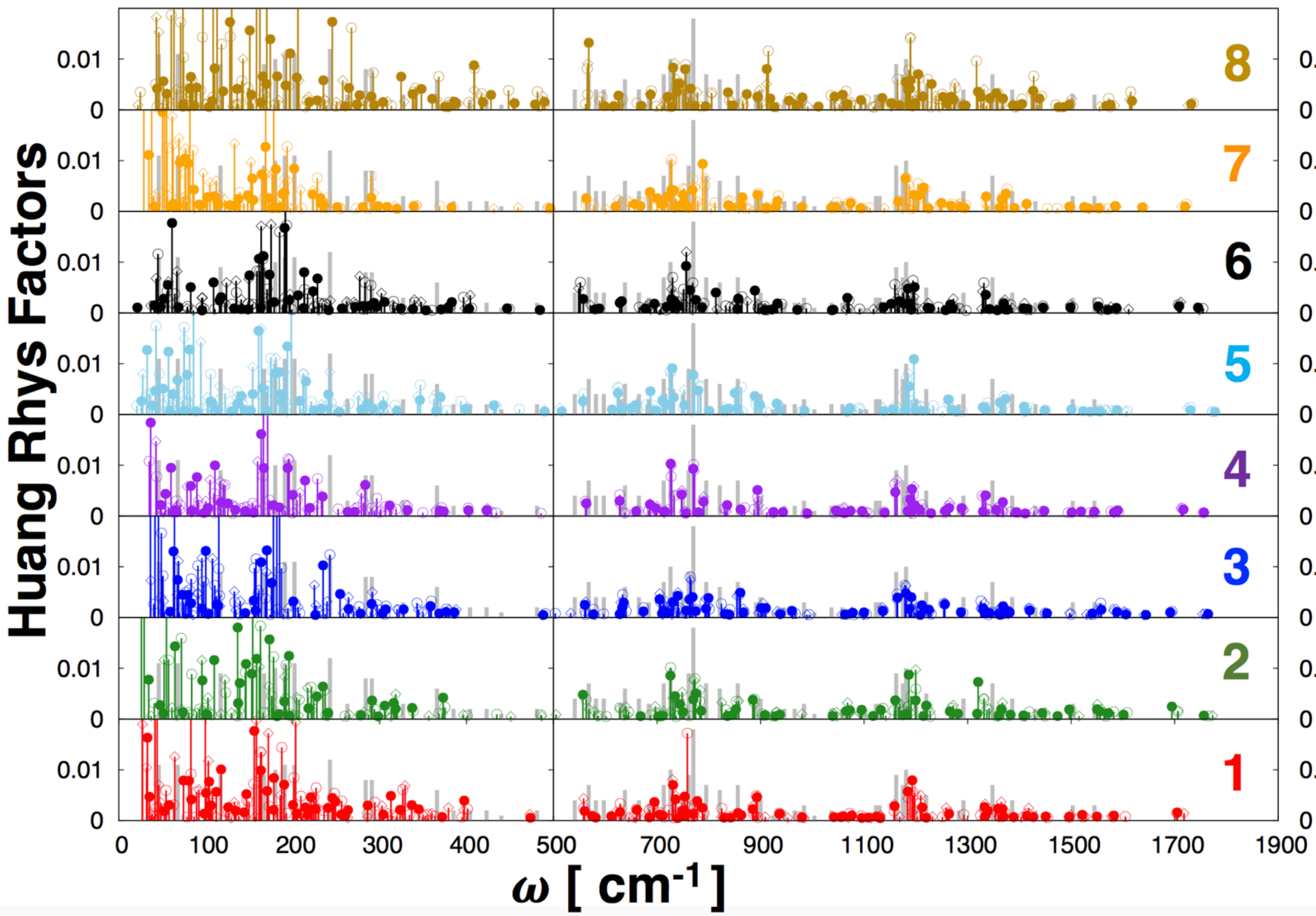

$$J_\alpha(\omega) = J_\alpha^{\mathrm{vib}}(\omega) + J_\alpha^{\mathrm{inter}}(\omega)$$

$$J^{(\alpha)}(\omega) = \frac{\pi}{2}\sum_i \frac{c_i^{(\alpha)2}}{\omega_i}\delta(\omega-\omega_i) = \quad 2\lambda\omega\tau_c/(1+\omega^2\tau_c^2) \quad \tau_c = 50 \text{ fs and } \lambda = 35 \text{ cm}^{-1}$$

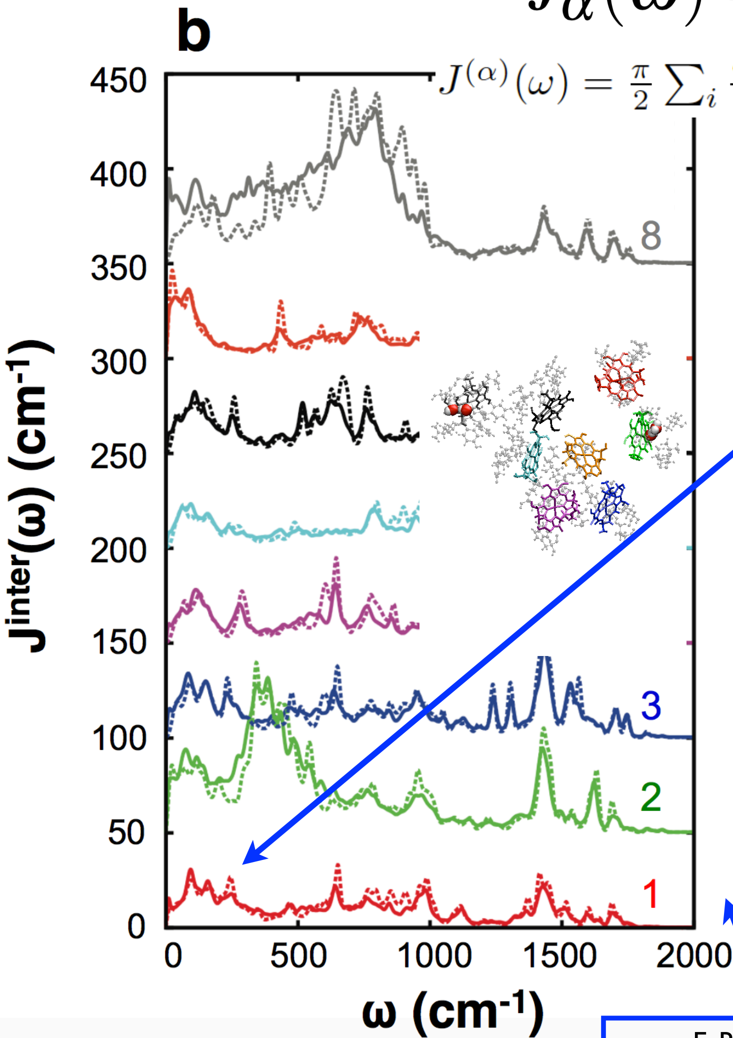

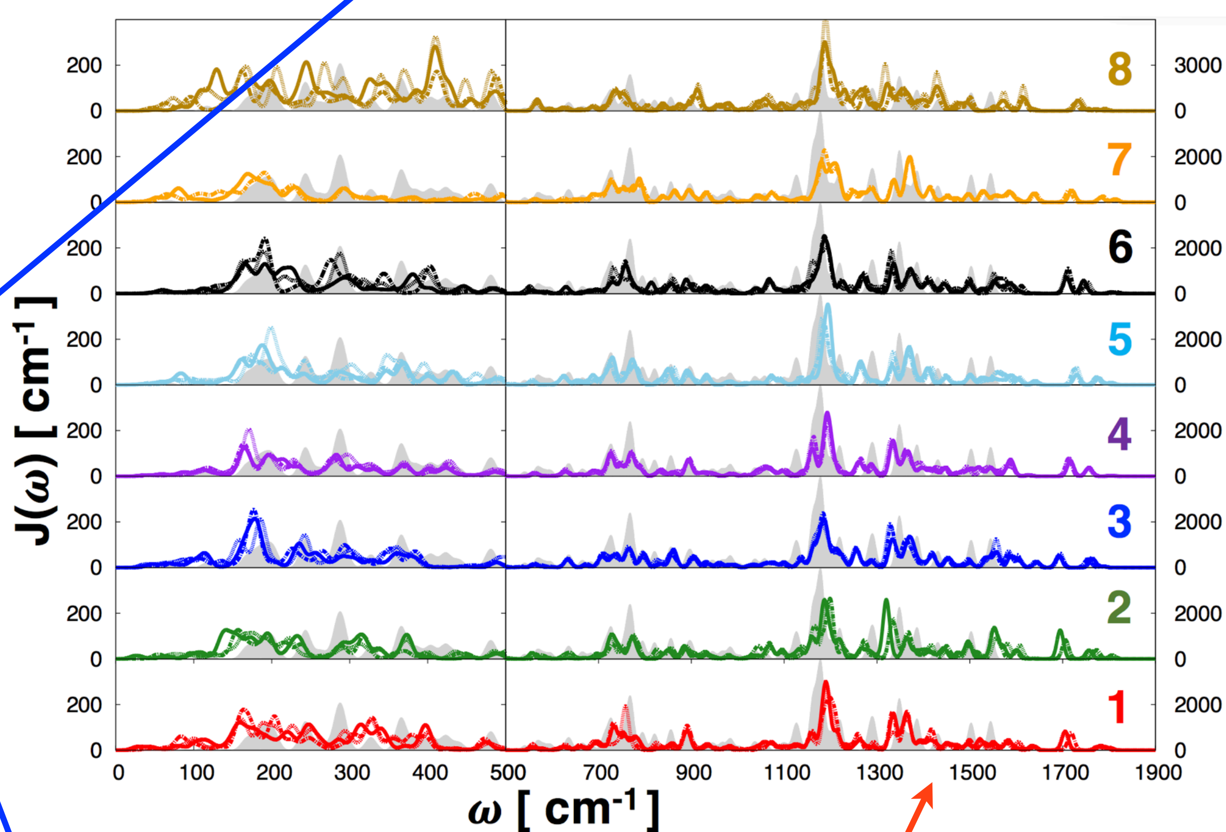

E. Rivera, D. Montemayor, M. Masia and D.F. Coker, J. Phys. Chem. B, 117, 55105521 (2013)

M.K. Lee & DFC, J. Phys. Chem. Lett. 7, 3171 (2016)

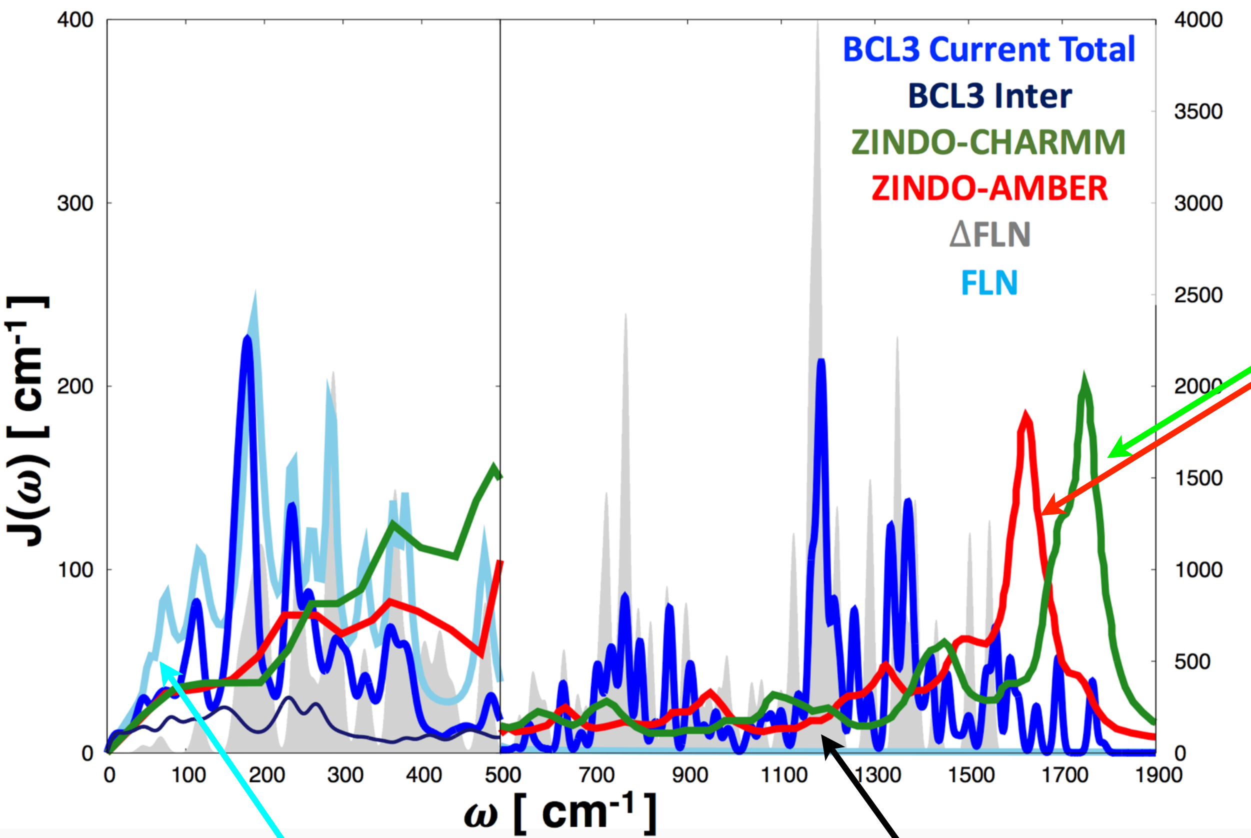

Kleinekathoefer, et al.
JPCB (2015)

$$J_{\alpha}^{\mathrm{MM}}(\omega) = \pi\omega \sum_{i_\alpha}\sum_{k_\alpha} \left(\frac{\omega_{k_\alpha} D_{k_\alpha i_\alpha}}{\Omega_{i_\alpha}} \right)^2 \lambda_{k_\alpha} \delta(\omega - \Omega_{i_\alpha})$$

$$J_{\alpha}(\omega) = \pi \sum_{i_\alpha} \omega_{i_\alpha} \lambda_{i_\alpha} \delta(\omega - \omega_{i_\alpha})$$

M. Ratsep & A. Freiberg J. Lumin. 127 (2007) 251.

M. Wendling et al. J. Phys. Chem. B 104 (2000) 5825.

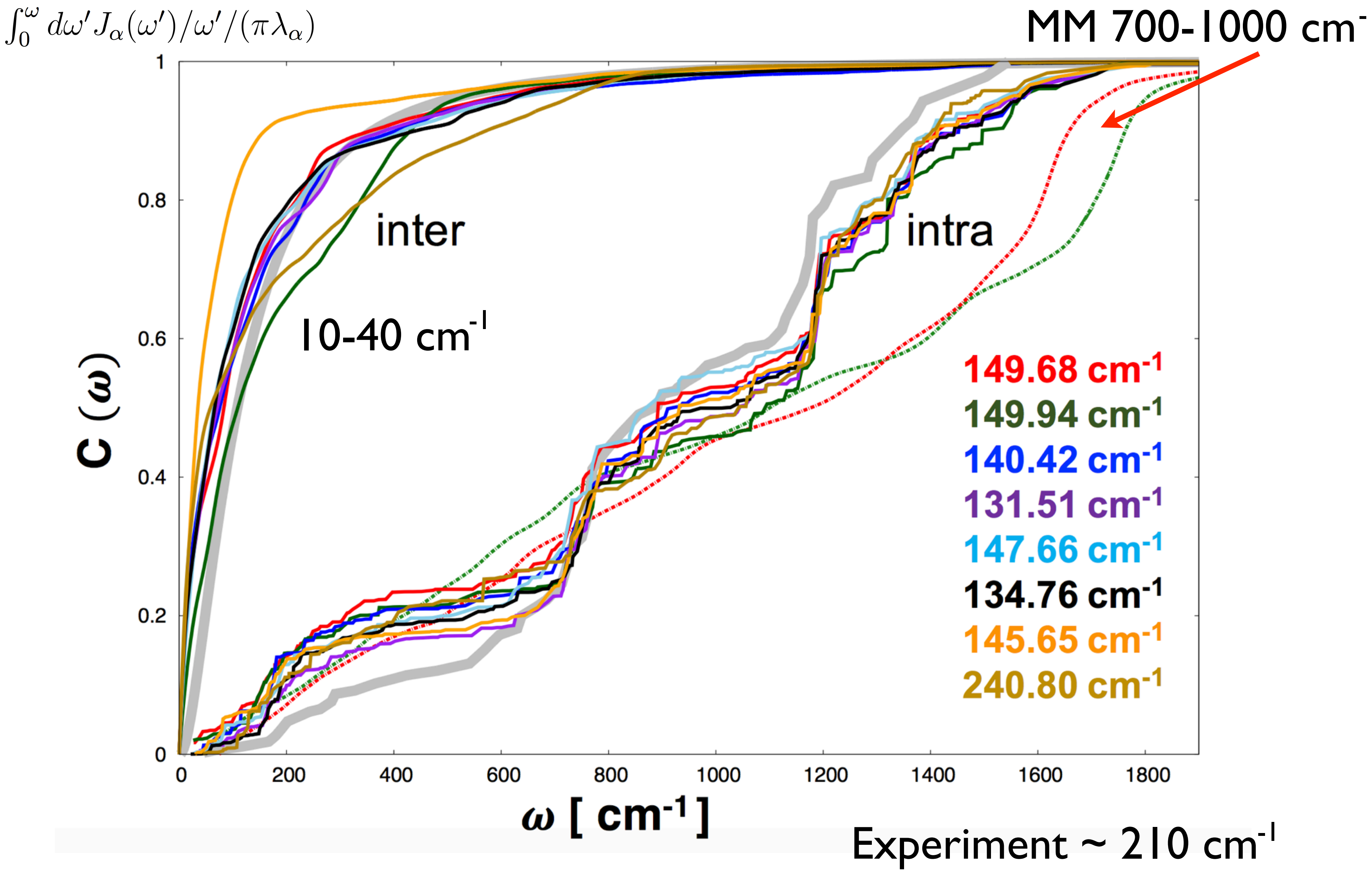

$\int_0^\omega d\omega' J_\alpha(\omega')/\omega'/(\pi\lambda_\alpha)$
MM 700-1000 cm-1
inter
intra
10-40 cm-1
C (ω)
ω [cm-1]
149.68 cm-1
149.94 cm-1
140.42 cm-1
131.51 cm-1
147.66 cm-1
134.76 cm-1
145.65 cm-1
240.80 cm-1
0
0.2
0.4
0.6
0.8
1
0
200
400
600
800
1000
1200
1400
1600
1800
Experiment ~ 210 cm-1

OUTLINE:

(1) Spectral Density Calculations

(2) Excitation Energy Calculations

(3) Dissipative Quantum Dynamics for General Regimes

(4) Issues with Linearized Dynamics of Higher Frequency Modes

(5) Spectra (PC645/HPC645) - Influence of Protonation and "Flickering" Pathways

(6) Quantum Dynamics and Nonlinear Spectroscopy

(7) Coherent State Density Matrix Dynamics (+PLDM)

Parameterized Model Site Hamiltonian

estimate from transition dipoles or densities - small fluctuations

$$\hat{H} = \sum_{\alpha=1}^{N_{state}} \epsilon_\alpha |\alpha\rangle\langle\alpha| + \sum_{\alpha\neq\beta}^{N_{state}} \Delta_{\alpha,\beta}[|\alpha\rangle\langle\beta| + |\beta\rangle\langle\alpha|]$$

Fluctuate like crazy!

$$+ \sum_{\alpha=1}^{N_{state}} \sum_{i=1}^{n^{(\alpha)}} c_i^{(\alpha)} Q_i^{(\alpha)} |\alpha\rangle\langle\alpha|$$

7 state FMO test

$$+ \sum_{\alpha=1}^{N_{state}} \sum_{i=1}^{n^{(\alpha)}} \frac{1}{2}[P_i^{(\alpha)2} + \omega_i^{(\alpha)2} Q_i^{(\alpha)2}]$$

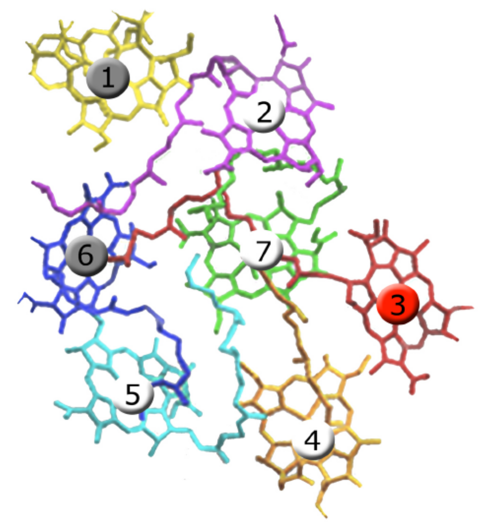

In principle Site dependent "spectral densities"

$$J^{(\alpha)}(\omega) = \frac{\pi}{2}\sum_i \frac{c_i^{(\alpha)2}}{\omega_i}\delta(\omega - \omega_i) = \quad 2\lambda\omega\tau_c/(1+\omega^2\tau_c^2) \quad \tau_c = 50 \text{ fs and } \lambda = 35 \text{ cm}^{-1}$$

Experimental fit assumes all have identical environments continuum of intermolecular modes

$$E^{\mathrm{CIS(D)}} = \langle \Phi_{\mathrm{CIS}} \mid V \mid U_2 \Phi_0 \rangle + \langle \Phi_{\mathrm{CIS}} \mid V \mid T_2 U_1 \Phi_0 \rangle$$

Double excitation from reference HF wavefunction. "Direct term" that describes excited state correlation pairs.

Double excitation of the "CIS inactive" electrons. This second 'indirect" term describes correlation with electrons not involved in the excitation.

Single excitation of the "CIS active" electrons

$$\omega^{\mathrm{SOS-CIS(D)}} = \langle \Phi_{\mathrm{CIS}} \mid V \mid c_U U_2^{\mathrm{OS}} \Phi_0 \rangle + \langle \Phi_{\mathrm{CIS}} \mid V \mid c_T T_2^{\mathrm{OS}} U_1 \Phi_0 \rangle$$

J. Phys. Chem. A **2007,** *111,* 5314−5326

Scaled Second-Order Perturbation Corrections to Configuration Interaction Singles: Efficient and Reliable Excitation Energy Methods

Young Min Rhee and Martin Head-Gordon*

Department of Chemistry, University of California and Chemical Sciences Division, Lawrence Berkeley National Laboratory, Berkeley, California 94720

Received: December 7, 2006; In Final Form: March 9, 2007

Two modifications of the perturbative doubles correction to configuration interaction with single substitutions (CIS(D)) are suggested, which are excited state analogues of ground state scaled second-order Møller−Plesset (MP2) methods. The first approach employs two parameters to scale the two spin components of the direct term of CIS(D), starting from the two-parameter spin-component scaled (SCS) MP2 ground state, and is termed SCS−CIS(D). An efficient resolution-of-the-identity (RI) implementation of this approach is described. The second approach employs a single parameter to scale only the opposite-spin direct term of CIS(D), starting from the one-parameter scaled opposite-spin (SOS) MP2 ground state, and is called SOS−CIS(D). By utilizing auxiliary basis expansions and a Laplace transform, a fourth-order algorithm for SOS−CIS(D) is described and implemented. The parameters that describe SCS−CIS(D) and SOS−CIS(D) are optimized based on a training set that includes valence excitations of various organic molecules and Rydberg transitions of water and ammonia, and they significantly improve upon CIS(D) itself. The accuracy of the two methods is found to be comparable. This arises from a strong correlation between the same-spin and the opposite-spin portions of the excitation energy terms. The methods are successfully applied to the zincbacteriochlorin−bacteriochlorin charge-transfer transition, for which time-dependent density functional theory, with presently available exchange-correlation functionals, is known to fail. The methods are also successfully applied to describe various electronic transitions outside of the training set. The efficiency of the SOS−CIS(D) and the auxiliary basis implementation of CIS(D) and SCS−CIS(D) are confirmed with a series of timing tests.

Standard MP2 correlation energy

$$E_C = E_C^{SS} + E_C^{OS},$$

Correlation for same spin

$$E_C^{SS} = \frac{1}{2}\sum_{ij} e_{ij} + \frac{1}{2}\sum_{\bar{i}\bar{j}} e_{\bar{i}\bar{j}},$$

Correlation for opposite spin

$$E_C^{OS} = \sum_{i\bar{j}} e_{i\bar{j}}.$$

$$e_{ij} = \sum_{ab} \left(T_{ij}^{ab} - T_{ij}^{ba}\right)(ia|jb),$$

$$e_{\bar{i}\bar{j}} = \sum_{\bar{a}\bar{b}} \left(T_{\bar{i}\bar{j}}^{\bar{a}\bar{b}} - T_{\bar{i}\bar{j}}^{\bar{b}\bar{a}}\right)(\bar{i}\bar{a}|\bar{j}\bar{b}),$$

$$e_{i\bar{j}} = \sum_{a\bar{b}} T_{i\bar{j}}^{a\bar{b}}(ia|\bar{j}\bar{b}).$$

$$T_{ij}^{ab} = \frac{(ia|jb)}{\epsilon_i + \epsilon_j - \epsilon_a - \epsilon_b},$$

$(ia|jb)=(i(1)a(1)|j(2)b(2))$

But in SOS-MP2:

$$E_C[SOS - MP2] = c_{OS} E_C^{OS}[MP2]$$

Neglect E^{SS} because much smaller than E^{OS}.

c_{os} = empirical parameter

Advanced Review

Spin-component-scaled electron correlation methods

Stefan Grimme,[1*] Lars Goerigk[2] and Reinhold F. Fink[3]

Spin-component-scaled (SCS) electron correlation methods for electronic structure theory are reviewed. The methods can be derived theoretically by applying special conditions to the underlying wave functions in perturbation theory. They are based on the insight that low-order wave function expansions treat the correlation effects of electron pairs with opposite spin (OS) and same spin (SS) differently because of their different treatment at the underlying Hartree–Fock level. Physically, this is related to the different average inter-electronic distances in the SS and OS electron pairs. The overview starts with the original SCS-MP2 method and discusses its strengths and weaknesses and various ways to parameterize the scaling factors. Extensions to coupled-cluster and excited state methods as well the connection to virtual-orbital dependent density functional approaches are highlighted. The performance of various SCS methods in large thermochemical benchmarks and for excitation energies is discussed in comparison with other common electronic structure methods.

How to cite this article:
WIREs Comput Mol Sci 2012, 2: 886–906 doi: 10.1002/wcms.1110

TABLE III. Computed (deviations between method and reference are shown, results were obtained with the def2-TZVPP basis set) vertical singlet excitation energies ΔE (in eV) for the complete dye bench-mark set.

Method	1	2	3	4	5	6	7	8	9	10	11	12
Reference[a]	2.95	2.02	2.12	2.72	2.33	2.66	3.66	2.52	3.37	3.15	2.60	3.60
B-LYP	−0.72	−0.06	−0.42	−0.35	−0.61	−0.26	−0.43	0.15	−0.53	−0.65	−0.55	−1.43
B3-LYP	−0.32	0.13	−0.09	−0.43	−0.38	−0.02	−0.20	0.38	−0.14	−0.41	−0.30	−0.86
PBE38	−0.01	0.27	0.19	0.00	−0.19	0.18	0.01	0.55	0.15	−0.22	−0.11	−0.39
BMK	0.00	0.30	0.25	0.06	−0.15	0.20	0.04	0.55	0.17	−0.17	−0.06	−0.36
CAM-B3LYP	0.06	0.26	0.30	0.07	−0.11	0.23	0.04	0.55	0.24	−0.15	−0.02	−0.13
B2-PLYP	−0.29	0.06	0.20	−0.13	−0.27	−0.01	−0.02	0.24	−0.07	−0.28	−0.16	−0.63
B2GP-PLYP	−0.17	0.08	0.35	−0.03	−0.18	0.08	0.08	0.28	0.06	−0.18	−0.06	−0.38
CIS	0.90	0.79	1.02	0.69	0.45	0.92	0.51	1.27	1.03	0.42	0.53	0.74
CIS(D)	0.05	0.02	0.77	0.19	0.09	0.28	0.45	0.16	0.55	0.21	0.23	0.05
SCS-CIS(D)′	0.13	0.02	0.96	0.26	0.20	0.41	0.49	0.19	0.60	0.28	0.33	0.12
SCS-CIS(D)$^{\lambda=0}$	−0.04	−0.30	0.74	0.03	−0.02	0.18	0.31	−0.06	0.46	0.12	0.12	−0.02
SCS-CIS(D)$^{\lambda=1}$	−0.17	−0.30	0.67	−0.05	−0.11	0.09	0.24	−0.13	0.33	0.00	0.02	−0.18
SOS-CIS(D)	−0.08	−0.36	0.70	−0.03	−0.10	0.13	0.27	−0.10	0.40	0.04	0.03	−0.09
CC2	−0.26	0.04	0.51	−0.06	−0.13	0.01	0.24	0.20	0.00	−0.10	0.01	−0.48
SCS-CC2	−0.06	0.05	0.77	0.08	0.06	0.20	0.34	0.25	0.12	0.04	0.17	−0.23

[a]Experimental vertical excitation energies from Table II.

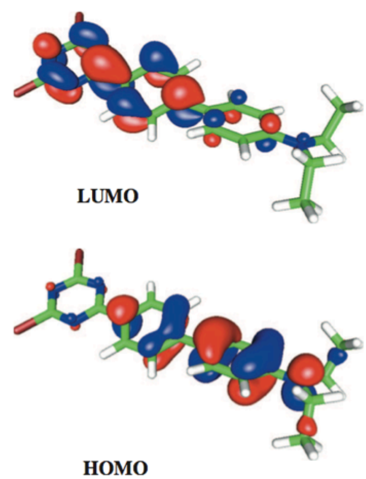

FIG. 2. Lowest unoccupied (LUMO; top) and highest occupied molecular orbitals (HOMO; bottom) for DBQ (**12**) obtained at the HF/def2-TZVPP level of theory.

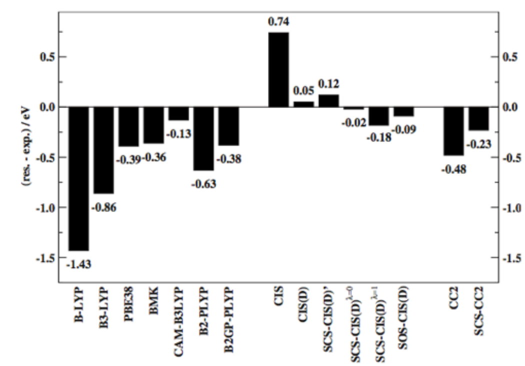

FIG. 3. Deviations for DBQ (**12**) in eV. All results were obtained with the def2-TZVPP basis.

OUTLINE:

(1) Spectral Density Calculations
(2) Excitation Energy Calculations
(3) Dissipative Quantum Dynamics for General Regimes
(4) Issues with Linearized Dynamics of Higher Frequency Modes
(5) Spectra (PC645/HPC645) - Influence of Protonation and "Flickering" Pathways
(6) Quantum Dynamics and Nonlinear Spectroscopy
(7) Coherent State Density Matrix Dynamics (+PLDM)

Partial Linearized Density Matrix (PLDM) dynamics:

Ehrenfest - like partially linearized propagator
useful for longer time propagation

Partial Linearized Density Matrix Propagation

PLDM: P. Huo and D.F. Coker, J. Chem. Phys. 135 201101 (2011).

ILDM: Dunkel, Bonella, Coker, J. Chem. Phys. 129,114106 (2008).

Miller-Meyer
Stock-Thoss

$$\hat{h}_{el} = \sum_{\beta,\lambda} |\beta\rangle\langle\beta|\hat{h}_{el}(\hat{R})|\lambda\rangle\langle\lambda| \qquad |\beta\rangle\langle\lambda| \rightarrow \hat{a}^\dagger_\beta \hat{a}_\lambda$$

$$|n\rangle \rightarrow |m_n\rangle = |0_1, ..., 1_n, ..0_{N_s}\rangle \qquad \hat{a}_\lambda = \frac{1}{\sqrt{2\hbar}}(\hat{q}_\lambda - i\hat{p}_\lambda) \qquad \hat{a}^\dagger_\lambda = \frac{1}{\sqrt{2\hbar}}(\hat{q}_\lambda + i\hat{p}_\lambda)$$

Total and "mapping" hamiltonian

$$\hat{H} = \hat{P}^2/2M + h_m(\hat{R},\hat{p},\hat{q}) \qquad \hat{h}_m(\hat{R}) = \frac{1}{2\hbar}\sum_\beta h_{\beta,\beta}(\hat{R})(\hat{q}^2_\beta + \hat{p}^2_\beta - \hbar) + \frac{1}{2\hbar}\sum_{\lambda\neq\beta} h_{\beta\lambda}(\hat{R})(\hat{q}_\beta\hat{q}_\lambda + \hat{p}_\beta\hat{p}_\lambda)$$

Density matrix propagation

$$\langle R_t n_t|\hat{\rho}(t)|R'_t n'_t\rangle = \sum_{n_0,n'_0}\int dR_0 dR'_0 \langle R_t n_t|e^{-\frac{i}{\hbar}\hat{H}t}|R_0 n_0\rangle \times \langle R_0 n_0|\hat{\rho}(0)|R'_0 n'_0\rangle\langle R'_0 n'_0|e^{\frac{i}{\hbar}\hat{H}t}|R'_t n'_t\rangle$$

Pengfei (Frank) Huo

Path integral mapping hamiltonian propagator

$$\langle R_N m_{n_t}|e^{-\frac{i}{\hbar}\hat{H}t}|R_0 m_{n_0}\rangle = \int \prod_{k=1}^{N-1} dR_k \frac{dP_k}{2\pi\hbar}\frac{dP_N}{2\pi\hbar} e^{\frac{i}{\hbar}S_0}$$

$$\times \langle n_t|e^{-\frac{i}{\hbar}\epsilon\hat{h}_m(R_{N-1})}\ldots e^{-\frac{i}{\hbar}\epsilon\hat{h}_m(R_0)}|n_0\rangle$$

Pechukas JCP 1969

$$S_0 = \epsilon \sum_{k=1}^{N} \left[P_k \frac{(R_k - R_{k-1})}{\epsilon} - \frac{P_k^2}{2M}\right]$$

$$T_{[n_t,n_0]} = \langle n_t|e^{-\frac{i}{\hbar}\epsilon\hat{h}_m(R_{N-1})}\ldots e^{-\frac{i}{\hbar}\epsilon\hat{h}_m(R_0)}|n_0\rangle$$

$$T_{[n_t,n_0]} = \int dq_0 dp_0 \frac{1}{4}(q_{n_t} + ip_{n_t})(q_{n_0} - ip_{n_0}) c_t e^{iS_1(t)}$$

$$\times \; e^{-\frac{i}{2}\sum_\beta (q_{\beta t}p_{\beta t} - q_{\beta 0}p_{\beta 0})} e^{-\frac{1}{2}\sum_\beta (q_{\beta 0}^2 + p_{\beta 0}^2)}$$

Coherent State description

$$c_t = e^{-\frac{i}{2\hbar}\int_0^t d\tau \sum_\beta \hat{h}_{\beta\beta}(R)}$$

$$S_1(t) = \int_0^t L_1(\tau)d\tau$$

$$L_1 = \sum_\beta p_\beta \dot{q}_\beta - h_m^{cl}(R) + \frac{1}{2}\sum_\beta h_{\beta\beta}(R)$$

$$h_m^{cl}(R,p,q) = \frac{1}{2}\sum_\beta h_{\beta\beta}(R)\left(p_\beta^2 + q_\beta^2\right) + \frac{1}{2}\sum_{\lambda\neq\beta} h_{\lambda\beta}(R)\left(p_\lambda p_\beta + q_\lambda q_\beta\right)$$

Bonella, Coker, J. Chem. Phys. 118,4370 (2003)
Dunkel, Bonella, Coker, J. Chem. Phys. 129,114106 (2008)

Partial Linearization in Forward-Backward Environment Path Difference

$$\langle R_t n_t|\hat{\rho}(t)|R_t' n_t'\rangle = \sum_{n_0,n_0'} \int dR_0 dR_0' \langle R_t n_t|e^{-\frac{i}{\hbar}\hat{H}t}|R_0 n_0\rangle$$
$$\times \langle R_0 n_0|\hat{\rho}(0)|R_0' n_0'\rangle \langle R_0' n_0'|e^{\frac{i}{\hbar}\hat{H}t}|R_t' n_t'\rangle$$

Transform to mean and difference paths

$$\bar{R} = (R + R')/2 \quad Z = (R - R')$$
$$\bar{P} = (P + P')/2 \quad Y = (P - P')$$

$$(S_0 - S_0') = \bar{P}_N Z_N - \bar{P}_1 Z_0 - \sum_{k=1}^{N-1} (\bar{P}_{k+1} - \bar{P}_k) Z_k$$
$$- \sum_{k=1}^{N} [\frac{\epsilon}{m} \bar{P}_k - (\bar{R}_k - \bar{R}_{k-1})] Y_k$$

Truncate to linear order in difference paths

$$\sum_\beta p_\beta \dot{q}_\beta - h_m^{cl}(\bar{R}, p, q) \sim \sum_\beta p_\beta \dot{q}_\beta - h_m^{cl}(R, p, q) = \frac{1}{2}\frac{d}{d\tau}\left(\sum_\beta p_\beta q_\beta\right)$$

$$(S_1 - S_1')[R(t), R'(t)]$$
$$= \int_0^t [\frac{1}{2}\frac{d}{d\tau} \sum_\beta (p_{\beta\tau} q_{\beta\tau} - p'_{\beta\tau} q'_{\beta\tau}) + \mathcal{O}(Z_\tau^2)$$
$$+ \frac{1}{2}\left(\nabla_{\bar{R}} h_m^{cl}(\bar{R}_\tau, p_\tau, q_\tau) + \nabla_{\bar{R}} h_m^{cl}(\bar{R}_\tau, p'_\tau, q'_\tau)\right) Z_\tau] d\tau$$

Q. Shi & E. Geva J. Phys. Chem. A 108, 6109 (2004)

R. Lambert & N. Makri J. Chem. Phys. 137, 22A552-3 (2010)

$$\langle \bar{R}_N + \frac{Z_N}{2} n_t | \hat{\rho}(t) | \bar{R}_N - \frac{Z_N}{2} n_t' \rangle = \sum_{n_0, n_0'} \int d\bar{R}_0 dq_0 dp_0 dq_0' dp_0' G_0 G_0'$$

$$\times \frac{1}{4}(q_{n_t} + ip_{n_t})(q_{n_0} - ip_{n_0}) \frac{1}{4}(q'_{n'_t} - ip'_{n'_t})(q'_{n'_0} + ip'_{n'_0})$$

$$\times \int \prod_{k=1}^{N-1} d\bar{R}_k \frac{d\bar{P}_k}{2\pi\hbar} \frac{d\bar{P}_N}{2\pi\hbar} (\hat{\rho})_W^{n_0, n_0'} (\bar{R}_0, \bar{P}_1) e^{\frac{i}{\hbar} \bar{P}_N Z_N}$$

$$\times \prod_{k=1}^{N-1} \delta\left(\frac{\bar{P}_{k+1} - \bar{P}_k}{\epsilon} - F_k \right) \prod_{k=1}^{N} \delta\left(\frac{\bar{P}_k}{M} - \frac{\bar{R}_k - \bar{R}_{k-1}}{\epsilon} \right)$$

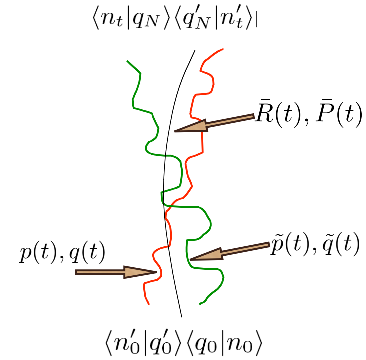

initial mapping distributions

$$G_0 = e^{-\frac{1}{2}\sum_\beta (q_{\beta 0}^2 + p_{\beta 0}^2)}$$

$$G_0' = e^{-\frac{1}{2}\sum_{\beta'} (q'^2_{\beta' 0} + p'^2_{\beta' 0})}$$

mapping equations of motion

$$\dot{q}_{n_t} = \partial h_m^{cl}(\bar{R}_t) / \partial p_{n_t}$$

$$\dot{p}_{n_t} = -\partial h_m^{cl}(\bar{R}_t) / \partial q_{n_t}$$

Effective back-reaction force

$$F_k = -\frac{1}{2}\left[\nabla_{\bar{R}_k} h_m^{cl}(\bar{R}_k, p_k, q_k) + \nabla_{\bar{R}_k} h_m^{cl}(\bar{R}_k, p_k', q_k')\right]$$

$$= -\frac{1}{4}\sum_\beta \nabla_{\bar{R}_k} h_{\beta\beta}(\bar{R}_k)\left(p_{\beta k}^2 + q_{\beta k}^2 + p'^2_{\beta k} + q'^2_{\beta k}\right)$$

$$-\frac{1}{4}\sum_{\lambda \neq \beta} \nabla_{\bar{R}_k} h_{\lambda\beta}\left(\bar{R}_k\right)\left(p_{\lambda k} p_{\beta k} + q_{\lambda k} q_{\beta k}\right)$$

$$-\frac{1}{4}\sum_{\lambda \neq \beta} \nabla_{\bar{R}_k} h_{\lambda\beta}\left(\bar{R}_k\right)\left(p'_{\lambda k} p'_{\beta k} + q'_{\lambda k} q'_{\beta k}\right)$$

Partial Linearized Density Matrix (PLDM) Dynamics: Approximate Open System Quantum Dynamics

P. Huo and D.F. Coker, J. Chem. Phys. 135 201101 (2011).

Canonical transformation:

$$\tilde{p}_\alpha = p_\alpha/\sqrt{2} \qquad \tilde{q}_\alpha = q_\alpha/\sqrt{2}$$

$$\tilde{p}'_\alpha = p'_\alpha/\sqrt{2} \qquad \tilde{q}'_\alpha = q'_\alpha/\sqrt{2}$$

Full system hamiltonian dynamics:

$$H = \frac{\bar{P}^2}{2M} + h_m^{can}(\bar{R}, \tilde{p}, \tilde{q}, \tilde{p}', \tilde{q}')$$

$$\begin{aligned} h_m^{can}(\bar{R}, \tilde{p}, \tilde{q}, \tilde{p}', \tilde{q}') \;=\; & \frac{1}{2}[\sum_\alpha h_{\alpha,\alpha}(\bar{R})(\tilde{p}_\alpha^2 + \tilde{q}_\alpha^2) + \sum_{\gamma \neq \alpha} h_{\gamma,\alpha}(\bar{R})(\tilde{p}_\gamma \tilde{p}_\alpha + \tilde{q}_\gamma \tilde{q}_\alpha) \\ & + \sum_\alpha h_{\alpha,\alpha}(\bar{R})(\tilde{p}'^{\,2}_\alpha + \tilde{q}'^{\,2}_\alpha) + \sum_{\gamma \neq \alpha} h_{\gamma,\alpha}(\bar{R})(\tilde{p}'_\gamma \tilde{p}'_\alpha + \tilde{q}'_\gamma \tilde{q}'_\alpha)] \end{aligned}$$

Iterative Implementation (IPLDM):

Second linearized density matrix propagation segment

Dunkel, Bonella, Coker, J. Chem. Phys. 129, 114106 (2008)

P. Huo & D.F. Coker, J. Chem. Phys. 137 22A535 (2012)

$$\langle \bar{R}_{2N} + \frac{Z_{2N}}{2} n_{2t} | \hat{\rho}(2t) | \bar{R}_{2N} - \frac{Z_{2N}}{2} n'_{2t} \rangle = \int \prod_{k=N+1}^{2N-1} d\bar{R}_k \frac{d\bar{P}_k}{2\pi} \frac{d\bar{P}_{2N}}{2\pi} e^{i\bar{P}_{2N} Z_{2N}}$$

$$\times r_{2t,n_{2t}}(\{\bar{R}_k\}) r'_{2t,n'_{2t}}(\{\bar{R}_k\}) e^{-i\epsilon \sum_{k=N+1}^{2N} (\theta_{n_{2t}}(\bar{R}_k) - \theta_{n'_{2t}}(\bar{R}_k))}$$

$$\times \prod_{k=N+1}^{2N-1} \delta\left(\frac{\bar{P}_{k+1} - \bar{P}_k}{\epsilon} - F_k^{\text{can}} \right) \prod_{k=N+1}^{2N} \delta\left(\frac{\bar{P}_k}{M} - \frac{\bar{R}_k - \bar{R}_{k-1}}{\epsilon} \right)$$

$$\sum_{n_t, n'_t} \int d\bar{R}_N \frac{d\bar{P}_N}{2\pi} dq_N dp_N dq'_N dp'_N r'_{t,n'_t} e^{-i\Theta'_{t,n'_t}} G'_t r_{t,n_t} e^{i\Theta_{t,n_t}} G_t$$

$$\times \delta(\bar{P}_N - \bar{P}_{N+1}) \delta\left(\frac{\bar{P}_N}{M} - \frac{\bar{R}_N - \bar{R}_{N-1}}{\epsilon} \right)$$

$$\times \int \prod_{k=1}^{N-1} d\bar{R}_k \frac{d\bar{P}_k}{2\pi} r_{t,n_t}(\{\bar{R}_k\}) r'_{t,n'_t}(\{\bar{R}_k\}) e^{-i\epsilon \sum_{k=1}^{N} (\theta_{n_t}(\bar{R}_k) - \theta_{n'_t}(\bar{R}_k))}$$

$$\times \prod_{k=1}^{N-1} \delta\left(\frac{\bar{P}_{k+1} - \bar{P}_k}{\epsilon} - F_k^{\text{can}} \right) \prod_{k=1}^{N} \delta\left(\frac{\bar{P}_k}{M} - \frac{\bar{R}_k - \bar{R}_{k-1}}{\epsilon} \right)$$

$$\times \sum_{n_0, n'_0} \int d\bar{R}_0 dq_0 dp_0 dq'_0 dp'_0 r'_{0,n'_0} e^{-i\Theta'_{0,n'_0}} G'_0 r_{0,n_0} e^{i\Theta_{0,n_0}} G_0 [\hat{\rho}]_W^{n_0,n'_0}(\bar{R}_0, \bar{P}_1)$$

An Algorithm:

$$(\sum_{n_t,n_t'} \int dq_N dp_N dq_N' dp_N')_{n_{2t},n_{2t}'}$$

Intermediate mapping integrals performed by steepest descent

$$(p_{n_0}^o, q_{n_0}^o) \; = \; (1/\sqrt{2}, 1/\sqrt{2}) \quad (p_{n_0}^u, q_{n_0}^u) \; = \; (0,0)$$

Intermediate state sums performed by importance sampled MC

Focusing

Bonella, Coker, J. Chem. Phys. 118,4370 (2003)

$$r_{\tau,n_t} r'_{\tau,n_t'} \exp[-i \int_0^\tau d\tau' (\theta_{n_t}(\tau') - \theta_{n_t'}(\tau'))]$$

$$M_{n_t,n_t'} = r_{t,n_t} r'_{t,n_t'} / \mathcal{N}(t) \qquad \mathcal{N}(t) = \sum_{n_t,n_t'} r_{t,n_t} r'_{t,n_t'}$$

Trajectory weights

$$\Omega_K \; = \; \left\{ \prod_{k=1}^{K-1} \mathcal{N}(kt) \exp[-i \int_{(k-1)t}^{kt} d\tau' (\theta_{n_{kt}}(\tau') - \theta_{n_{kt'}}(\tau'))] \right\}$$

$$\times \;\; r_{Kt,n_{Kt}} r'_{Kt,n_{Kt}'} \exp[-i \int_{(K-1)t}^{Kt} d\tau' (\theta_{n_{Kt}}(\tau') - \theta_{n_{Kt}'}(\tau'))]$$

Algorithm: Iterative Scheme LAND-Map

$$M_{n_t,n'_t} = r_{t,n_t} r'_{t,n'_t} / \sum_{n_t,n'_t} r_{t,n_t} r'_{t,n'_t}$$

$$C_{m_t,m'_t} = \sum_{n_t=1}^{m_t} \sum_{n'_t=1}^{m'_t} M_{n_t,n'_t}$$

$$\xi \in (0,1]$$

$$\succ C_{m_t,m'_t} \quad \xi$$

$$m_t = n_t^* \text{ and } m'_t = n'^*_t$$

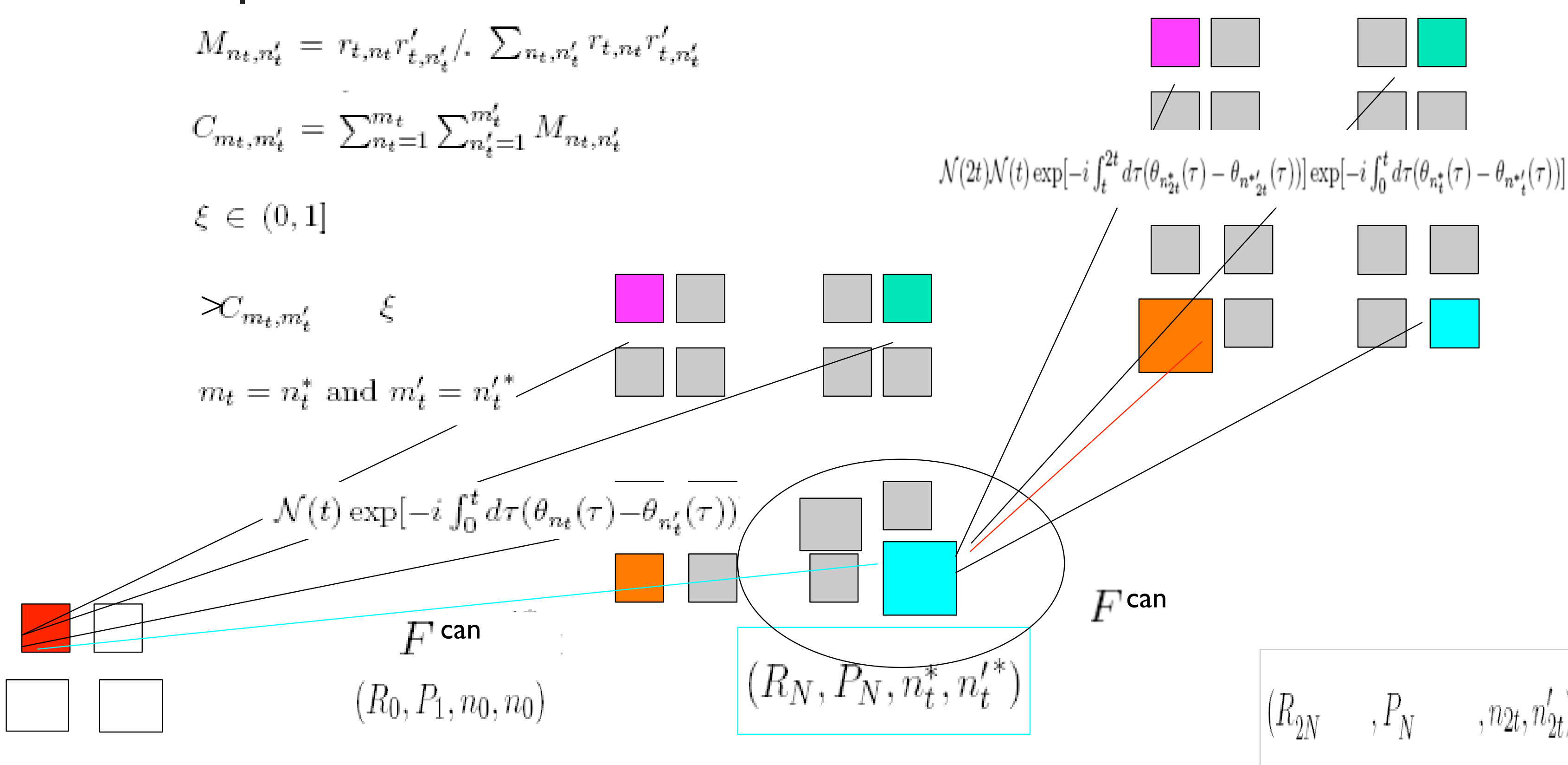

$$\begin{pmatrix} \boxed{\rho_{11}(0)} & \rho_{12}(0) \\ \rho_{21}(0) & \rho_{22}(0) \end{pmatrix} \quad \begin{pmatrix} \rho_{11}(t) & \rho_{12}(t) \\ \rho_{21}(t) & \rho_{22}(t) \end{pmatrix} \quad \begin{pmatrix} \rho_{11}(2t) & \rho_{12}(2t) \\ \rho_{21}(2t) & \rho_{22}(2t) \end{pmatrix} \quad \cdots\cdot$$

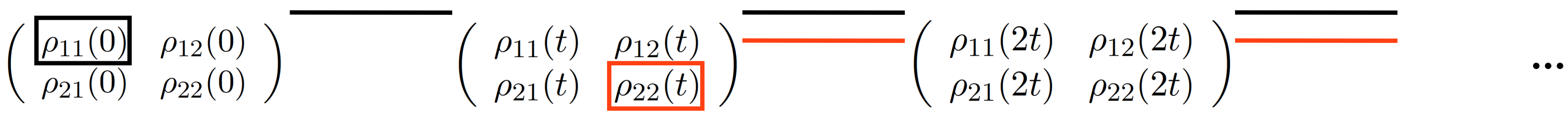
ρ11(0) ρ12(0)
ρ21(0) ρ22(0)
ρ11(t) ρ12(t)
ρ21(t) ρ22(t)
ρ11(2t) ρ12(2t)
ρ21(2t) ρ22(2t)
....

$$\begin{pmatrix} \boxed{\rho_{11}(0)} & \rho_{12}(0) \\ \rho_{21}(0) & \rho_{22}(0) \end{pmatrix} \quad \begin{pmatrix} \rho_{11}(t) & \rho_{12}(t) \\ \rho_{21}(t) & \boxed{\rho_{22}(t)} \end{pmatrix} \quad \begin{pmatrix} \rho_{11}(2t) & \rho_{12}(2t) \\ \boxed{\rho_{21}(2t)} & \rho_{22}(2t) \end{pmatrix} \quad \ldots.$$

Accumulating phase weights for different branching trajectories gives a representation of interference effects

1D nonadiabatic test models: PLDM, LSC-IVR, PBME

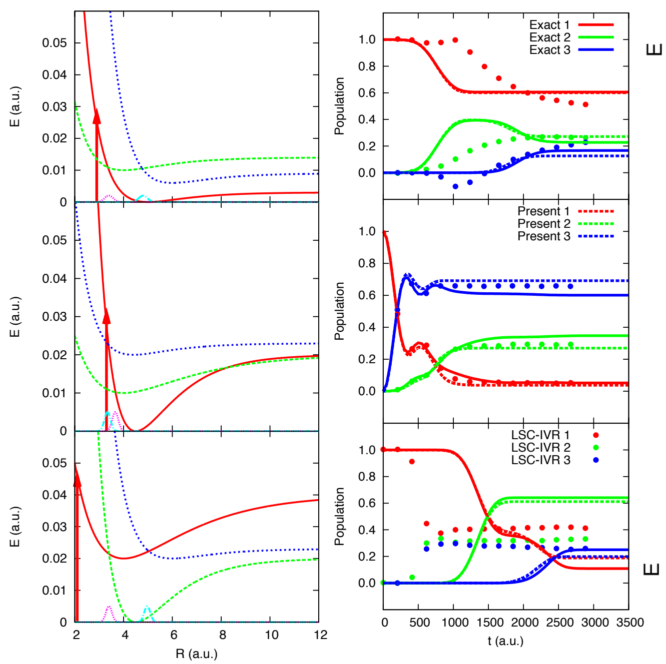

P. Huo and D.F. Coker, J. Chem. Phys. 135 201101 (2011).

Tully models

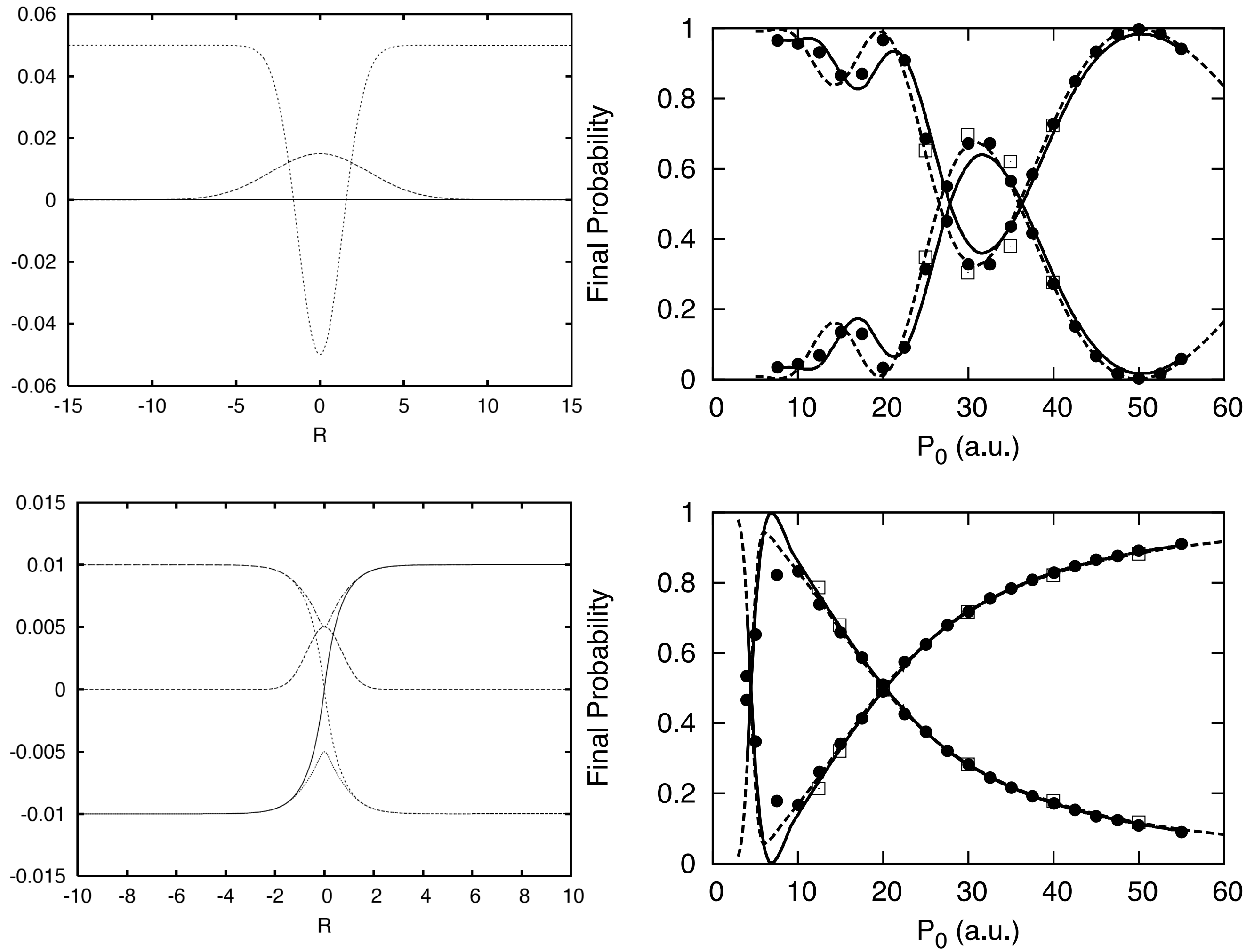

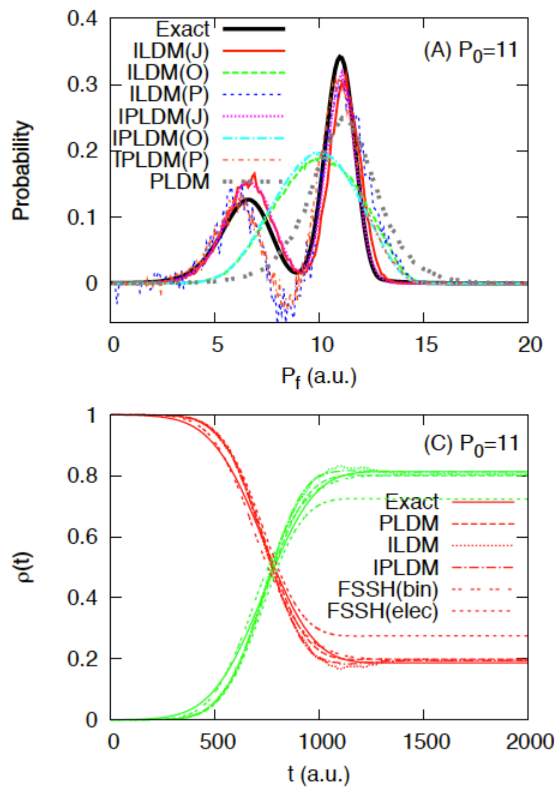

(1) Tully 1 momentum distribution bifurcation

P. Huo & D.F. Coker, J. Chem. Phys. 137 22A535 (2012)

(2) Asymmetric Spin-Boson Relaxation-Thermalization

$$\hat{H} = \hat{H}_s + \hat{H}_b + \hat{H}_{s-b}$$

$$= \epsilon\hat{\sigma}_z - \hbar\Omega\hat{\sigma}_x + \sum_j \left\{ \left[\frac{P_j^2}{2M_j} + \frac{1}{2}\omega_j^2 R_j^2 \right] \hat{1} - \hbar c_j R_j \hat{\sigma}_z \right\}$$

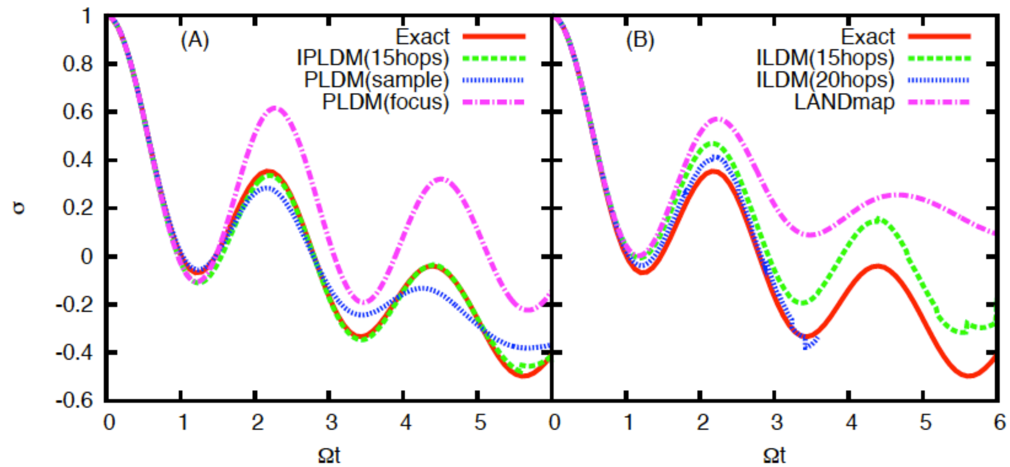

FIG. 7: $\langle\sigma_z(t)\rangle$ versus Ωt for spin-boson model, with $\Omega/\omega_c = 0.4$, $\zeta = 0.13$, $\epsilon = 0.4$, $\beta\hbar\omega_c = 12.5$. (A) Left panel gives results obtained with linearized and iterative algorithms based on the PLDM approximate short time propagator. (B) Right panel shows results obtained using LANDmap approximate short time propagator as the basis of iteration. In each panel results are explored as a function on the number of iterations.

PLDM

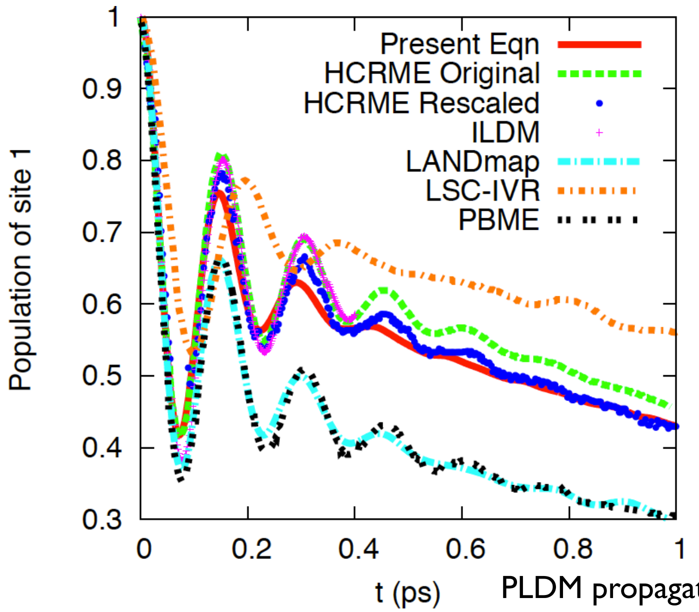

Seven state FMO spin-boson

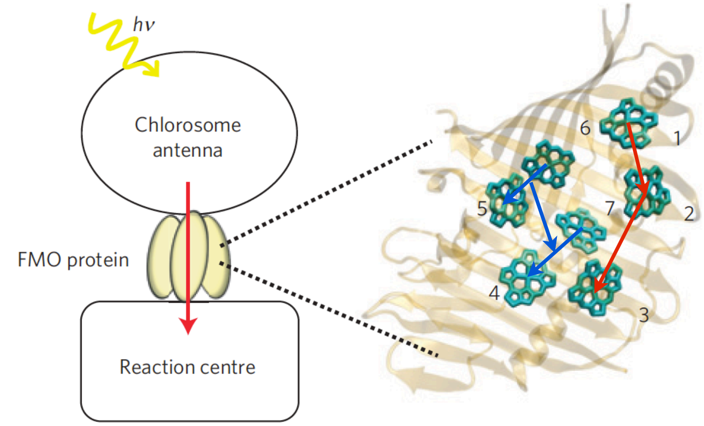

Experimentally fit spectral density

PLDM propagation & Thermal Equilibration

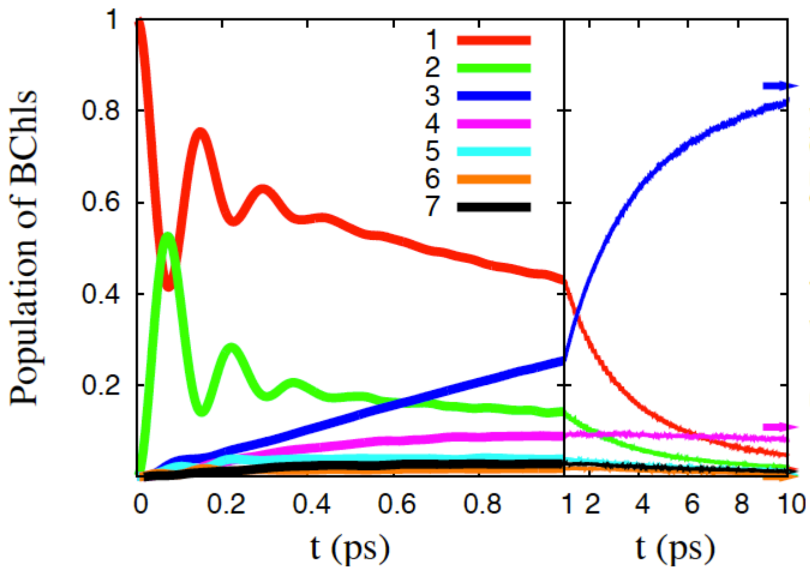

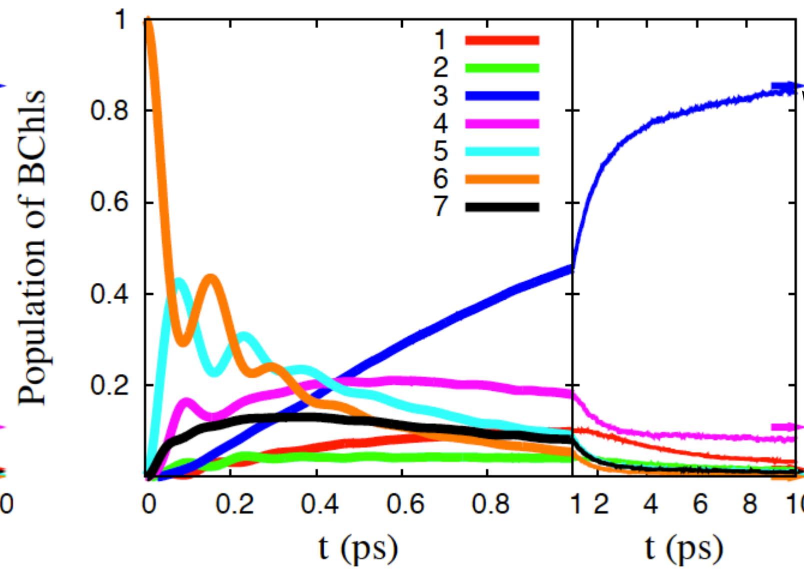

Diabatic projected thermal density

PLDM propagation & Thermal Equilibration

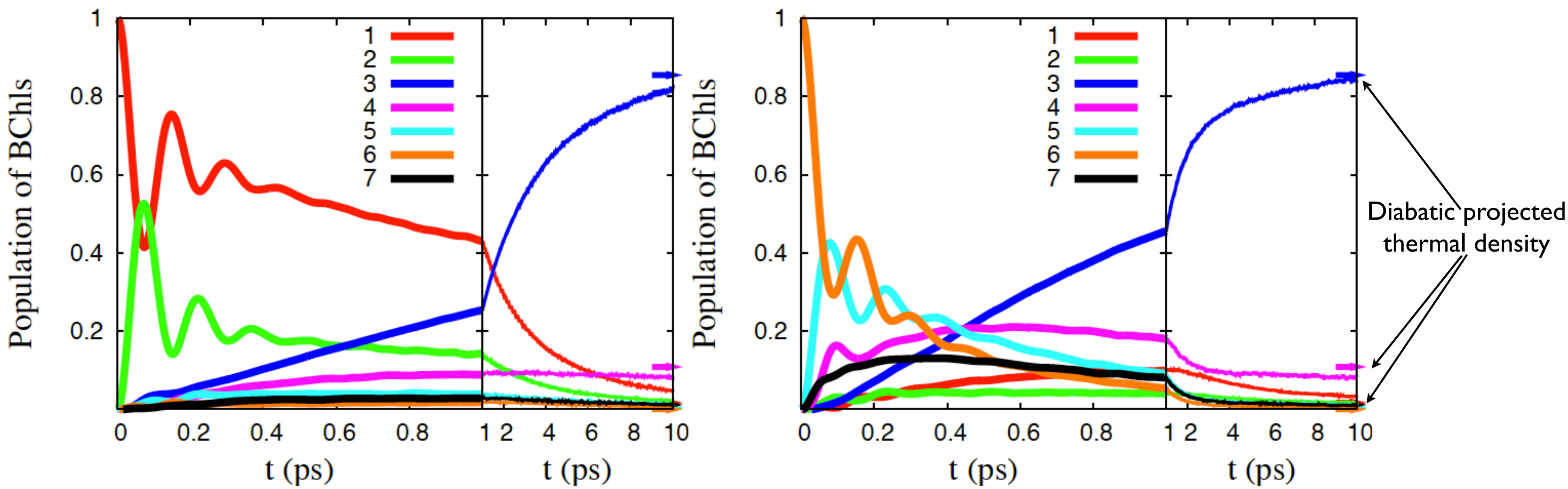

C.-Y. Hsieh and R. Kapral, JCP 138, 134110 (2013)

IPLDM = "Jump FB solution"

Equivalent to exact solution of
Mixed Quantum Classical Liouville (MQCL) equation

Important properties:

(1) Exact for the spin-boson:
D. MacKernan, G. Ciccotti, R. Kapral, JCP 116, 2346 (2002)

(2) Stationary solution of MQCL equation, $\hat{\rho}_{We}(R,P)$, and the partial Wigner transform of the quantum equilibrium canonical density matrix, $\hat{\rho}^{Q}_{We}(R,P)$, agree to $\mathcal{O}(\hbar)$:
S. Neilsen, G. Ciccotti, R. Kapral, JCP 115, 5805 (2001)

OUTLINE:

(1) Spectral Density Calculations
(2) Excitation Energy Calculations
(3) Dissipative Quantum Dynamics for General Regimes
(4) Issues with Linearized Dynamics of Higher Frequency Modes
(5) Spectra (PC645/HPC645) - Influence of Protonation and "Flickering" Pathways
(6) Quantum Dynamics and Nonlinear Spectroscopy
(7) Coherent State Density Matrix Dynamics (+PLDM)

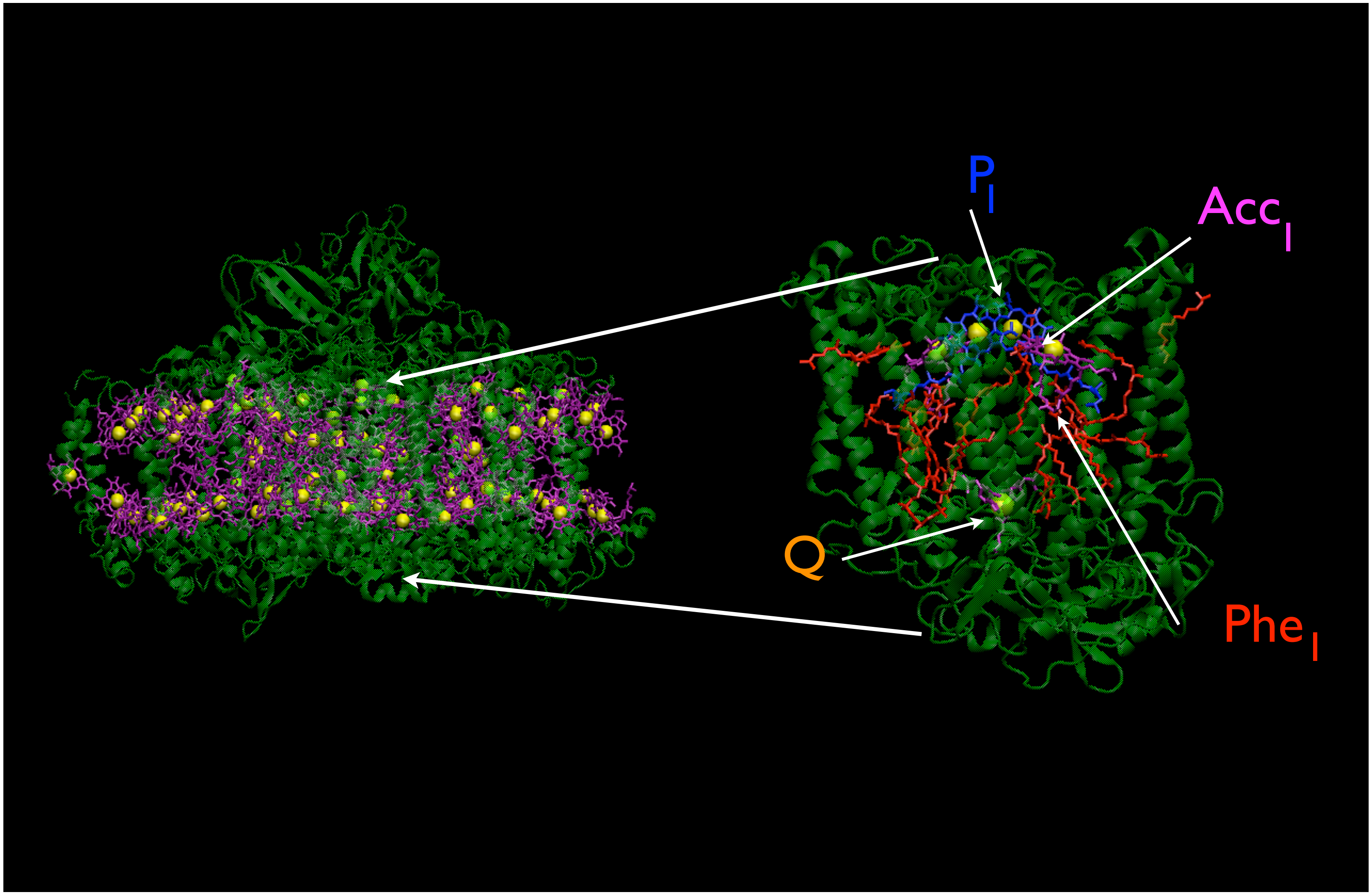

P_I
Acc_I
Q
Phe_I

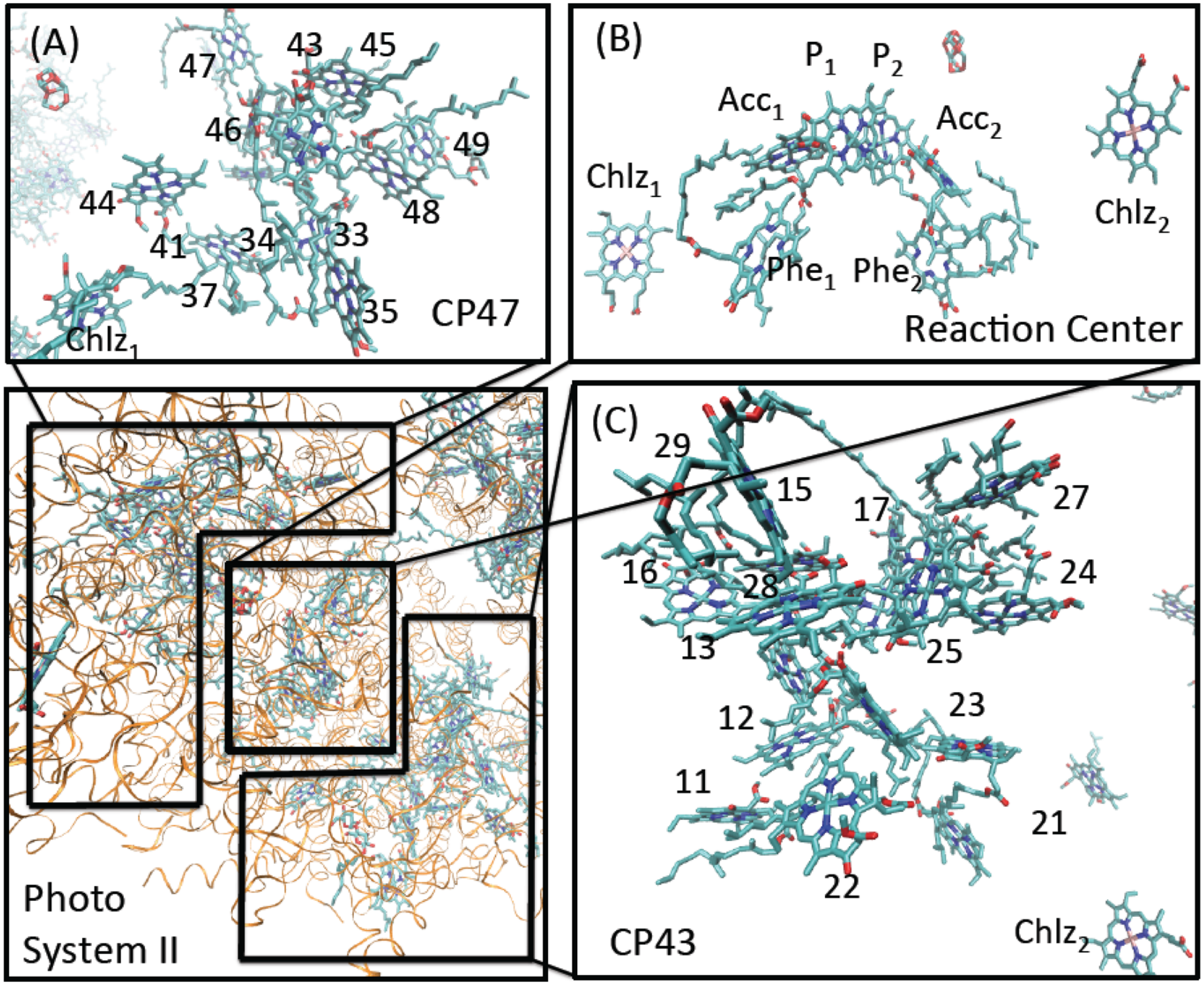

Photo System II Harvesting, Photo Protection and Charge Separation

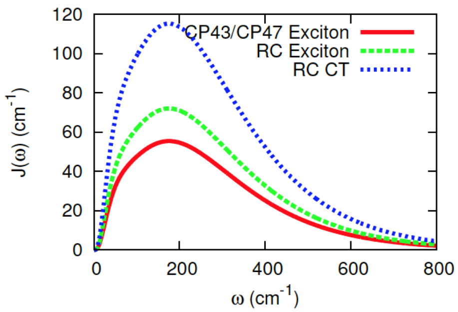

FIG. 2: Spectral density used in the model hamiltonian of PSII complex[14]. The exciton state spectral density in the harvesting complex CP43, CP47 is represented by red solid line. The spectral density for exciton (EX) and charge transfer (CT) state in reaction center are represented by green dash and blue dotted line respectively.

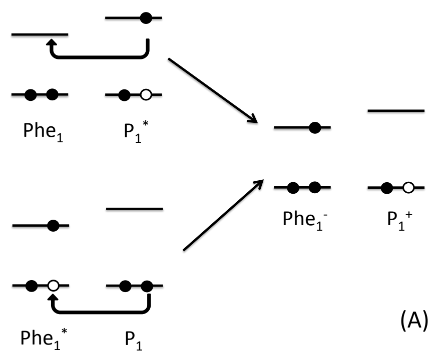

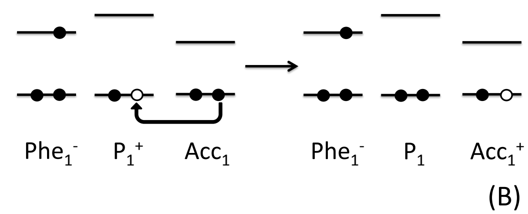

Exciton-Charge Transfer "wiring" diagram Light harvesting & Reaction Center Sub-Units

Exciton Couplings (Tom Renger & Coworkers)
BioPhys. J. 986 (2005), JACS 130 4431 (2008)

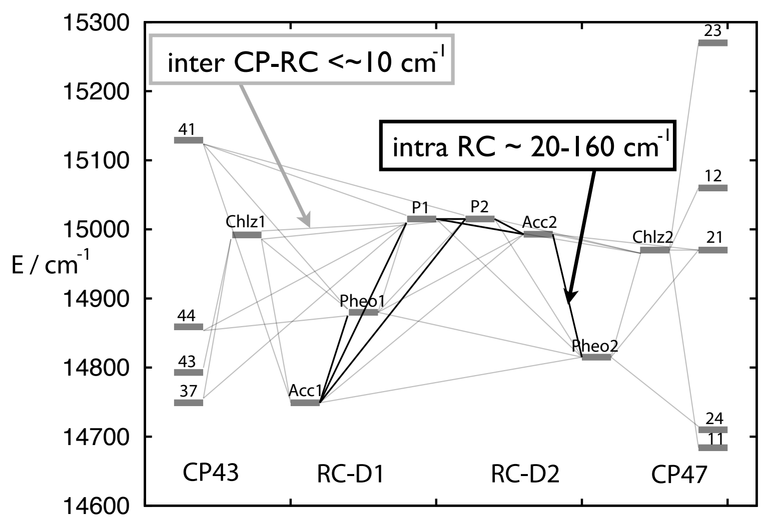

Exciton-CT & CT-CT Couplings
Mukamel & Coworkers, JCP 133, 184501(2010)

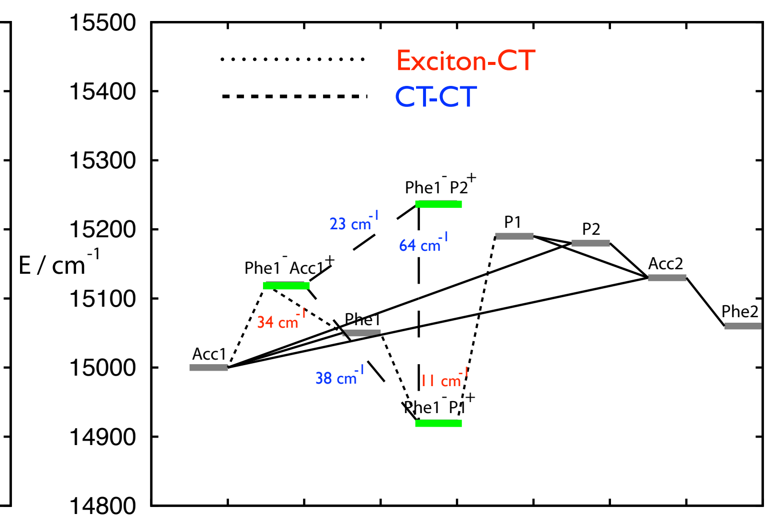

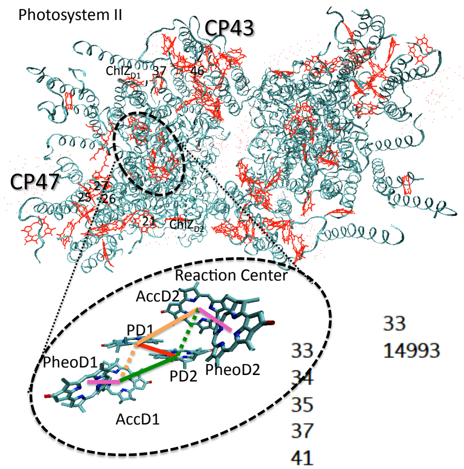

(1) Raszewski G, Saenger W, Renger T (2008) Light Harvesting in Photosystem II Core Complexes Is Limited by the Transfer to the Trap: Can the Core Complex Turn into a Photoprotective Mode? J. Am. Chem. Soc. 130:4431-4446.

Harvesting Network Hamiltonians

H_{ij} (cm^{-1})

CP43

	33	34	35	37	41	42	43	44	45	46	47	48	49
33	14993	-7	0	-2	-3	12	16	1	-9	3	-2	0	1
34		14859	-25	60	1	-6	-8	3	19	-12	10	-6	-1
35			14925	-20	-2	0	-5	-3	-4	-11	-4	13	4
37				14749	2	4	2	6	-2	21	3	-3	4
41					15129	-13	-76	-11	18	-2	-1	1	-4
42						14925	20	10	-25	11	4	-6	9
43							14793	-10	64	-3	-6	24	-24
44								14859	6	56	29	-16	9
45									14793	-50	78	3	-8
46										15038	-59	-9	10
47											15038	-15	9
48												14925	-41
49													14993

CP47

	11	12	13	14	15	16	17	21	22	23	24	25	26	27	28	29
11	14684	-49	-12	4	-2	-4	-1	4	-6	-2	-2	3	-2	-1	-2	-1
12		15060	-83	20	5	-6	-5	5	-20	-13	-4	6	-9	-2	4	-2
13			14793	0	-6	-59	-3	-8	32	15	2	-10	4	-2	-1	-3
14				14950	-47	-13	65	5	-11	-6	-1	21	-35	8	-3	0
15					14810	72	-20	-2	1	-5	-3	-6	-7	-4	13	11
16						14880	7	-3	8	-4	6	-4	9	4	1	9
17							15130	0	4	1	6	-2	17	3	-2	2
21								14970	-17	-83	-16	20	-5	-3	3	-1
22									14810	48	99	-16	10	4	-2	6
23										15270	-13	52	0	-6	32	-7
24											14710	-12	56	37	-18	8
25												15060	-64	95	25	2
26													14860	-63	-3	2
27														14880	-12	13
28															14970	-8
29																14530

Harvesting Network Dynamics

Site disorder: $\sigma = 0\ \text{cm}^{-1}$ $\sigma = 180\ \text{cm}^{-1}$

CP47

CP43

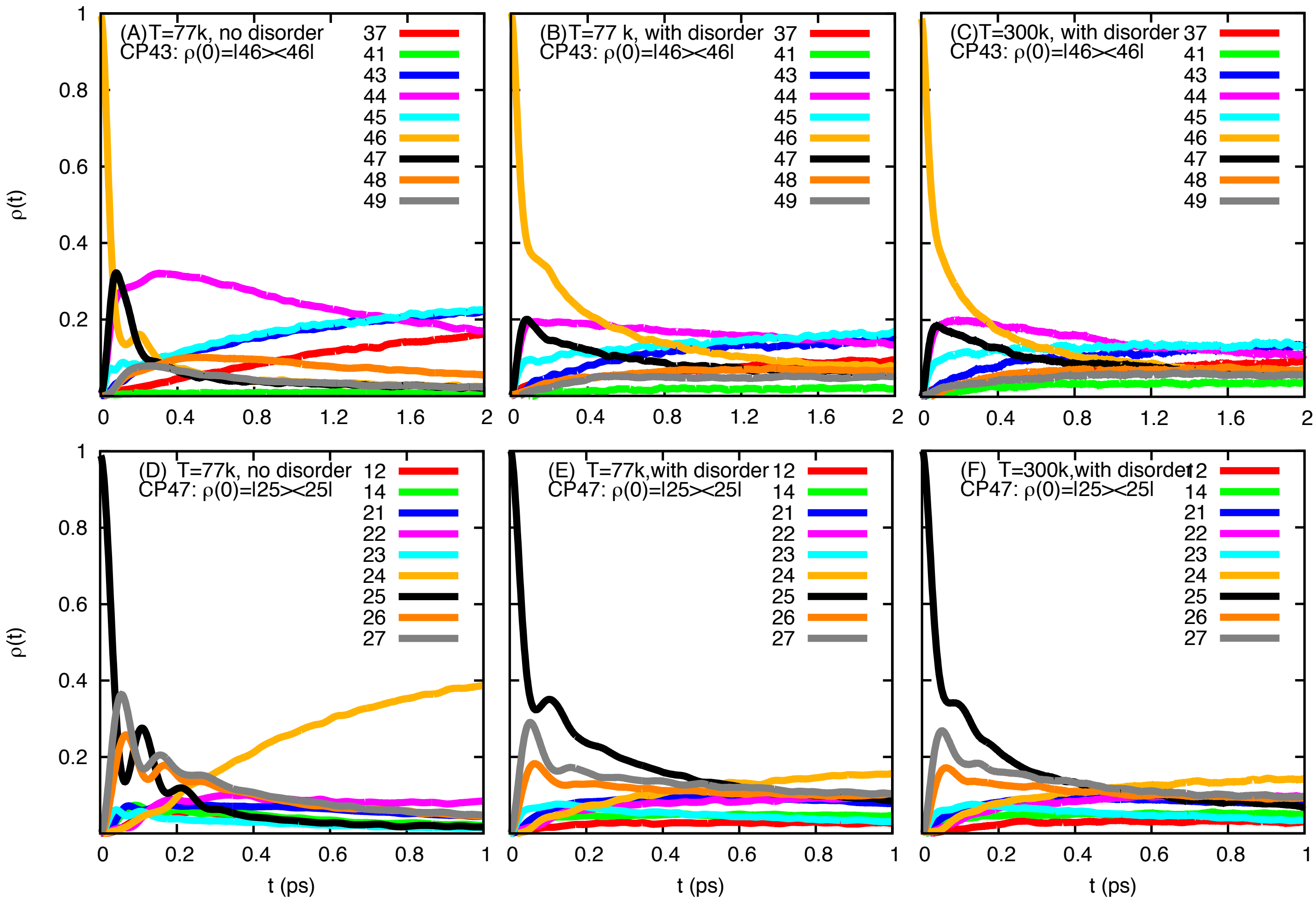

EX and CT Reaction Center Dynamics

PSII RC exciton dissociation - Romero

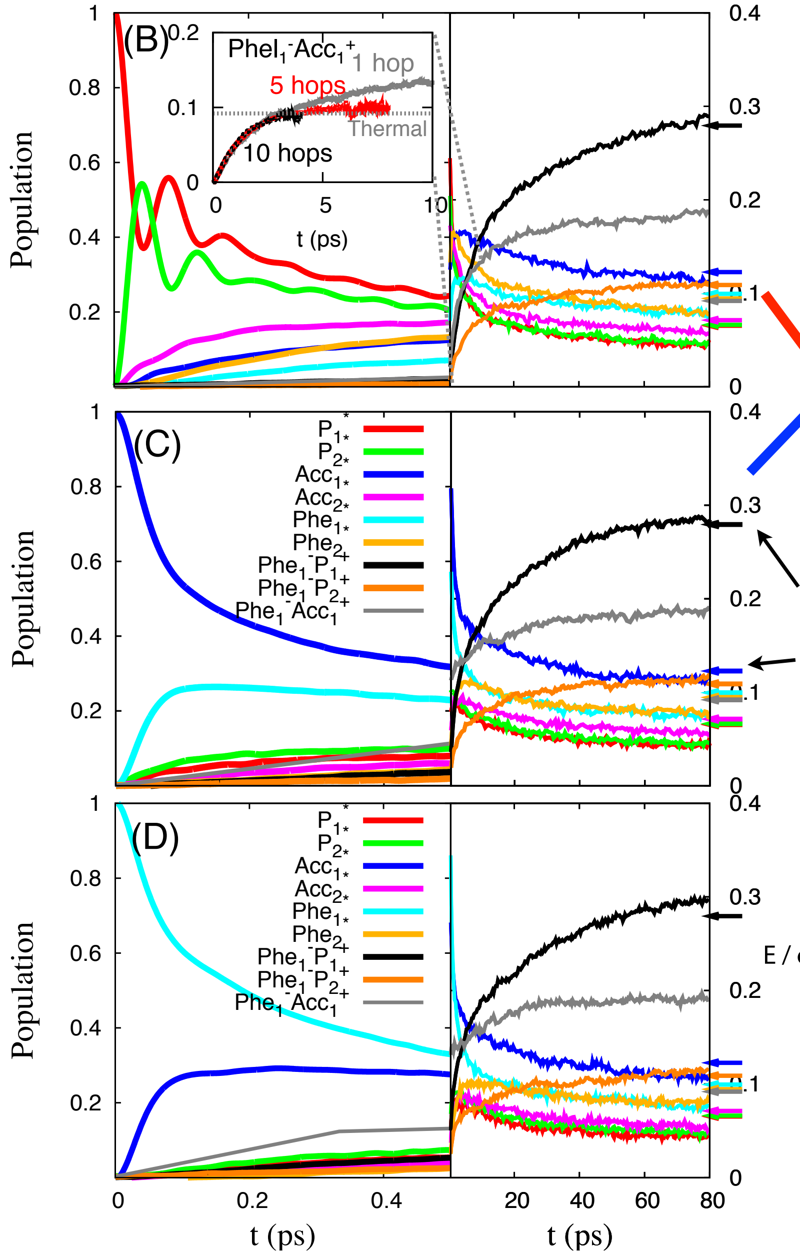

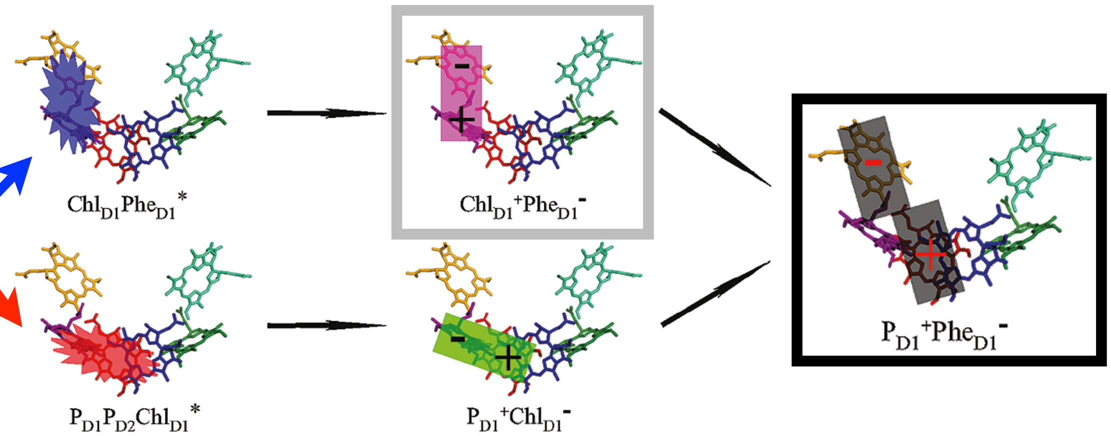

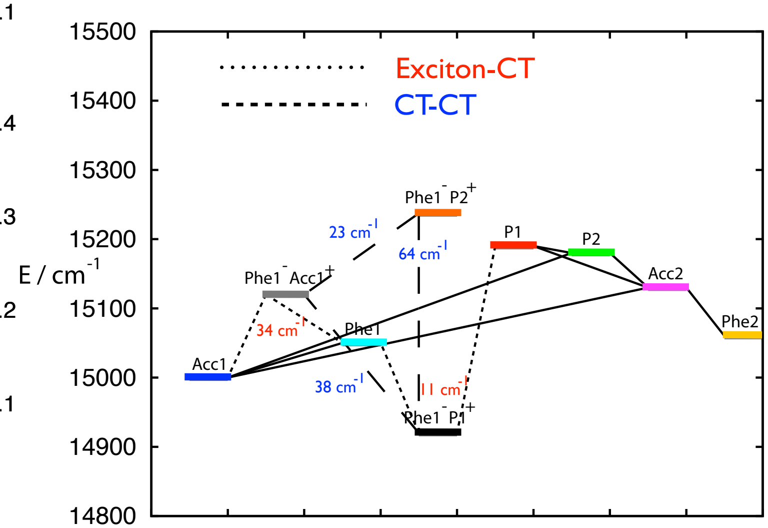

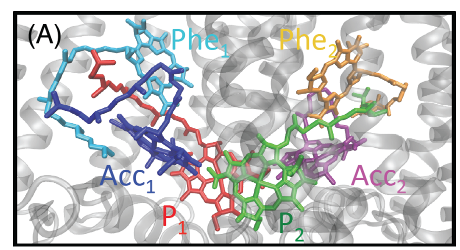

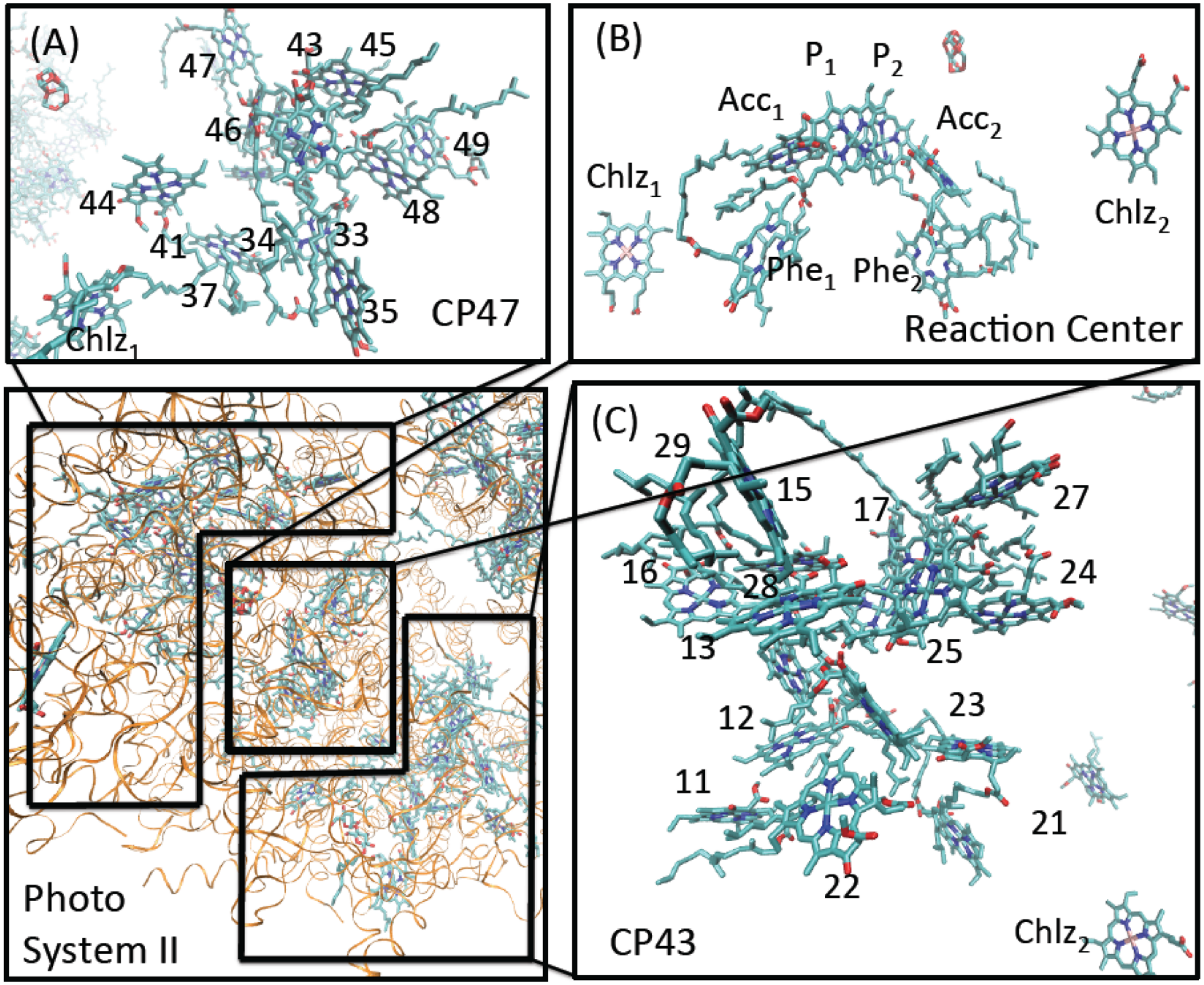

Photo System II
Harvesting,
Photo Protection
and Charge
Separation

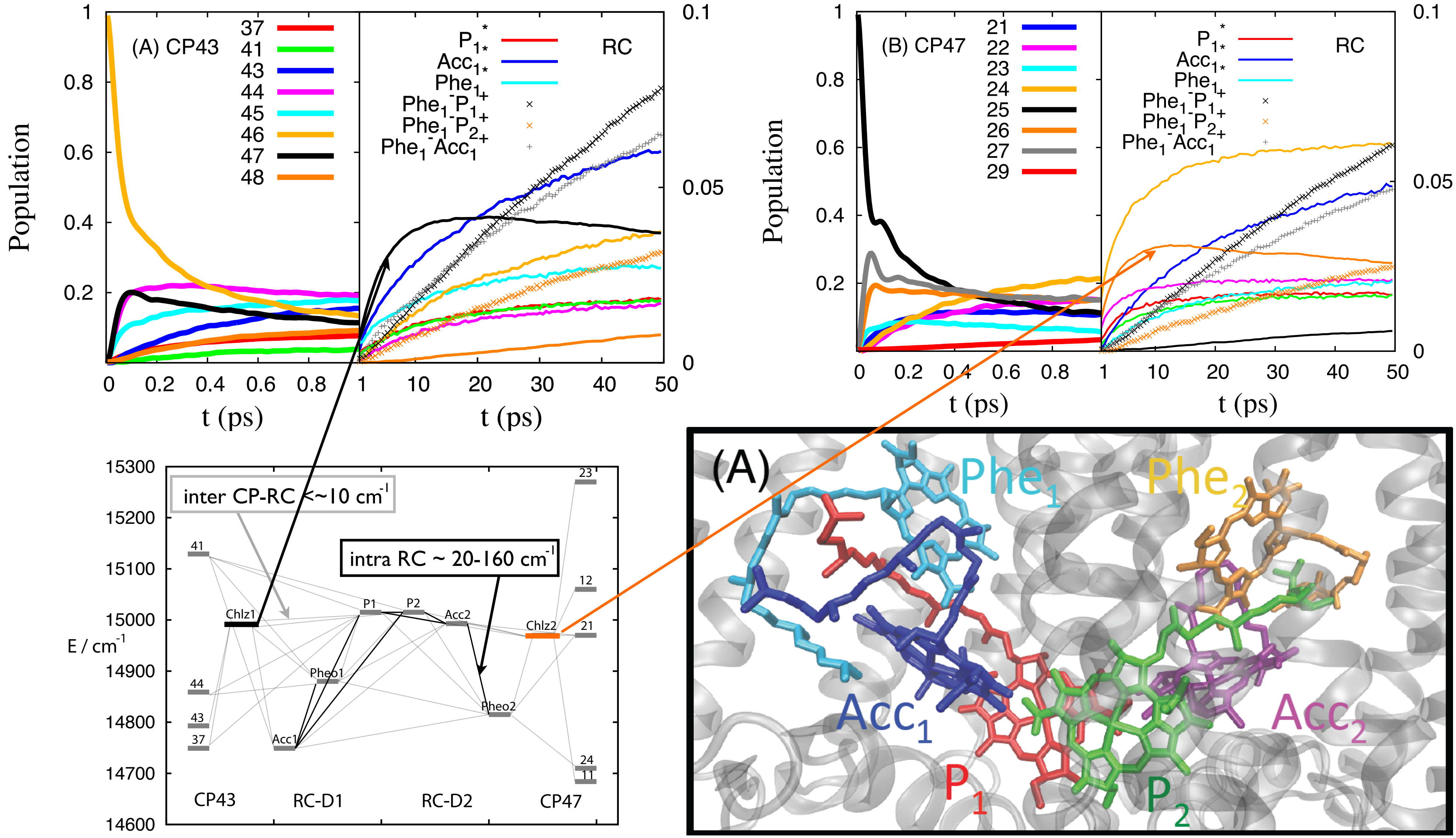

(A) CP43
37
41
43
44
45
46
47
48
Population
t (ps)
RC
(B) CP47
21
22
23
24
25
26
27
29
inter CP-RC <~10 cm-1
intra RC ~ 20-160 cm-1
E / cm-1
Chlz1
P1
P2
Acc2
Chlz2
Pheo1
Pheo2
Acc1
CP43
RC-D1
RC-D2
CP47
(A)
Phe1
Phe2
Acc1
Acc2
P1
P2

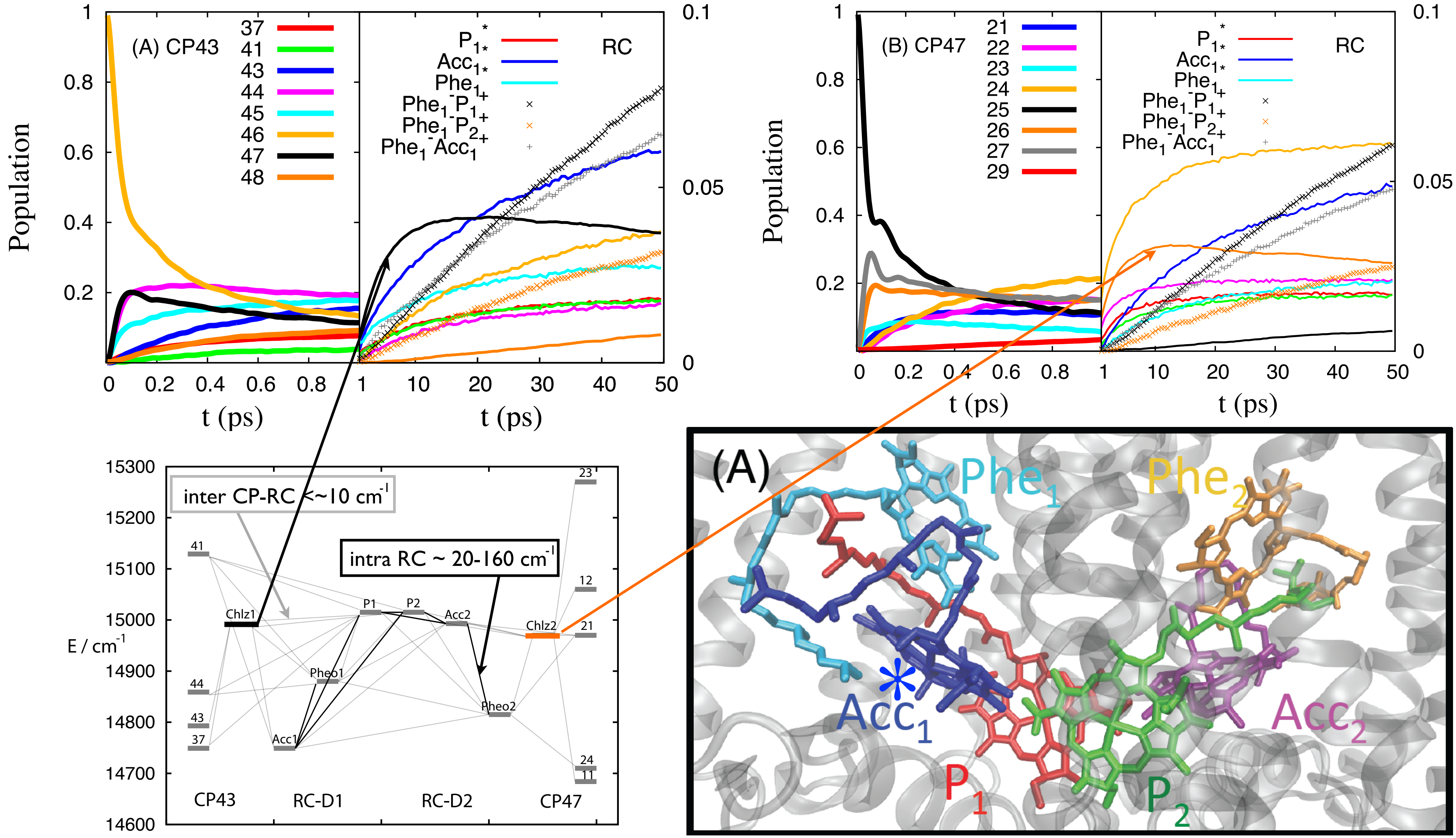

(A) CP43
37
41
43
44
45
46
47
48
Population
t (ps)
RC
(B) CP47
21
22
23
24
25
26
27
29
inter CP-RC <~10 cm-1
intra RC ~ 20-160 cm-1
E / cm-1
Chlz1
P1
P2
Acc2
Chlz2
Pheo1
Pheo2
Acc1
CP43
RC-D1
RC-D2
CP47
(A)
Phe1
Phe2
Acc1
Acc2
P1
P2

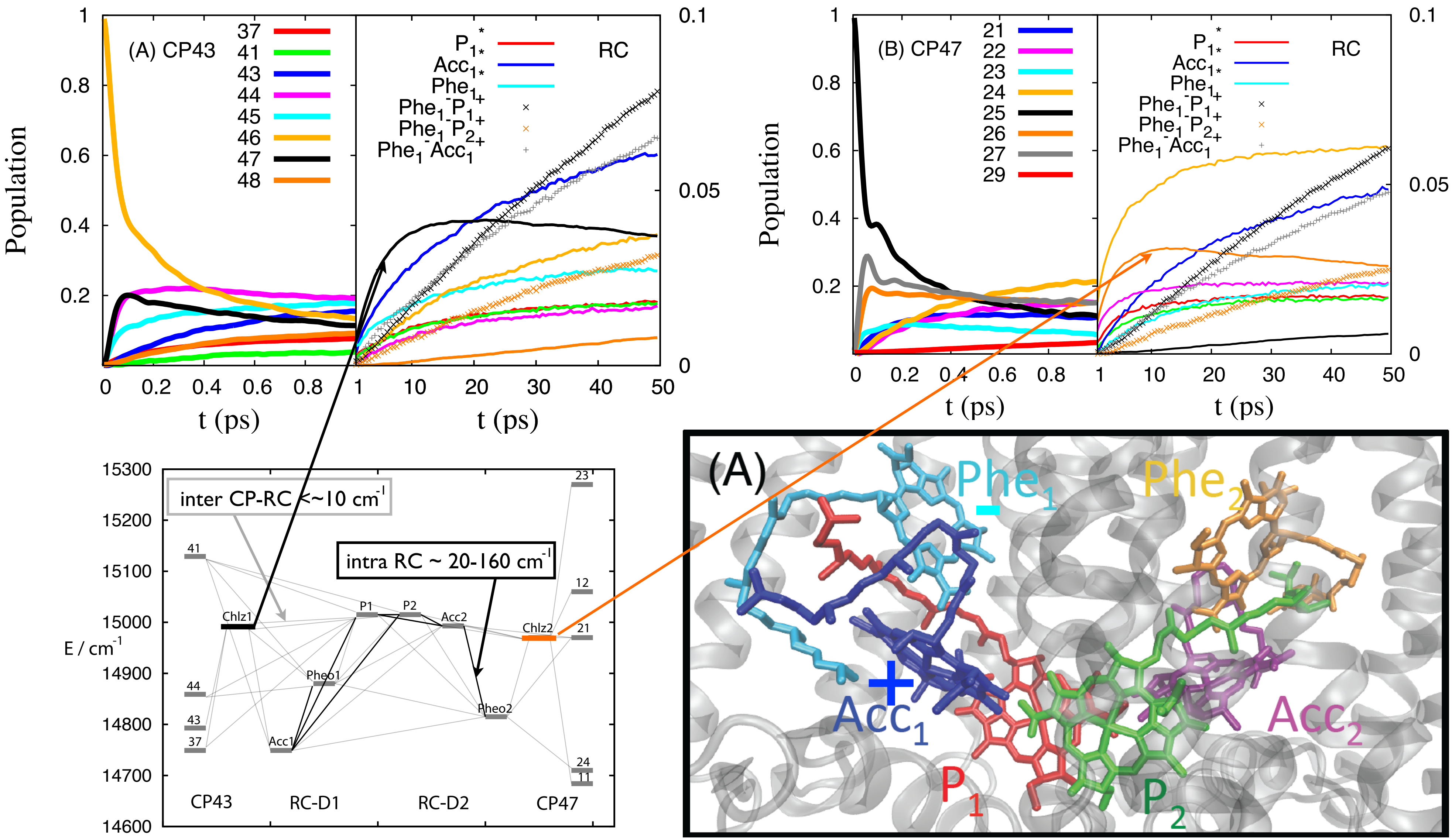

(A) CP43
37
41
43
44
45
46
47
48
Population
t (ps)
P1*
Acc1*
Phe1*
Phe1-P1+
Phe1-P2+
Phe1-Acc1+
RC
(B) CP47
21
22
23
24
25
26
27
29
inter CP-RC <~10 cm-1
intra RC ~ 20-160 cm-1
E / cm-1
Chlz1
P1
P2
Acc2
Chlz2
Pheo1
Pheo2
Acc1
CP43
RC-D1
RC-D2
CP47
(A)
Phe1
Phe2
Acc1
Acc2
P1
P2

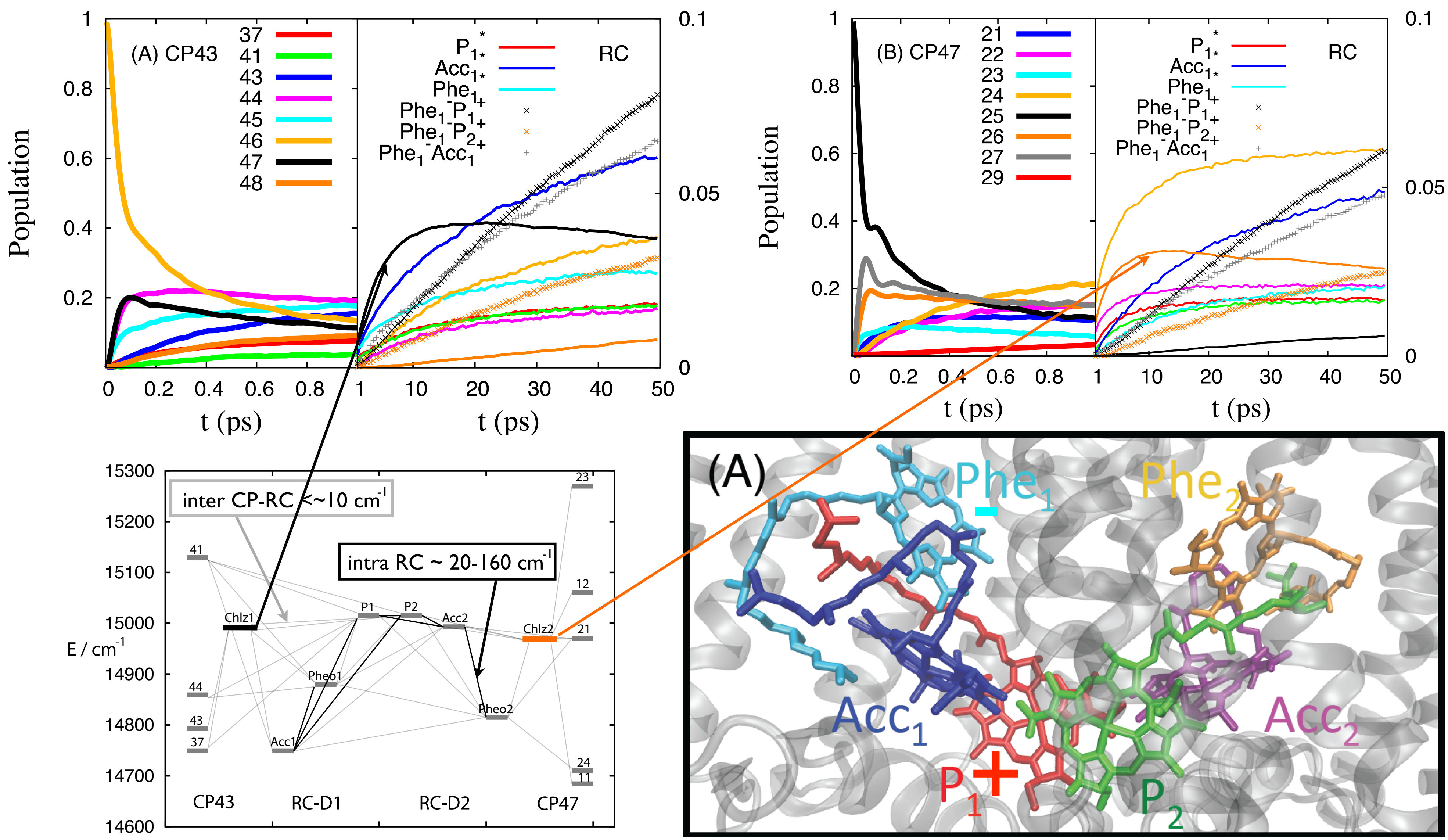
(A) CP43
37
41
43
44
45
46
47
48
Population
t (ps)
RC
(B) CP47
21
22
23
24
25
26
27
29
inter CP-RC <~10 cm-1
intra RC ~ 20-160 cm-1
E / cm-1
Chlz1
Chlz2
P1
P2
Acc1
Acc2
Pheo1
Pheo2
CP43
RC-D1
RC-D2
CP47
(A)
Phe1
Phe2
Acc1
Acc2
P1
P2

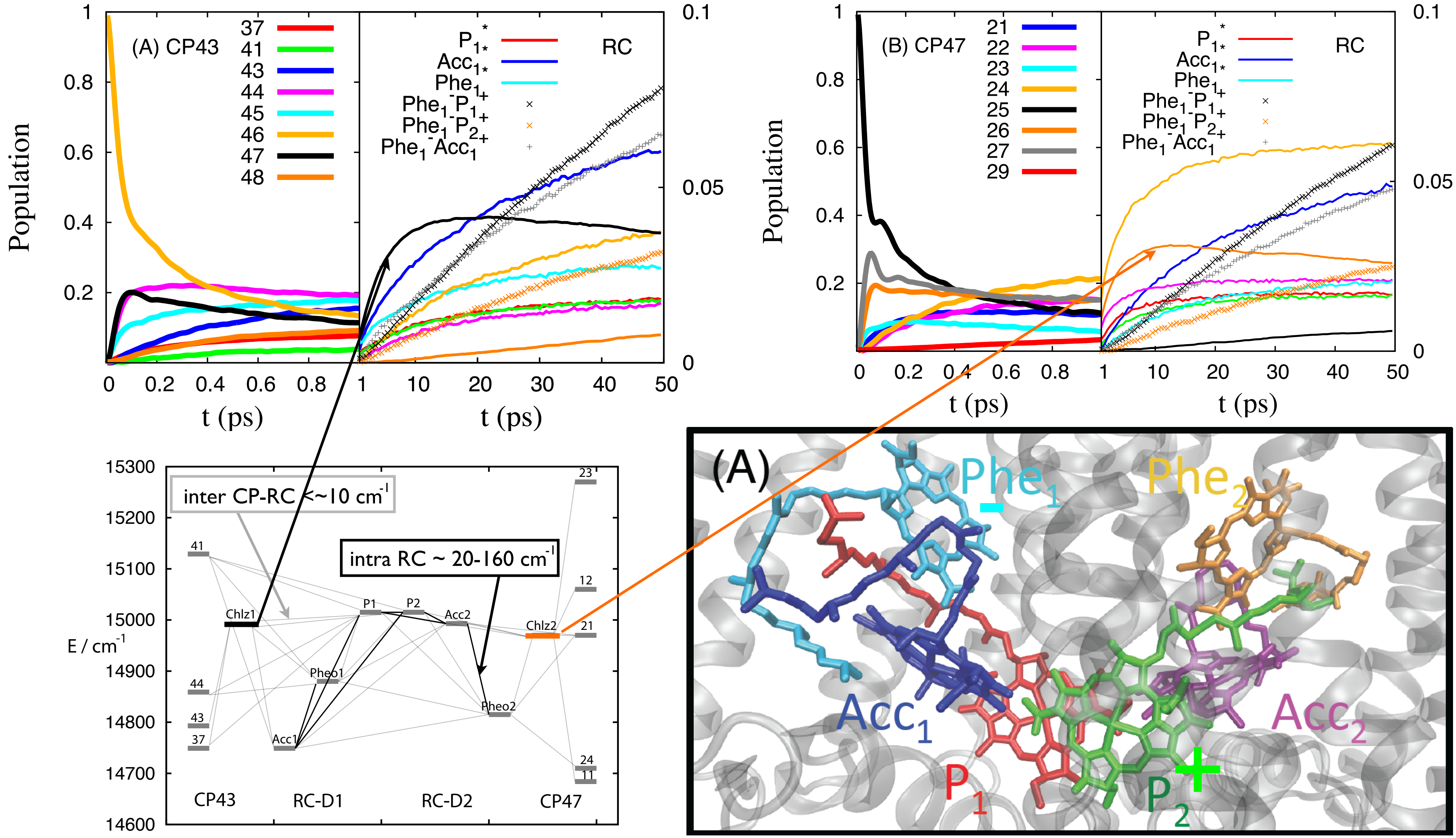

(A) CP43
37
41
43
44
45
46
47
48
Population
t (ps)
RC
(B) CP47
21
22
23
24
25
26
27
29
inter CP-RC <~10 cm-1
intra RC ~ 20-160 cm-1
E / cm-1
Chlz1
P1
P2
Acc2
Chlz2
Pheo1
Pheo2
Acc1
CP43
RC-D1
RC-D2
CP47
(A)
Phe1
Phe2
Acc1
Acc2
P1
P2

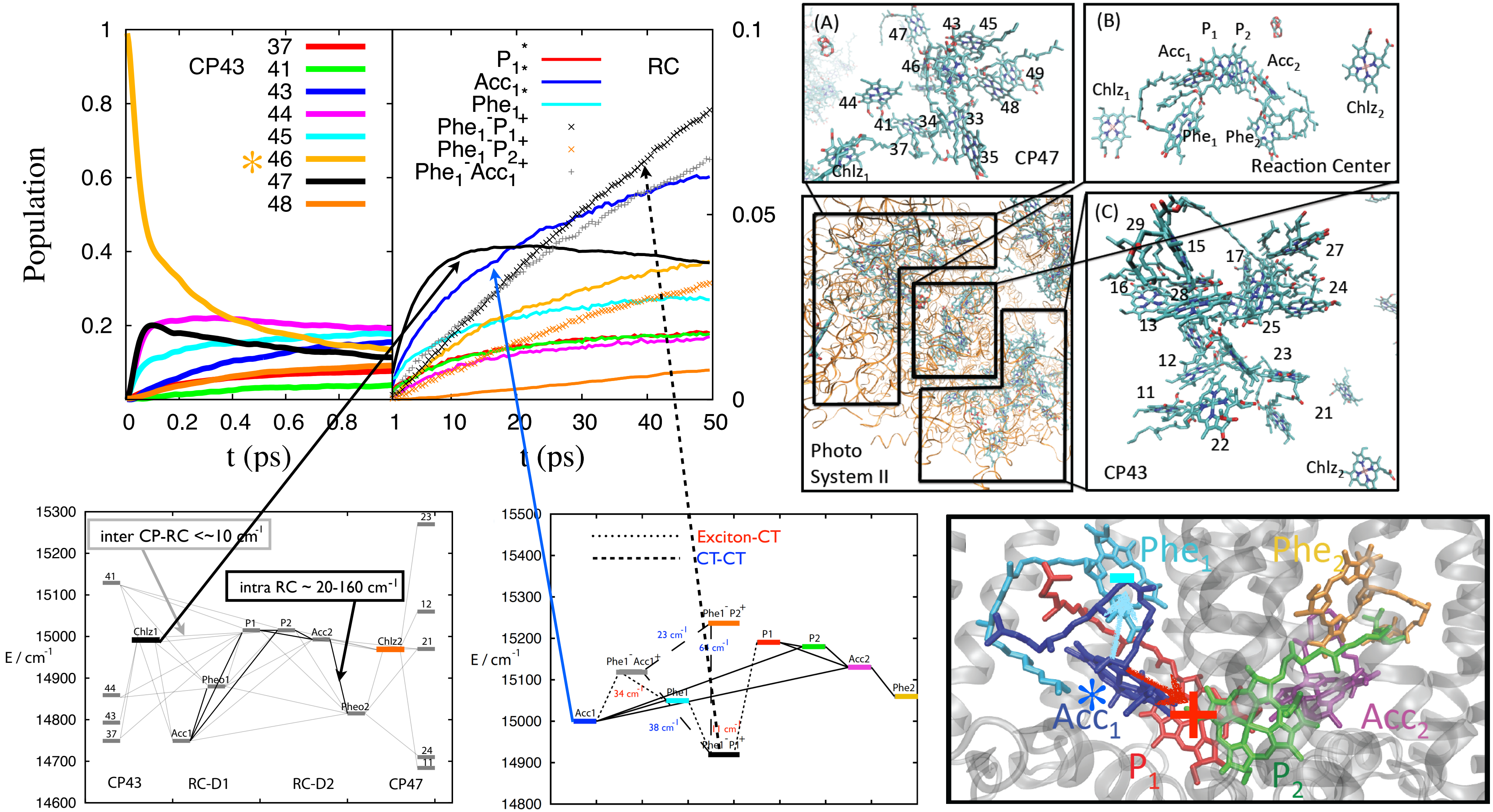

Population
CP43
37
41
43
44
45
46
47
48
RC
P1*
Acc1*
Phe1*
Phe1- P1+
Phe1- P2+
Phe1- Acc1+
t (ps)
t (ps)
(A)
CP47
Chlz1
(B)
P1
P2
Acc1
Acc2
Chlz1
Chlz2
Phe1
Phe2
Reaction Center
(C)
CP43
Chlz2
Photo
System II
E / cm-1
inter CP-RC <~10 cm-1
intra RC ~ 20-160 cm-1
Chlz1
P1
P2
Acc2
Chlz2
Pheo1
Pheo2
Acc1
CP43
RC-D1
RC-D2
CP47
Exciton-CT
CT-CT
Phe1- P2+
Phe1- Acc1+
Phe1
Phe1- P1+
Acc1
Acc2
Phe2
23 cm-1
64 cm-1
34 cm-1
38 cm-1
Phe1
Phe2
Acc1
Acc2
P1
P2

OUTLINE:

(1) Spectral Density Calculations
(2) Excitation Energy Calculations
(3) Dissipative Quantum Dynamics for General Regimes
(4) Issues with Linearized Dynamics of Higher Frequency Modes
(5) Spectra (PC645/HPC645) - Influence of Protonation and "Flickering" Pathways
(6) Quantum Dynamics and Nonlinear Spectroscopy
(7) Coherent State Density Matrix Dynamics (+PLDM)

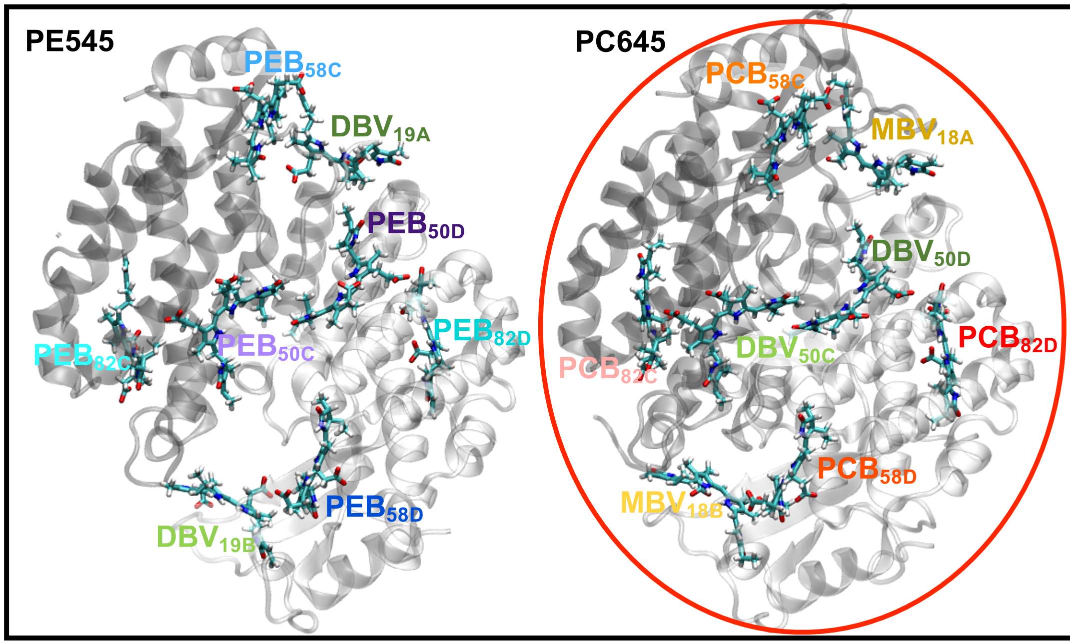

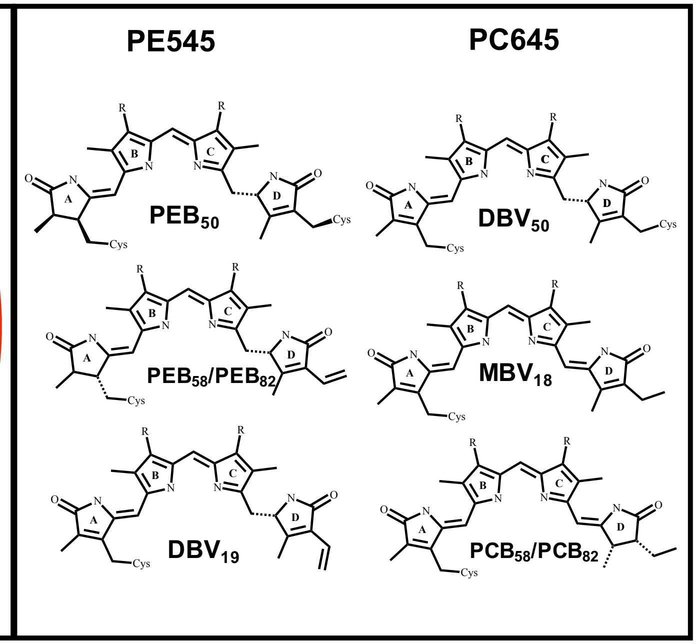

MBV - no aspartic acid coordination

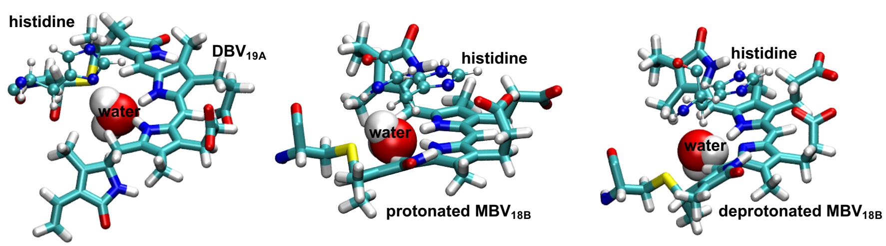

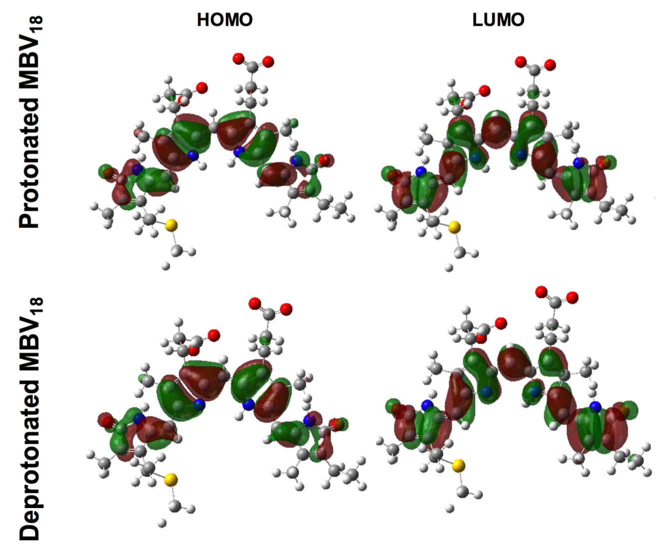

PE545 PC645

M.K. Lee, K. Bravaya, DFC, J. Am. Chem. Soc., 139, 7803-7814 (2017)

Approximate Exciton - Vibronic Lineshapes
Renger & Marcus JCP 116, 9997 (2002)

$$\hat{H}_{ex-vib} = \sum_\alpha \sum_i^{n(\alpha)} c_i^{(\alpha)} \hat{Q}_i^{(\alpha)} |\alpha\rangle\langle\alpha|$$

$$\hat{H} = \hat{H}_{ex} + \hat{H}_{ex-vib} + \hat{H}_{vib} \qquad \hat{H}_{vib} = \sum_\alpha \sum_i^{n(\alpha)} \tfrac{1}{2}[\hat{P}_i^{(\alpha)2} + \omega_i^{(\alpha)2}\hat{Q}_i^{(\alpha)2}]$$

$$\hat{H}_{ex} = \sum_\alpha \epsilon_\alpha |\alpha\rangle\langle\alpha| + \sum_{\alpha\neq\beta} \Delta_{\alpha\beta}|\alpha\rangle\langle\beta| \quad (H_{ex} \text{ eigen states}) \quad |M\rangle = \sum_\alpha a_\alpha^{(M)}|\alpha\rangle \quad \hbar\omega_{LK} = E_L - E_K$$

Linear Absorption $A(\omega) \propto \omega \sum_M |\mu_M|^2 D_M(\omega)$ $\quad D_M(\omega) = \mathrm{Re}\int_0^\infty dt e^{i\omega t}\rho_{M0}(t) \quad \mu_M = \langle 0|\mu|M\rangle = \sum_\alpha a_\alpha^{(M)}\mu_\alpha$

Non-Markovian, 2nd order cumulant Master Equation for reduced density matrix in secular approximation

$$\dot{\rho}_{M0}(t) = -i\omega_{M0}\rho_{M0}(t) - \frac{1}{\hbar^2}\sum_{KL}\int_0^t d\tau C_{MKKL}(\tau)e^{i\omega_{LK}\tau}\rho_{L0}(t) \qquad C_{MNKL}(t) = \sum_\alpha\sum_\beta a_\alpha^{(M)}a_\alpha^{(N)}a_\beta^{(K)}a_\beta^{(L)}\langle\delta\epsilon^\alpha(t)\delta\epsilon^\beta(0)\rangle$$

$$\langle\delta\epsilon^\alpha(t)\delta\epsilon^\alpha(0)\rangle = \langle e^{iH_{vib}^{(\alpha)}t/\hbar}\delta\epsilon^\alpha e^{-iH_{vib}^{(\alpha)}t/\hbar}\delta\epsilon^\alpha\rangle = \frac{\hbar}{\pi}\int_0^\infty d\omega J^{(\alpha)}(\omega)[(n(\omega)+1)e^{-i\omega t} + n(\omega)e^{i\omega t}]$$

$$\rho_{M0}(t) = \exp[-i\omega_{M0}t - \frac{1}{\hbar^2}\sum_K\int_0^t d\tau(t-\tau)C_{MKKM}(\tau)e^{i\omega_{MK}\tau}] \qquad n(\omega) = 1/(e^{\beta\hbar\omega}-1)$$

$$D_M(\omega) = \mathrm{Re}\int_0^\infty dt e^{i(\omega-\tilde{\omega}_{M0})t}e^{[G_M(t)-G_M(0)]}e^{-t/\tau_M} \qquad \tilde{C}_{MK}(\omega_{MK}) = \int_0^\infty d\tau C_{MKKM}(\tau)e^{i\omega_{MK}\tau}$$

$$\tilde{\omega}_{M0} = \omega_{M0} - E_\lambda^M/\hbar + \sum_{K\neq M}\mathrm{Im}\tilde{C}_{MK}(\omega_{MK}) \qquad E_\lambda^M = \frac{1}{\pi}\int_0^\infty d\omega J^{MM}(\omega)/\omega$$

$$\mathrm{Re}\tilde{C}_{MK}(\omega) = \frac{1}{\hbar}[(1+n(\omega))J^{MK}(\omega) + n(-\omega)J^{MK}(-\omega)] \qquad J^{MK}(\omega) = \sum_\alpha |a_\alpha^{(M)}|^2|a_\alpha^{(K)}|^2 J^{(\alpha)}(\omega)$$

$$\tau_M^{-1} = \frac{1}{2}\sum_K k_{M\to K} \qquad k_{M\to K} = 2\mathrm{Re}\tilde{C}_{MK}(\omega_{MK}) \qquad G_M(t) = \frac{\hbar}{\pi}\int_0^\infty d\omega(J^{MM}(\omega)/\omega^2)[(n(\omega)+1)e^{-i\omega t} + n(\omega)e^{i\omega t}]$$

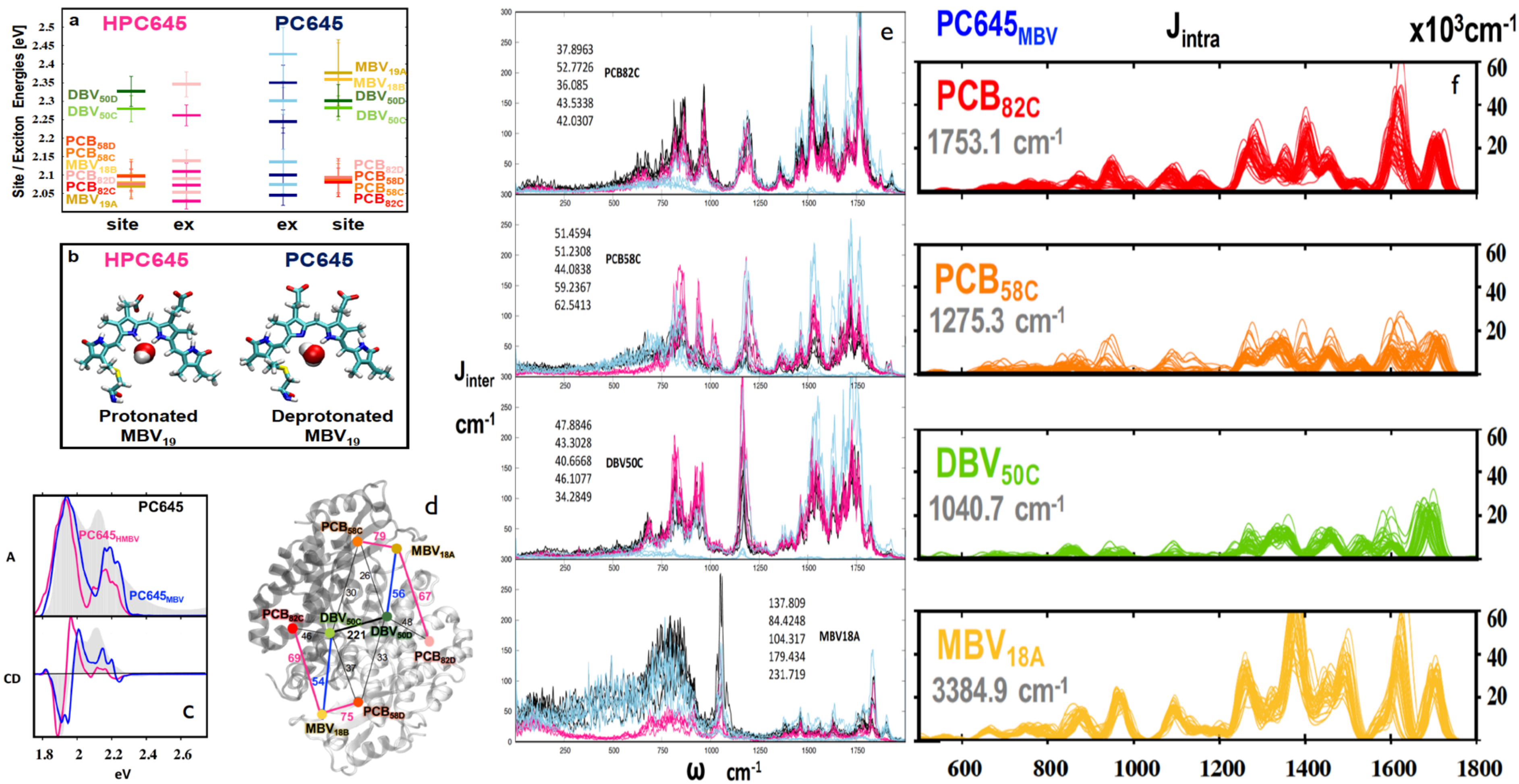

a
HPC645
PC645
Site / Exciton Energies [eV]
DBV50D
DBV50C
PCB58D
PCB58C
MBV18B
PCB82D
PCB82C
MBV19A
MBV19A
MBV18B
DBV50D
DBV50C
PCB82D
PCB58D
PCB58C
PCB82C
site
ex
ex
site
b
HPC645
PC645
Protonated MBV19
Deprotonated MBV19
PC645
PC645HMBV
PC645MBV
A
CD
C
eV
d
PCB58C
MBV18A
PCB82C
DBV50C
DBV50D
PCB82D
MBV18B
PCB58D
e
37.8963
52.7726
36.085
43.5338
42.0307
PCB82C
51.4594
51.2308
44.0838
59.2367
62.5413
PCB58C
47.8846
43.3028
40.6668
46.1077
34.2849
DBV50C
137.809
84.4248
104.317
179.434
231.719
MBV18A
Jinter cm-1
ω cm-1
PC645MBV
Jintra
x10³cm-1
f
PCB82C
1753.1 cm-1
PCB58C
1275.3 cm-1
DBV50C
1040.7 cm-1
MBV18A
3384.9 cm-1

OUTLINE:

(1) Spectral Density Calculations
(2) Excitation Energy Calculations
(3) Dissipative Quantum Dynamics for General Regimes
(4) Issues with Linearized Dynamics of Higher Frequency Modes
(5) Spectra (PC645/HPC645) - Influence of Protonation and "Flickering" Pathways
(6) Quantum Dynamics and Nonlinear Spectroscopy
(7) Coherent State Density Matrix Dynamics (+PLDM)

Ultrafast Nonlinear Spectroscopy

$$\hat{H}_{tot}(t) = \hat{H} + \hat{H}'(t) \qquad \hat{H}'(t) = -\hat{\boldsymbol{\mu}} \cdot \boldsymbol{E}(\boldsymbol{r}, t)$$

$$P^{(n)} = \mathrm{Tr}[\hat{\mu}\hat{\rho}^{(n)}] \qquad \hat{\rho}^{(n)} = \left[\hat{\mu}, \hat{\rho}^{(n-1)}\right]$$

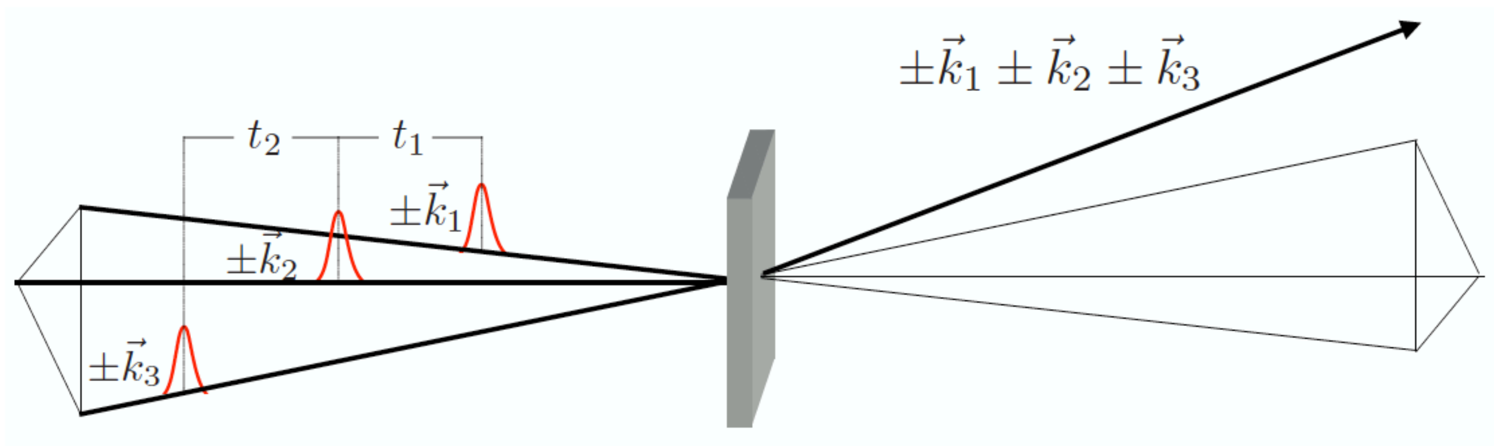

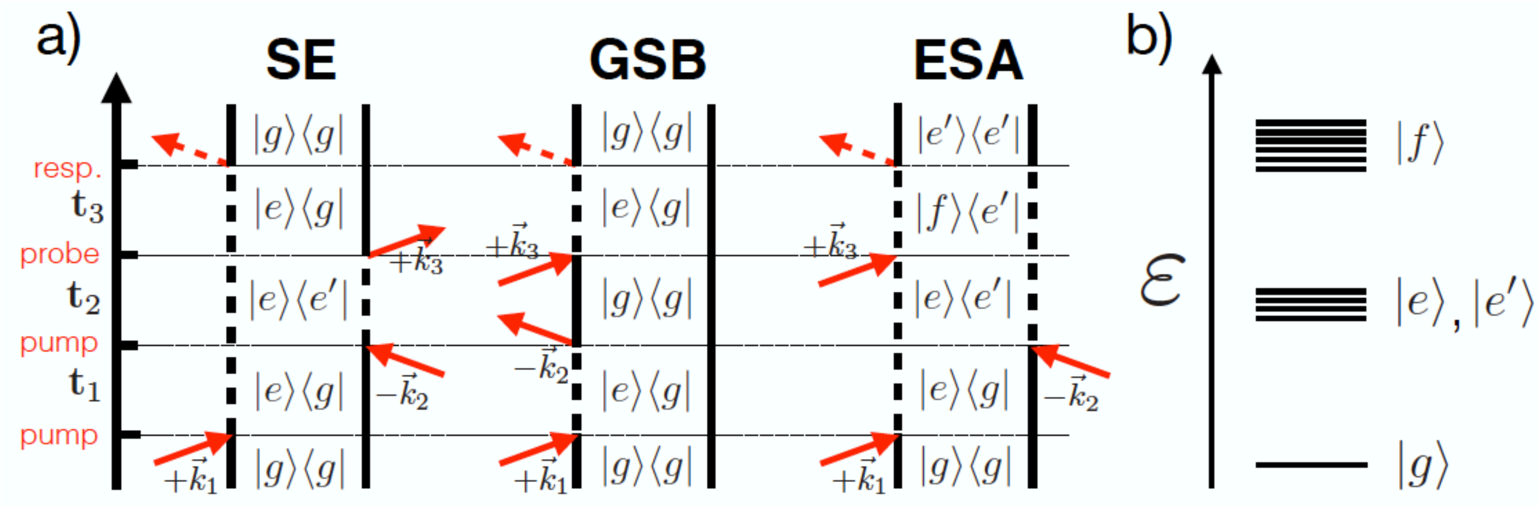

$$P^{(1)}(t) = \int_0^\infty dt_1 \; R^{(1)}(t_1) \; E(t - t_1) \quad R^{(1)}(t_1) = i\mathrm{Tr}[\hat{\mu}(t_1)\hat{\mu}^\times(0)\hat{\rho}(0)]$$

$$\hat{\mu}(t) = e^{+i\hat{H}t}\hat{\mu}e^{-i\hat{H}t}$$

$$P^{(3)}(t) = \int_0^\infty dt_3 \int_0^\infty dt_2 \int_0^\infty dt_1 \; R^{(3)}(t_3, t_2, t_1) \times E(t - t_3)E(t - t_3 - t_2)E(t - t_3 - t_2 - t_1)$$

$$\hat{\mu}^\times(t) \bullet = [\hat{\mu}(t), \bullet]$$

$$\begin{aligned} R^{(3)}(t_3, t_2, t_1) &= (i)^3 \langle \hat{\mu}(t_3 + t_2 + t_1) \; \hat{\mu}^\times(t_2 + t_1) \; \hat{\mu}^\times(t_1) \; \hat{\mu}^\times(0) \rangle \\ &= (i)^3 \, \mathrm{Tr}[\hat{\mu}(t_3 + t_2 + t_1) \; \hat{\mu}^\times(t_2 + t_1) \; \hat{\mu}^\times(t_1) \; \hat{\mu}^\times(0)\hat{\rho}(0)] \end{aligned}$$

$$R^{(3)}(t_3,t_2,t_1) = (i)^3 \sum_{n_{t_3}} \left(\prod_{k=N_2+N_1+1}^{N_3+N_2+N_1} \int d\bar{R}_k \frac{d\bar{P}_k}{2\pi} \right) \sum_{n_{t_2},n'_{t_2}} \int d\bar{R}_{N_2+N_1} \frac{d\bar{P}_{N_2+N_1}}{2\pi} dx_{t_2} dp_{t_2} dx'_{t_2} dp'_{t_2} \; G_{t_2} G'_{t_2}$$

$$\times \left(\mu\rho^{(3)}\right)_{n_{t_3} n_{t_3}} \prod_{k=N_2+N_1+1}^{N_3+N_2+N_1-1} \delta\left(\frac{\bar{P}_{k+1}-\bar{P}_k}{\epsilon} - F_k \right) \prod_{k=N_2+N_1+1}^{N_3+N_2+N_1} \delta\left(\frac{\bar{R}_k - \bar{R}_{k-1}}{\epsilon} - \frac{\bar{P}_k}{M} \right) \delta\left(\bar{P}_{N_2+N_1+1} - \bar{P}_{N_2+N_1} \right)$$

$$\times \delta\left(\frac{\bar{R}_{N_2+N_1} - \bar{R}_{N_2+N_1-1}}{\epsilon} - \frac{\bar{P}_{N_2+N_1}}{M} \right) \left(\prod_{k=N_1+1}^{N_2+N_1-1} \int d\bar{R}_k \frac{d\bar{P}_k}{2\pi} \right) \sum_{n_{t_1},n'_{t_1}} \int d\bar{R}_{N_1} \frac{d\bar{P}_{N_1}}{2\pi} dx_{t_1} dp_{t_1} dx'_{t_1} dp'_{t_1} \; G_{t_1} G'_{t_1}$$

$$\times \left(\mu^{\times}\rho^{(2)}\right)_{n_{t_2} n'_{t_2}} \prod_{k=N_1+1}^{N_2+N_1-1} \delta\left(\frac{\bar{P}_{k+1}-\bar{P}_k}{\epsilon} - F_k \right) \prod_{k=N_1+1}^{N_2+N_1} \delta\left(\frac{\bar{R}_k - \bar{R}_{k-1}}{\epsilon} - \frac{\bar{P}_k}{M} \right) \delta\left(\bar{P}_{N_1+1} - \bar{P}_{N_1} \right)$$

$$\times \delta\left(\frac{\bar{R}_{N_1} - \bar{R}_{N_1-1}}{\epsilon} - \frac{\bar{P}_{N_1}}{M} \right) \left(\prod_{k=1}^{N_1-1} \int d\bar{R}_k \frac{d\bar{P}_k}{2\pi} \right) \sum_{n_0,n'_0} \int d\bar{R}_0 dx_0 dp_0 dx'_0 dp'_0 \; G_{t_0} G'_{t_0}$$

$$\times \left(\mu^{\times}\rho^{(1)}\right)_{n_{t_1} n'_{t_1}} \prod_{k=1}^{N_1-1} \delta\left(\frac{\bar{P}_{k+1}-\bar{P}_k}{\epsilon} - F_k \right) \prod_{k=1}^{N_1} \delta\left(\frac{\bar{R}_k - \bar{R}_{k-1}}{\epsilon} - \frac{\bar{P}_k}{M} \right) \left(\mu^{\times}\rho^{(0)}\right)_W^{n_0 n'_0} (\bar{R}_0, \bar{P}_1)$$

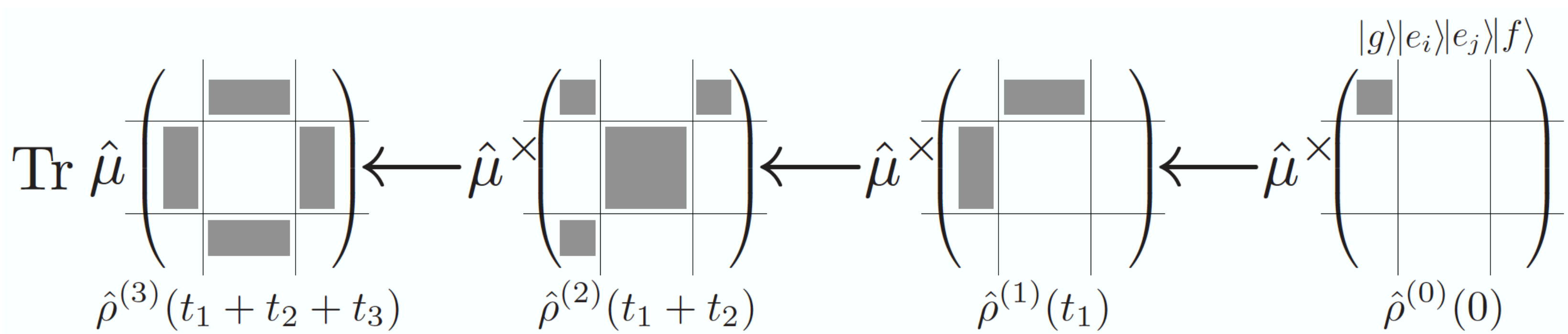

$$\hat{H}_0 = \sum_{i,j=0}^{1} \epsilon_{ij} |ij\rangle\langle ij| + \sum_{ij\in 01,10} \Delta_{ij,ji} |ij\rangle\langle ji| + \sum_{ij\in 01,10,11} \sum_{m=1}^{M} c_{ij}^m \hat{R}_m |ij\rangle\langle ij| + \sum_{m=1}^{M} \frac{1}{2}\left(\hat{P}_m^2 + \omega_m^2 \hat{R}_m^2\right) \hat{\mathbb{1}}$$

$$J(\omega) = 2\lambda \frac{\omega/\omega_c}{(1+(\omega/\omega_c)^2)} = \frac{\pi}{2}\sum_i \frac{c_i^2}{\omega_i}\delta(\omega-\omega_i) \qquad (\omega_c^{-1} = 300 \text{ fs})$$

Coupled Dimer

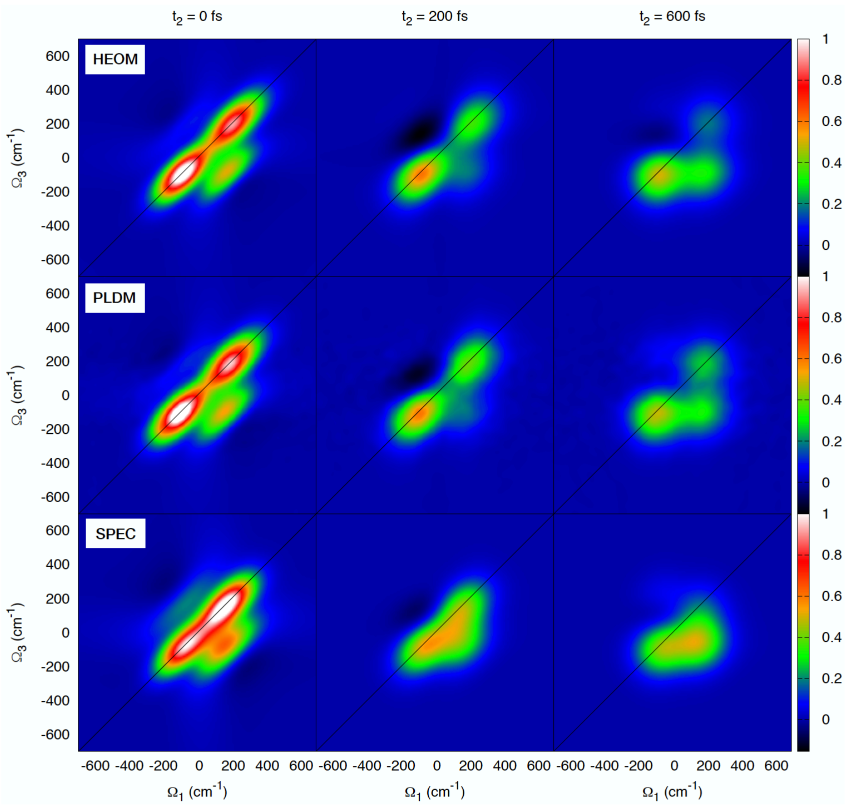

Figure 4: Comparison of HEOM, PLDM, and SPECTRON 2DES at different t_2 times for a coupled dimer at 300 K with $\epsilon_{10} - \epsilon_{01} = 100$ cm^{-1}, $\Delta_{01,10} = 100$ cm^{-1}, and $\mu_{00,01}/\mu_{00,10} = -0.2$. The bath has a cutoff frequency of $\omega_c = 18$ cm^{-1} and a reorganization energy of $\lambda = 50$ cm^{-1}. The PLDM calculation presented here is averaged over only 60,000 trajectories initialized from each element of $(\mu^\times \rho^{(0)})$ with nonzero amplitude.

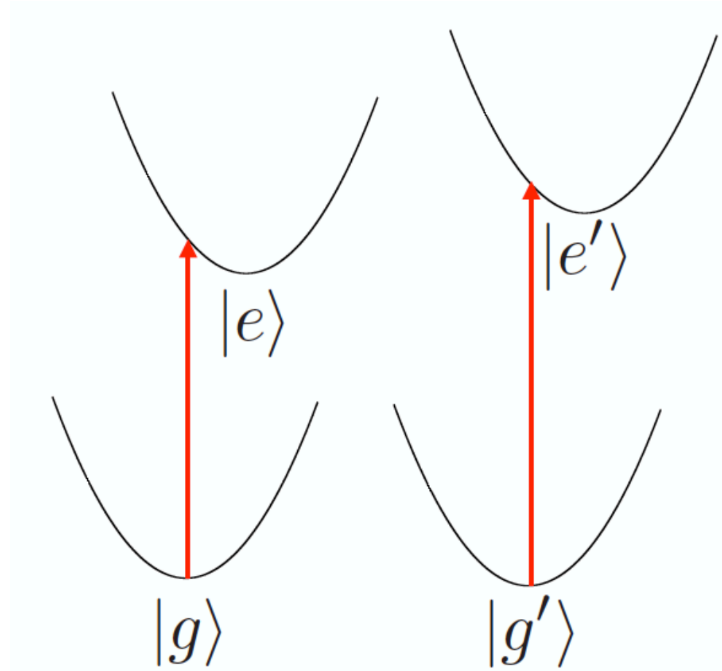

J. Provazza, F. Segatta, M. Garavelli, D.F. Coker
J. Chem. Theor. Comput. 14, 856-866 (2018)

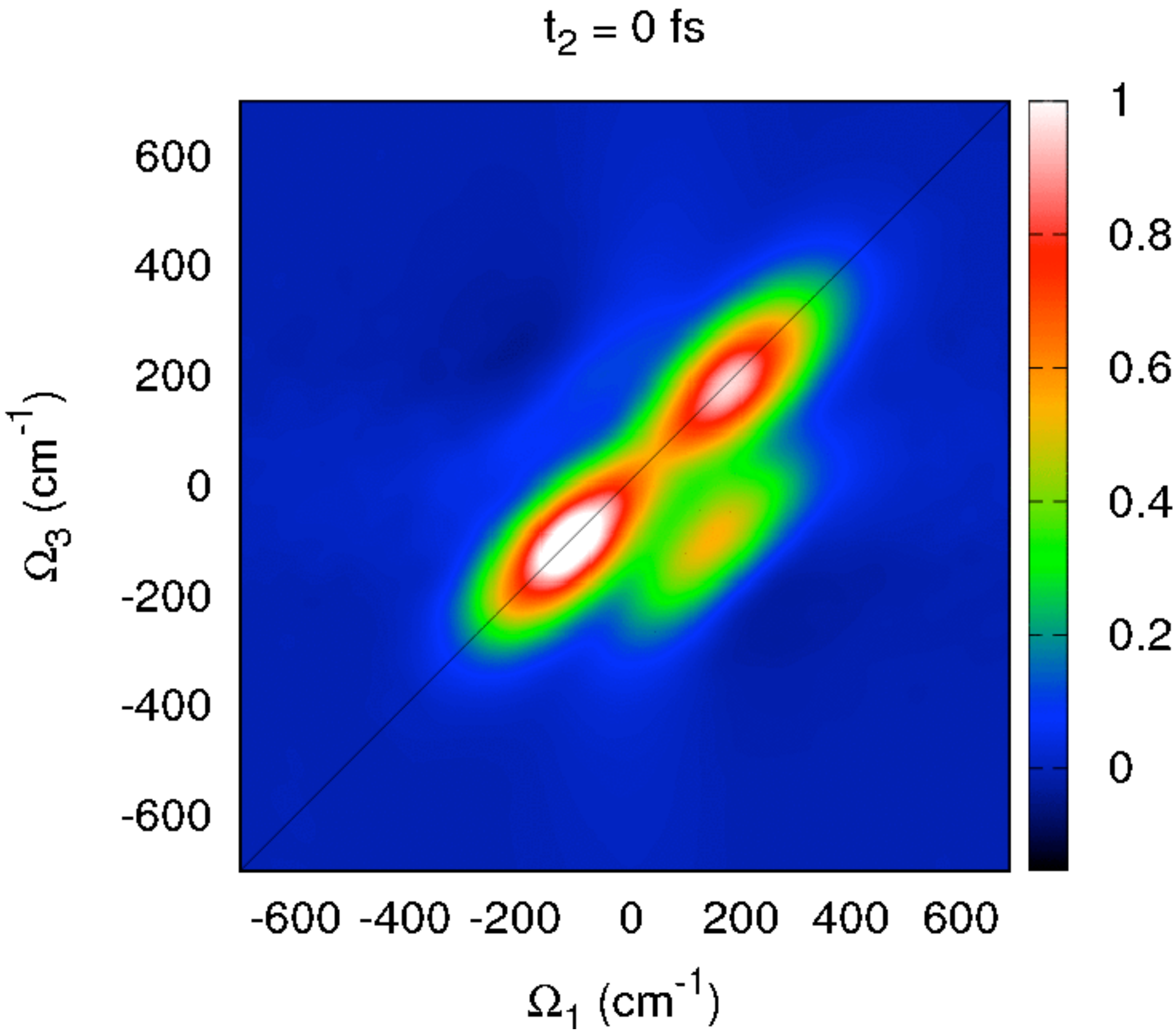

t2 = 0 fs
600
400
200
0
-200
-400
-600
Ω3 (cm-1)
-600 -400 -200 0 200 400 600
Ω1 (cm-1)
1
0.8
0.6
0.4
0.2
0

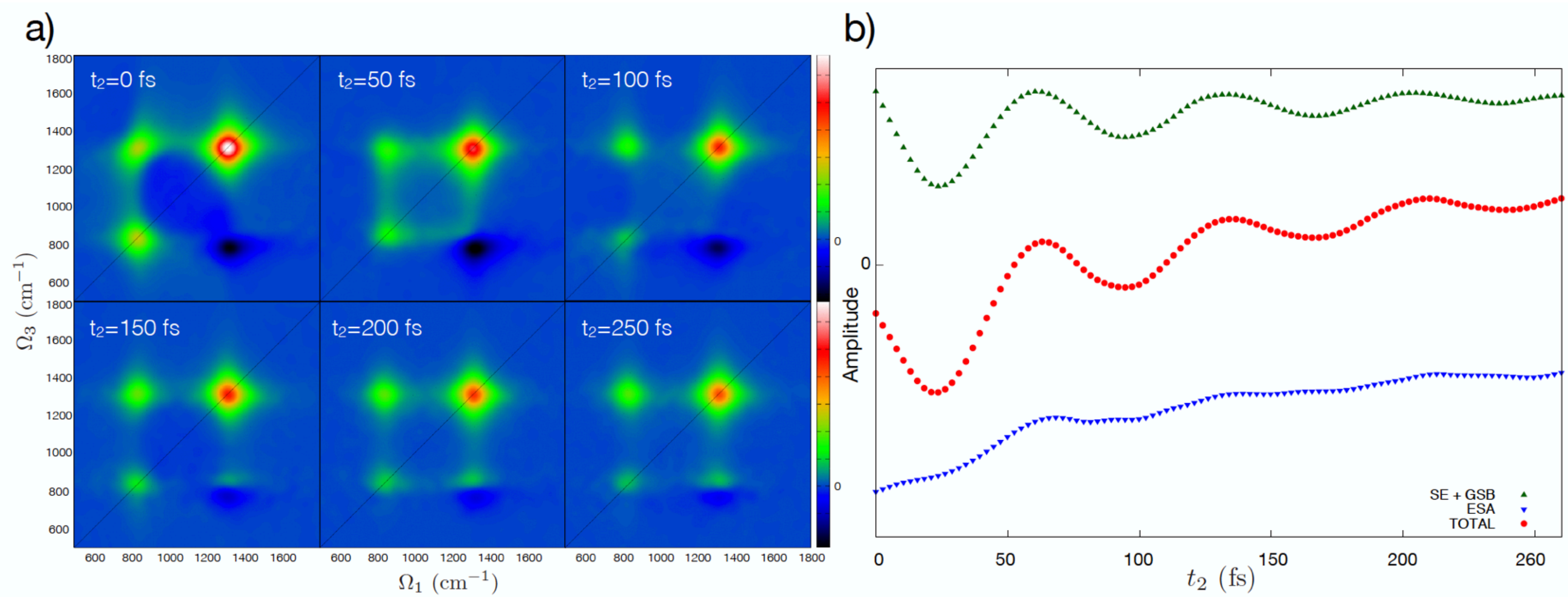

Figure 5: 2DES for a coupled dimer at 300 K with $\epsilon_{10} - \epsilon_{01} = 200$ cm^{-1}, $\Delta_{01,10} = 200$ cm^{-1}, and $\mu_{00,01}/\mu_{00,10} = 2.4$. The spectral density parameters employed were $\lambda = 50$ cm^{-1}, $\omega_c = 200$ cm^{-1}. Panel a) shows the spectra for varying t_2 waiting time. Panel b) shows the amplitude of the energy transfer-related cross-peak at $(\Omega_1, \Omega_3) \approx (1325$ cm$^{-1}, 875$ cm$^{-1})$. The amplitude evolves with coherent oscillations resonant with the energy difference between exciton states.

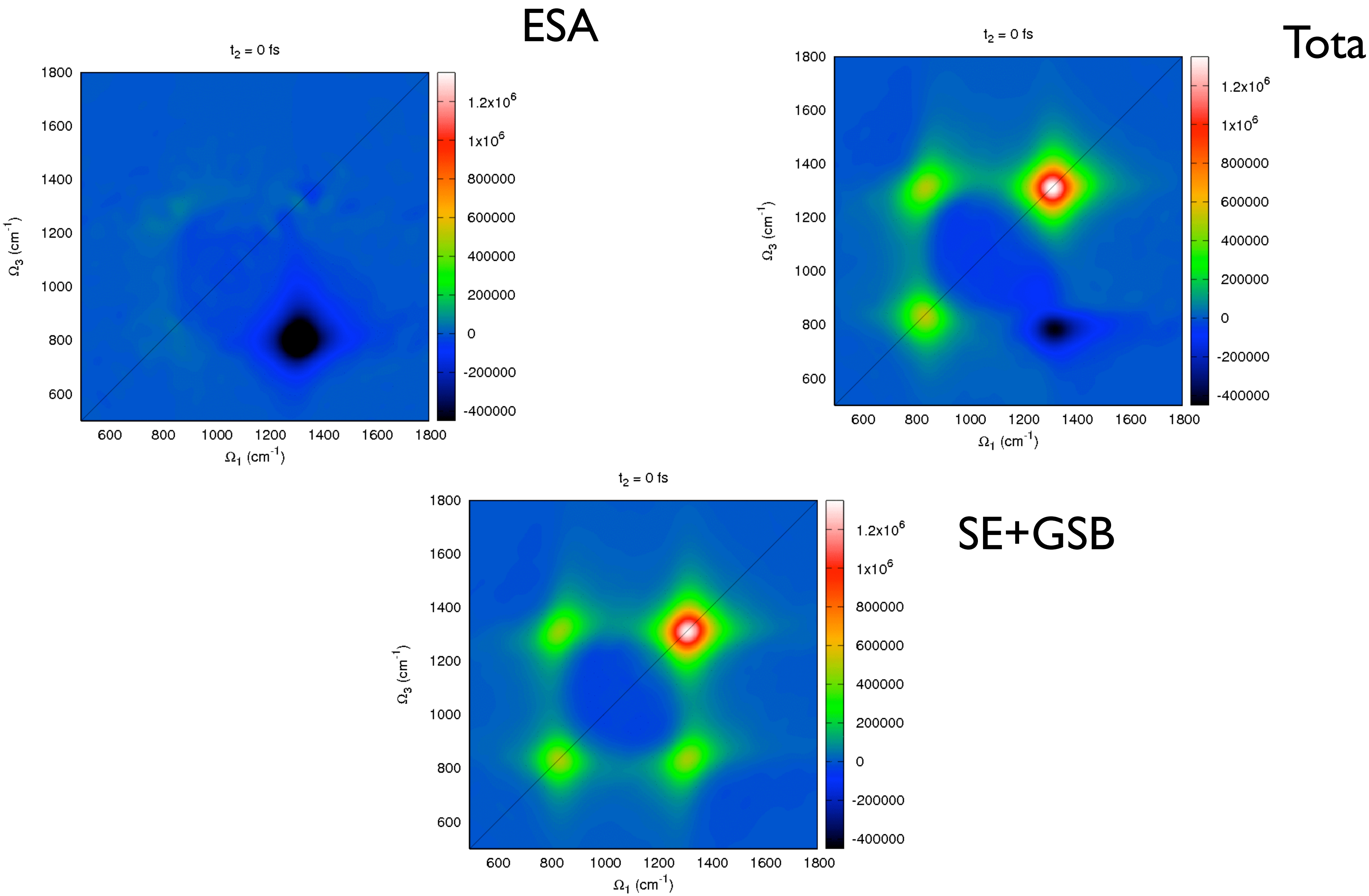
ESA
Total
SE+GSB
t_2 = 0 fs
Ω_1 (cm^{-1})
Ω_3 (cm^{-1})
600
800
1000
1200
1400
1600
1800
1.2x10^6
1x10^6
800000
600000
400000
200000
0
-200000
-400000

$$\hat{H}_0 = \sum_{n_u=0}^{\infty} \epsilon_g^{(n_u)} |g_{n_u}\rangle\langle g_{n_u}| + \sum_{n_s=0}^{\infty} \epsilon_e^{(n_s)} |e_{n_s}\rangle\langle e_{n_s}| + \sum_{n_s=0}^{\infty}\sum_{m=1}^{M_c} c_m \hat{R}_m |e_{n_s}\rangle\langle e_{n_s}| + \sum_{m=1}^{M_c} \frac{1}{2}\left(\hat{P}_m^2 + \omega_m^2 \hat{R}_m^2\right)\hat{\mathbb{1}}$$

$$\epsilon_g^{(n_u)} = \epsilon_g + \left(n_u + \tfrac{1}{2}\right)\Omega_d \qquad \epsilon_e^{(n_s)} = \epsilon_e - \Lambda_d + \left(n_s + \tfrac{1}{2}\right)\Omega_d$$

$$S = 0.45 \qquad S = \Lambda_d/\Omega_d$$

$$\Lambda_d = \frac{c_d^2}{2\Omega_d^2}$$

JCTC 14, 856-866 (2018)

$$\langle e_{n_s}|\hat{\mu}|g_{m_u}\rangle = \mu_{eg}\langle n_s|m_u\rangle = \mu_{eg}\int dx\ \langle n|x - c/\Omega_d^2\rangle\langle x|m\rangle$$

Vibronic Monomer

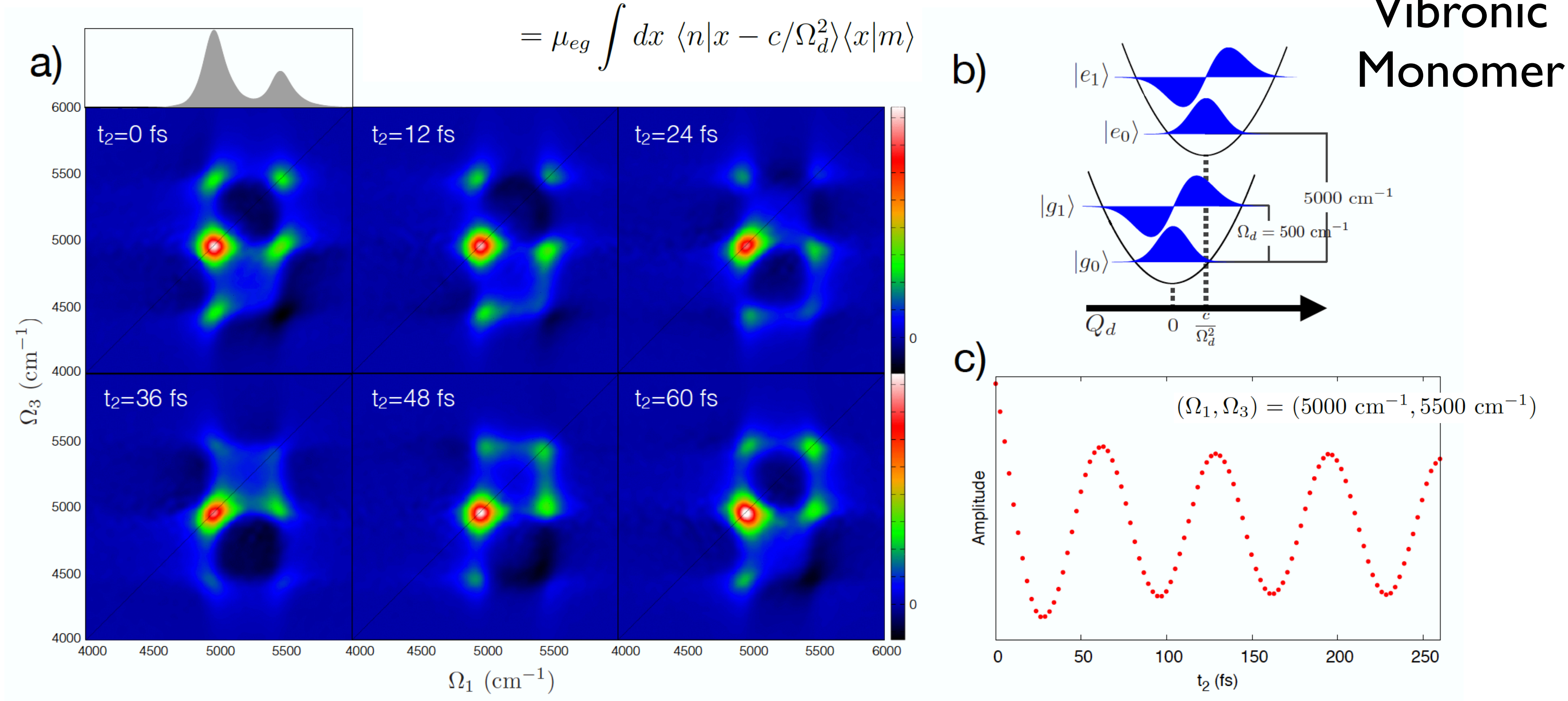

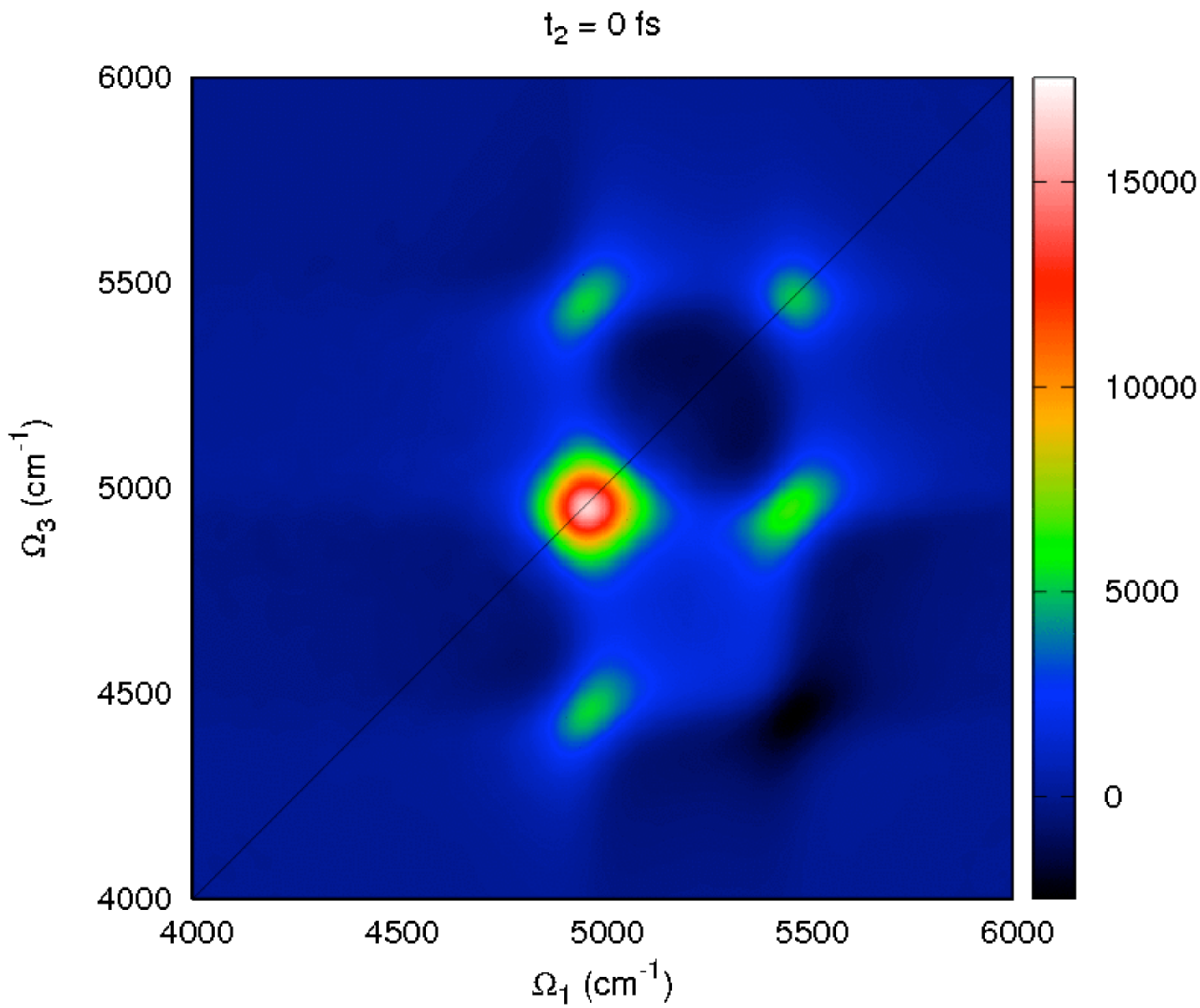

t2 = 0 fs
6000
5500
5000
4500
4000
4000
4500
5000
5500
6000
Ω3 (cm-1)
Ω1 (cm-1)
15000
10000
5000
0

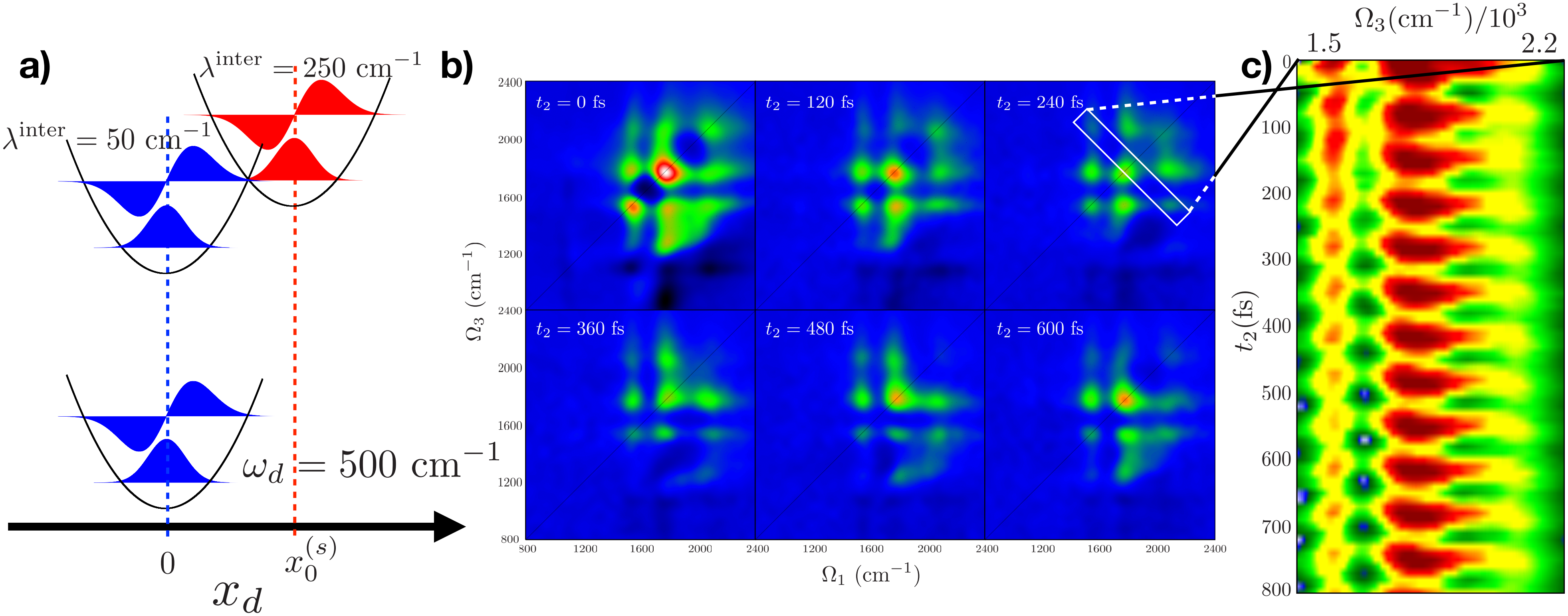

a)
$\lambda^{\text{inter}} = 250\ \text{cm}^{-1}$
$\lambda^{\text{inter}} = 50\ \text{cm}^{-1}$
$\omega_d = 500\ \text{cm}^{-1}$
0
$x_0^{(s)}$
x_d
b)
$t_2 = 0$ fs
$t_2 = 120$ fs
$t_2 = 240$ fs
$t_2 = 360$ fs
$t_2 = 480$ fs
$t_2 = 600$ fs
$\Omega_3\ (\text{cm}^{-1})$
$\Omega_1\ (\text{cm}^{-1})$
800
1200
1600
2000
2400
c)
$\Omega_3(\text{cm}^{-1})/10^3$
1.5
2.2
$t_2(\text{fs})$
0
100
200
300
400
500
600
700
800

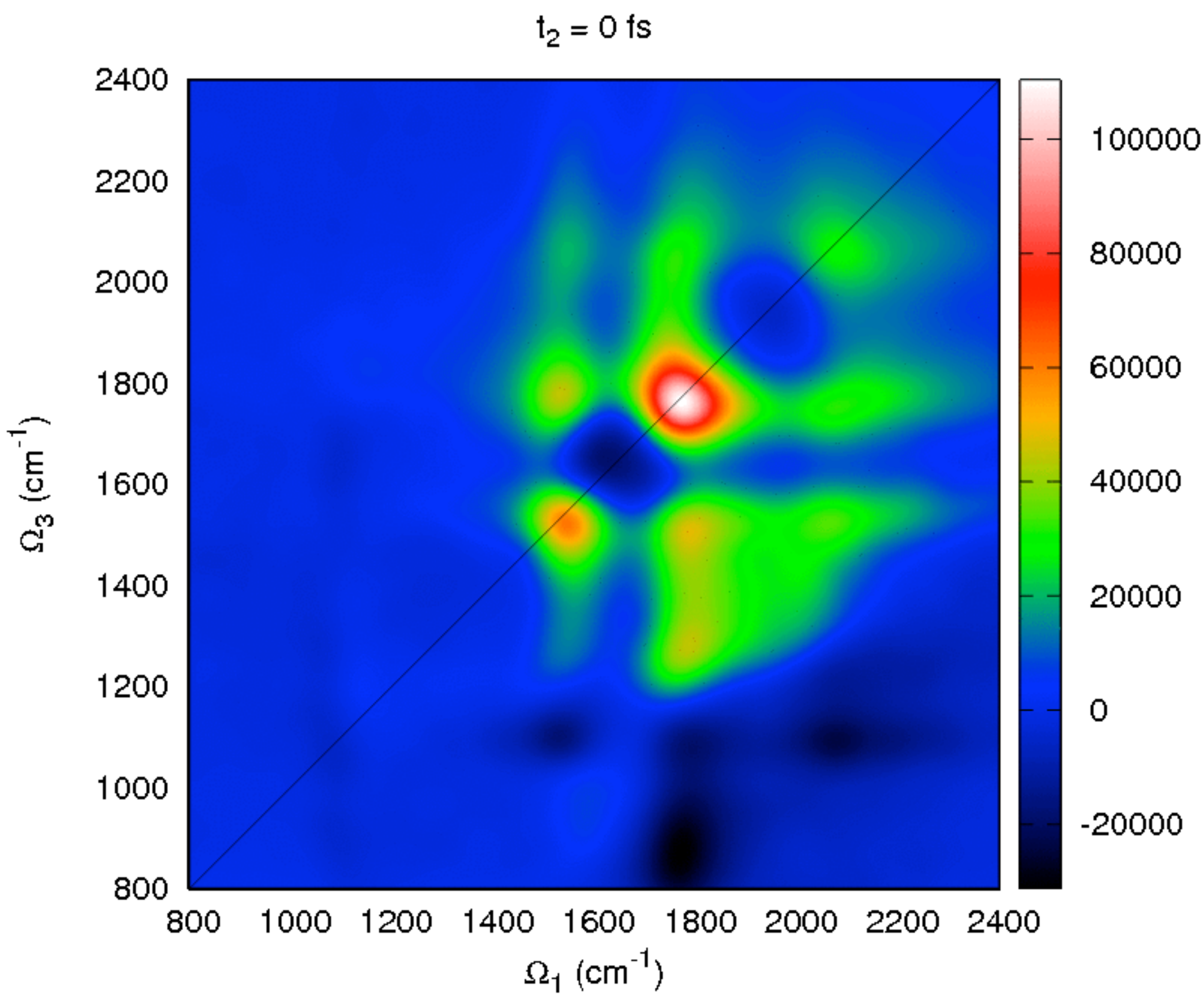

t_2 = 0 fs
2400
2200
2000
1800
1600
1400
1200
1000
800
Ω_3 (cm^{-1})
800
1000
1200
1400
1600
1800
2000
2200
2400
Ω_1 (cm^{-1})
100000
80000
60000
40000
20000
0
-20000

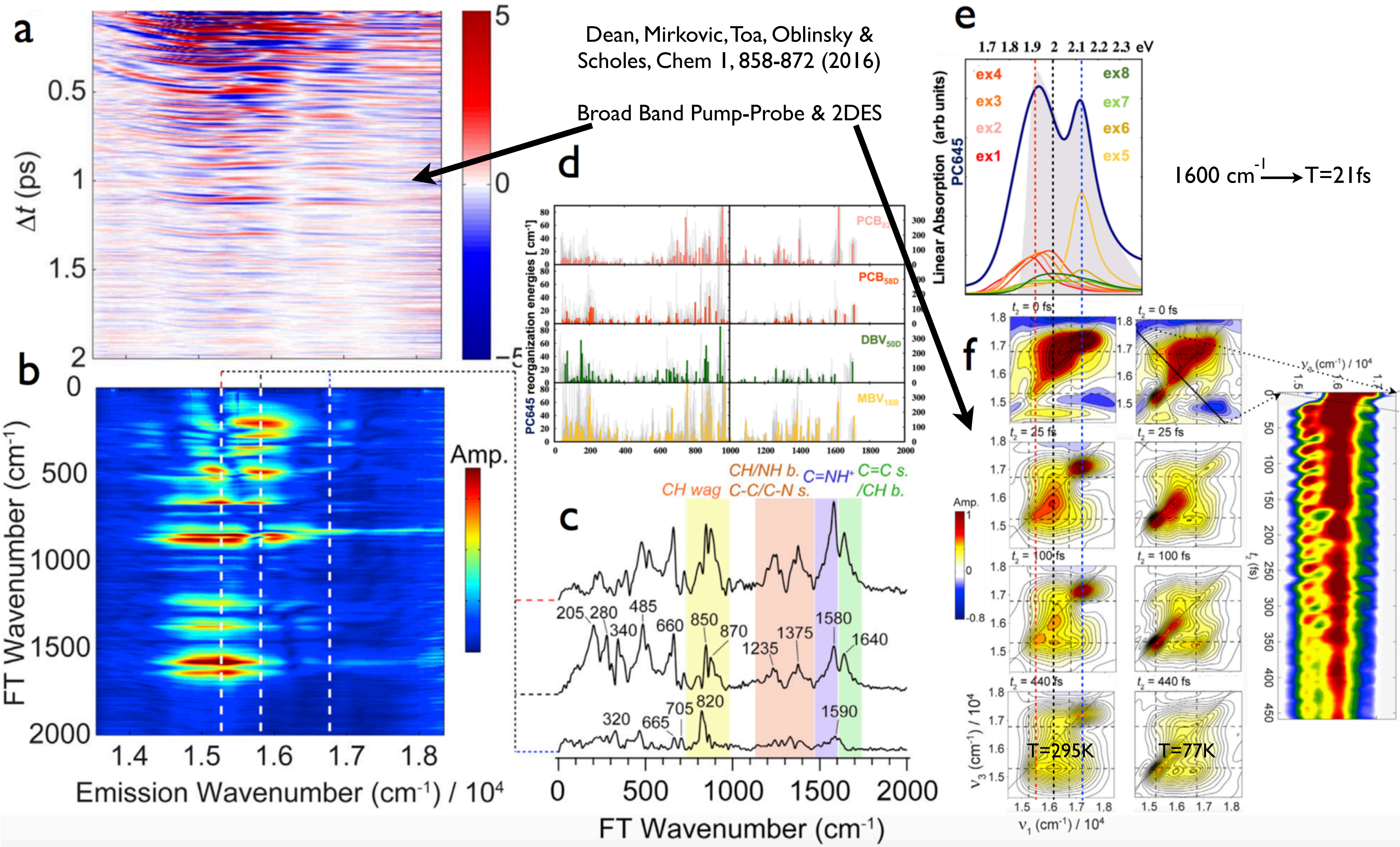

Dean, Mirkovic, Toa, Oblinsky & Scholes, Chem 1, 858-872 (2016)
Broad Band Pump-Probe & 2DES
1600 cm-1 → T=21fs
a
b
c
d
e
f
Δt (ps)
FT Wavenumber (cm-1)
Emission Wavenumber (cm-1) / 10^4
Amp.
CH wag
CH/NH b.
C-C/C-N s.
C=NH+
C=C s.
/CH b.
205
280
340
485
660
850
870
1235
1375
1580
1640
320
665
705
820
1590
FT Wavenumber (cm-1)
PC645 reorganization energies [cm-1]
PCB82
PCB58D
DBV50D
MBV18B
Linear Absorption (arb units)
PC645
ex4
ex3
ex2
ex1
ex8
ex7
ex6
ex5
eV
T=295K
T=77K

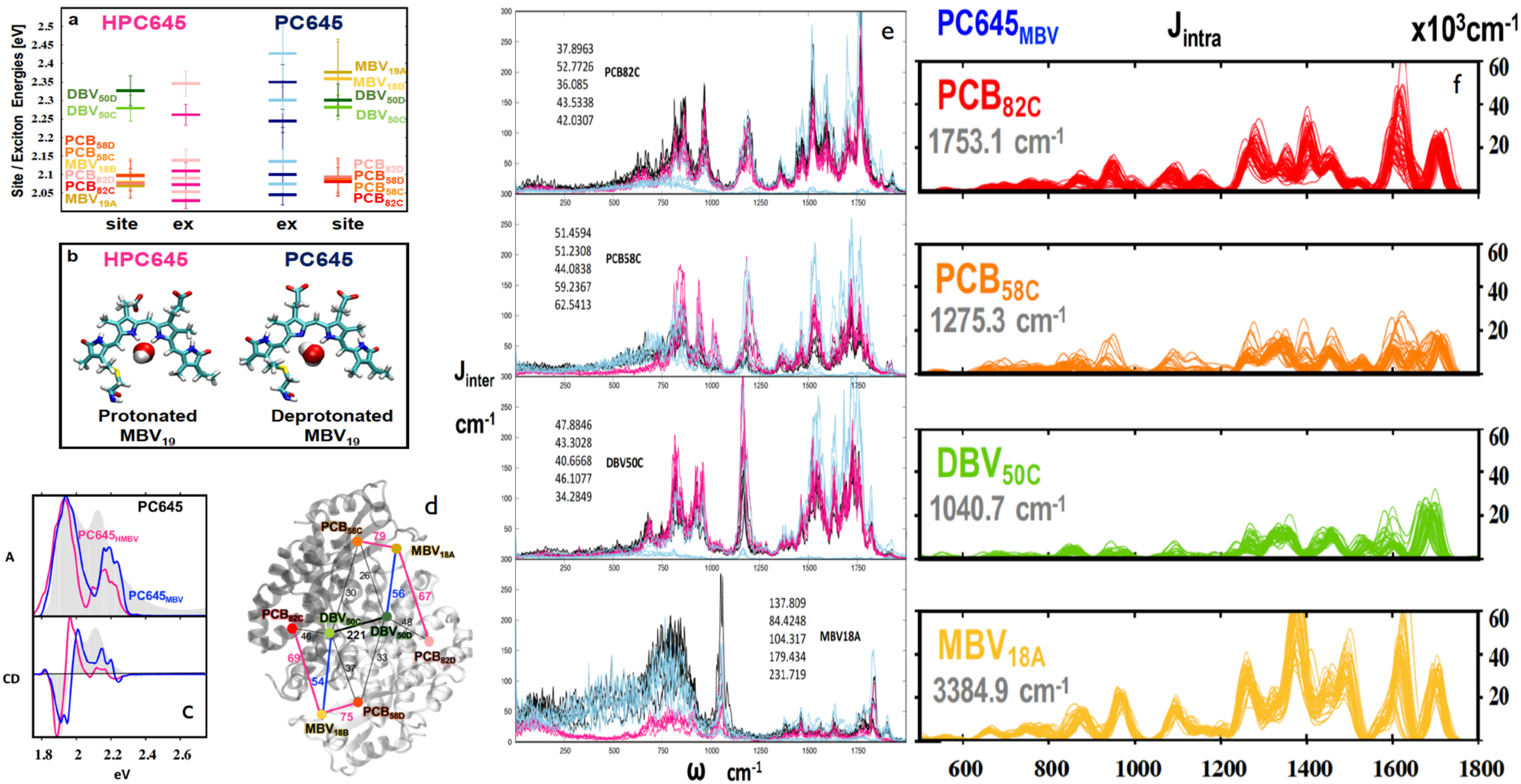

a
HPC645
PC645
Site / Exciton Energies [eV]
site
ex
ex
site
b
HPC645
PC645
Protonated MBV19
Deprotonated MBV19
PC645
A
CD
C
eV
d
e
PCB82C
PCB58C
DBV50C
MBV18A
J inter cm-1
ω cm-1
PC645MBV
J intra
x10³cm-1
f
PCB82C
1753.1 cm-1
PCB58C
1275.3 cm-1
DBV50C
1040.7 cm-1
MBV18A
3384.9 cm-1

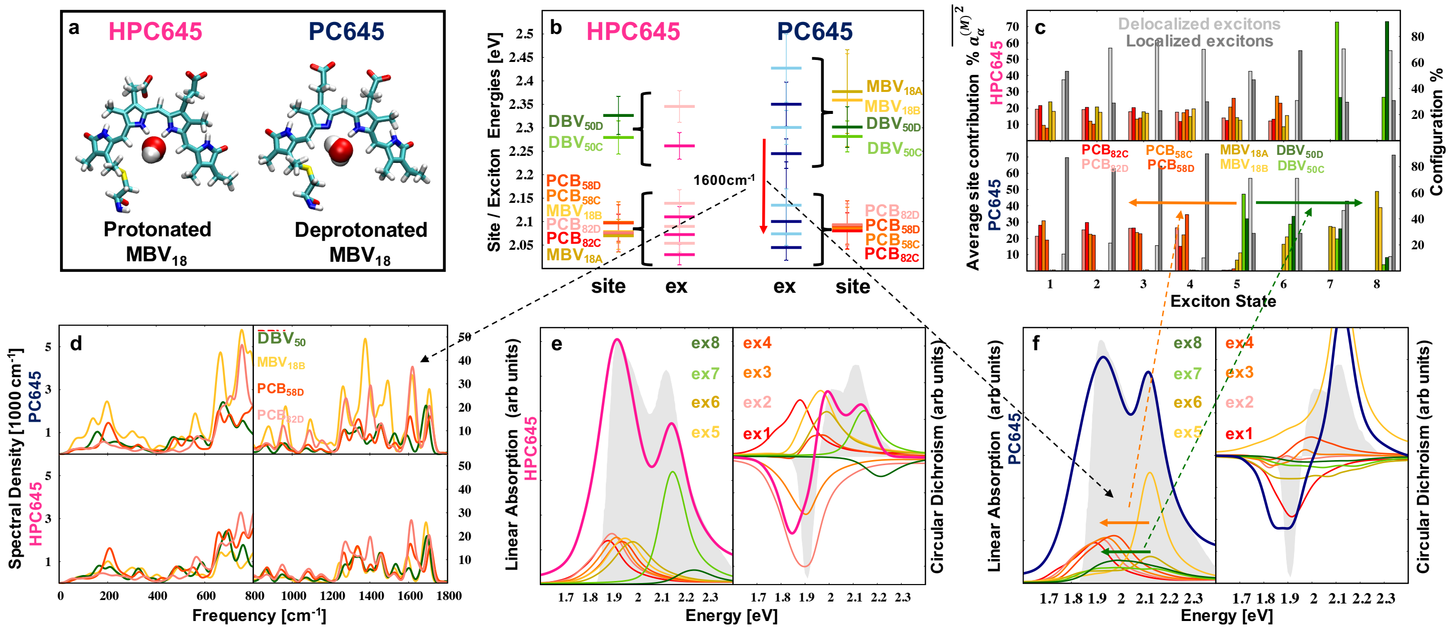

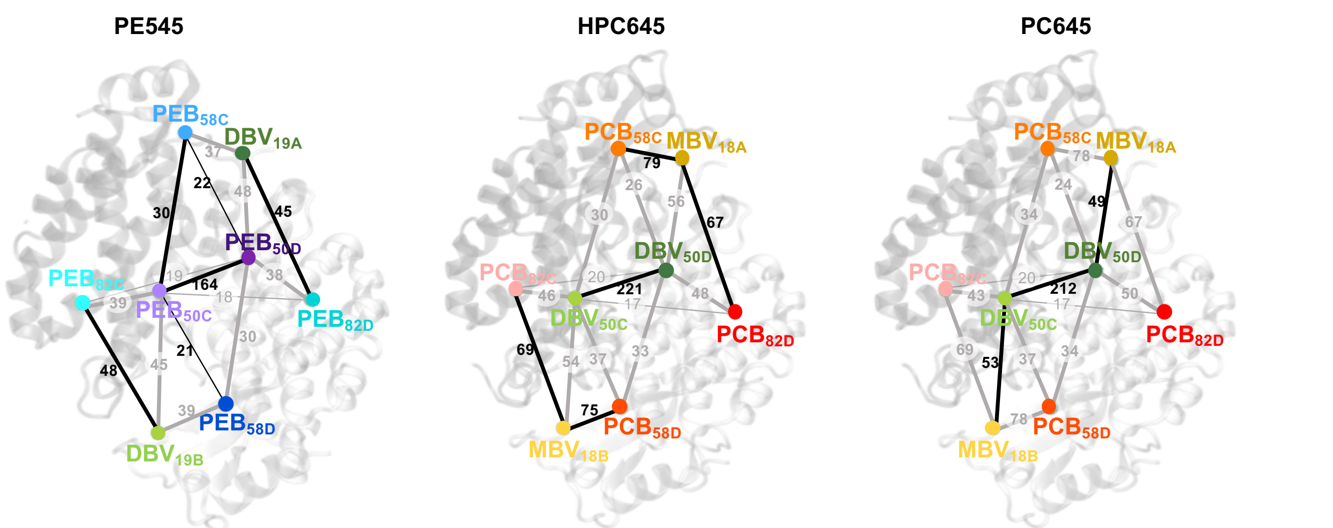

“Flickering” EET pathways

Protonation state control of (de)-localization

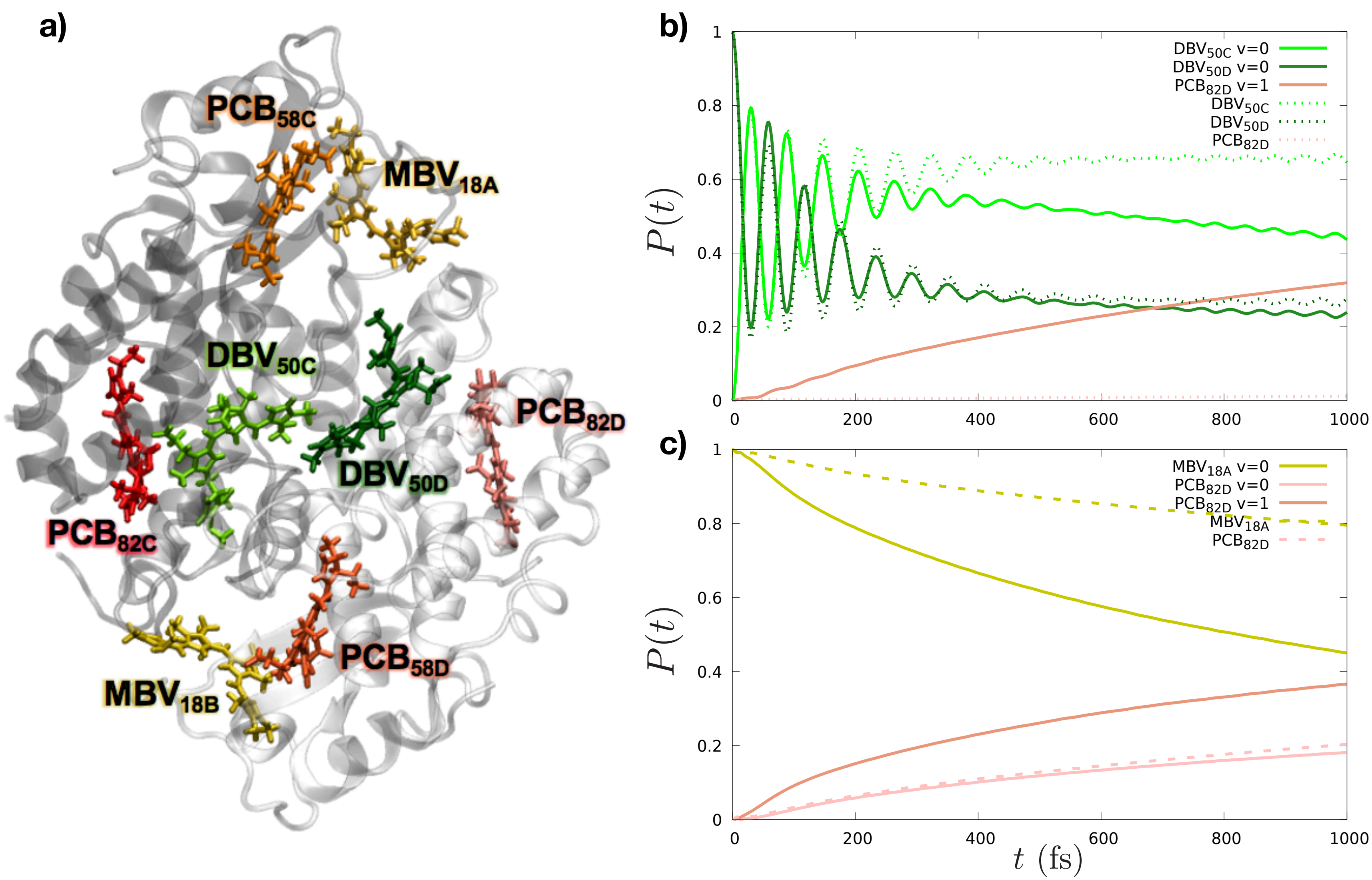

a)
PCB58C
MBV18A
DBV50C
DBV50D
PCB82D
PCB82C
PCB58D
MBV18B
b)
DBV50C v=0
DBV50D v=0
PCB82D v=1
DBV50C
DBV50D
PCB82D
P(t)
c)
MBV18A v=0
PCB82D v=0
PCB82D v=1
MBV18A
PCB82D
P(t)
t (fs)

OUTLINE:

(1) Spectral Density Calculations
(2) Excitation Energy Calculations
(3) Dissipative Quantum Dynamics for General Regimes
(4) Issues with Linearized Dynamics of Higher Frequency Modes
(5) Spectra (PC645/HPC645) - Influence of Protonation and "Flickering" Pathways
(6) Quantum Dynamics and Nonlinear Spectroscopy
(7) Coherent State Density Matrix Dynamics (+PLDM)

CSDM

$$\hat{H}_{\text{map}} = \sum_{k=1}^{N_{osc}} \left(\frac{\hat{P}_k^2}{2M_k} + \frac{1}{2} M_k \Omega_k^2 \hat{Q}_k^2 \right) + \frac{1}{2\hbar} \sum_{\alpha,\beta=1}^{N_{st}} h_{\alpha,\beta}(\{\hat{Q}_i\})(\hat{q}_\alpha \hat{q}_\beta + \hat{p}_\alpha \hat{p}_\beta - \hbar \delta_{\alpha,\beta})$$

$$e^{-\frac{i}{\hbar}\hat{H}t} \propto \int d\vec{q}_0 d\vec{p}_0 d\vec{Q}_0 d\vec{P}_0 \;\; |\vec{q}_t, \vec{p}_t\rangle \, |\vec{Q}_t, \vec{P}_t\rangle \, C_t e^{\frac{i}{\hbar}S_t} \, \langle \vec{q}_0, \vec{p}_0| \, \langle \vec{Q}_0, \vec{P}_0|$$

$$\gamma_i = m_i \omega_i / 2\hbar$$

$$\langle x|q,p\rangle = \exp[-\gamma(q-x)^2 + ip(x-q)/\hbar]$$

$$C_t = \det[\frac{1}{2}(\frac{\partial \vec{q}_t}{\partial \vec{q}_0} + \frac{\partial \vec{p}_t}{\partial \vec{p}_0} - i2\hbar\gamma \frac{\partial \vec{q}_t}{\partial \vec{p}_0} + \frac{i}{2\hbar\gamma}\frac{\partial \vec{p}_t}{\partial \vec{q}_0})]^{\frac{1}{2}}$$

$$C_t = \det[\frac{1}{2} \begin{pmatrix} C_t^{QQ} & C_t^{Qq} \\ C_t^{qQ} & C_t^{qq} \end{pmatrix}]^{\frac{1}{2}}$$

$$C_t^{QQ} = \det[\frac{1}{2}(\frac{\partial Q_t}{\partial Q_0} + \frac{\partial P_t}{\partial P_0} - im\omega \frac{\partial Q_t}{\partial P_0} + \frac{i}{m\omega}\frac{\partial P_t}{\partial Q_0})]^{\frac{1}{2}}$$

$$= \det[\frac{1}{2}(\frac{\partial a_{cl}(Q_t,P_t)}{\partial(\mathrm{Re}(a_{cl}^\dagger(Q_0,P_0)))} + i\frac{\partial a_{cl}(Q_t,P_t)}{\partial(\mathrm{Im}(a_{cl}^\dagger(Q_0,P_0)))})]^{\frac{1}{2}}$$

$$a_{cl}(Q,P) \;=\; \sqrt{\tfrac{M\Omega}{2\hbar}}(Q + \tfrac{i}{M\Omega}P)$$

$$V(Q) = \tfrac{1}{2}M\Omega^2 Q^2 + \Gamma(t)Q$$

$$a_{cl}(Q_t,P_t) = a_{cl}(Q_0,P_0)e^{-i\Omega t} - \frac{i}{\sqrt{2M\Omega\hbar}} \int_o^t d\tau \; \Gamma(\tau) e^{-i\Omega(t-\tau)}$$

$$C_t \approx \det[\frac{1}{2} \begin{pmatrix} C_t^{QQ} & 0 \\ C_t^{qQ} & C_t^{qq} \end{pmatrix}]^{\frac{1}{2}} = \det[\frac{1}{2}C_t^{QQ}]^{\frac{1}{2}} \det[\frac{1}{2}C_t^{qq}]^{\frac{1}{2}} \;=\; \exp[-\tfrac{i}{2}\textstyle\sum_{k=1}^{N_{osc}} \Omega_k t] \;\; \exp[-\tfrac{i}{2}\sum_\alpha \int_0^t d\tau h_{\alpha,\alpha}(\{\hat{Q}_i\})]$$

$$\langle q,p|\nu\rangle_{\gamma=\frac{m\omega}{2\hbar}} = \frac{1}{\sqrt{\nu!}} \left(a_{cl}^\dagger(q,p)\right)^\nu \langle q,p|0\rangle_{\gamma=\frac{m\omega}{2\hbar}}$$

$$\langle q,p|0\rangle_{\gamma=\frac{m\omega}{2\hbar}} = \left(\tfrac{\pi\hbar}{m\omega}\right)^{\frac{1}{4}} \exp[-\tfrac{m\omega}{4\hbar}q^2 - \tfrac{1}{4\hbar m\omega}p^2 + \tfrac{i}{2\hbar}pq]$$

$$\langle n_f, \vec{\nu}_f | \hat{\rho}(t) | n'_f, \vec{\nu}'_f \rangle \approx \int d\vec{q}_0 d\vec{p}_0 d\vec{q}'_0 d\vec{p}'_0 d\vec{Q}_0 d\vec{P}_0 d\vec{Q}'_0 d\vec{P}'_0 \langle \vec{Q}_0 \vec{P}_0 | 0 \rangle \langle 0 | \vec{Q}'_0, \vec{P}'_0 \rangle \langle \vec{q}_0 \vec{p}_0 | 0 \rangle \langle 0 | \vec{q}'_0, \vec{p}'_0 \rangle$$

$$\times \langle 0 | \vec{Q}_t \vec{P}_t \rangle \langle \vec{Q}'_t, \vec{P}'_t | 0 \rangle \langle 0 | \vec{q}_t \vec{p}_t \rangle \langle \vec{q}'_t, \vec{p}'_t | 0 \rangle \, e^{i\left(\tilde{S}_t[\vec{q},\vec{p},\vec{Q},\vec{P}] - \tilde{S}_t[\vec{q}',\vec{p}',\vec{Q}',\vec{P}']\right)}$$

$$\times \sum_{n_0, n'_0 = 1}^{N_{st}} \rho_s^{(n_0, n'_0)} T_s^{(n_f, n_0)}(q_{n_{f_t}}, p_{n_{f_t}}, q_{n_{0_0}}, p_{n_{0_0}}) T_s^{*(n'_f, n'_0)}(q'_{n'_{f_t}}, p'_{n'_{f_t}}, q'_{n'_{0_0}}, p'_{n'_{0_0}})$$

$$\times \sum_{\vec{\nu}_0, \vec{\nu}'_0} \rho_b^{(\vec{\nu}_0, \vec{\nu}'_0)} T_b^{(\vec{\nu}_f, \vec{\nu}_0)}(\vec{Q}, \vec{P}) T_b^{*(\vec{\nu'}_f, \vec{\nu'}_0)}(\vec{Q}', \vec{P}')$$

$$\tilde{S}_t[\vec{q}, \vec{p}, \vec{Q}, \vec{P}] \; = \; \int_0^t d\tau \;\; \vec{p} \cdot \dot{\vec{q}} + \vec{P} \cdot \dot{\vec{Q}} - H_{\text{map}} - \tfrac{1}{2} \textstyle\sum_\alpha h_{\alpha,\alpha}(\{Q_i\})$$

$$T_s^{(n_f, n_0)}(q_{n_{f_t}}, p_{n_{f_t}}, q_{n_{0_0}}, p_{n_{0_0}}) \; = \; \tfrac{1}{2}(q_{n_{f_t}} + i p_{n_{f_t}})(q_{n_{0_0}} - i p_{n_{0_0}})$$

$$T_b^{(\vec{\nu}_f, \vec{\nu}_0)}(\vec{Q}, \vec{P}) \; = \; \textstyle\prod_{k=1}^{N_{osc}} \left(\frac{1}{\sqrt{\nu_0^{(k)}!}} a_{cl}^\dagger(Q_{k_0}, P_{k_0}) \right)^{\nu_0^{(k)}} \frac{1}{\sqrt{\nu_f^{(k)}!}} \left(a_{cl}(Q_{k_t}, P_{k_t}) \right)^{\nu_f^{(k)}})$$

$$
\begin{aligned}
\langle n_f, \vec{\nu}_f | \hat{\rho}(t) | n'_f, \vec{\nu}'_f \rangle \propto \int & d\vec{q}_0 d\vec{p}_0 d\vec{q}'_0 d\vec{p}'_0 d\vec{Q}_0 d\vec{P}_0 d\vec{Q}'_0 d\vec{P}'_0 \\
& \times \mathcal{G}(\vec{q}_0, \vec{p}_0) \mathcal{G}(\vec{q}'_0, \vec{p}'_0) \mathcal{F}(\vec{Q}_0, \vec{P}_0) \mathcal{F}(\vec{Q}'_0, \vec{P}'_0) e^{\frac{i}{2}\left(\Theta_t[\vec{Q}, \vec{P}, \vec{p}, \vec{q}] - \Theta^*_t[\vec{Q}', \vec{P}', \vec{p}', \vec{q}']\right)} \\
& \times \sum_{n_0, n'_0 = 1}^{N_{st}} \rho_s^{(n_0, n'_0)} T_s^{(n_f, n_0)}(q_{n_{f_t}}, p_{n_{f_t}}, q_{n_{0_0}}, p_{n_{0_0}}) T_s^{*(n'_f, n'_0)}(q'_{n'_{f_t}}, p'_{n'_{f_t}}, q'_{n'_{0_0}}, p'_{n'_{0_0}}) \\
& \times \sum_{\vec{\nu}_0, \vec{\nu}'_0} \rho_b^{(\vec{\nu}_0, \vec{\nu}'_0)} T_b^{(\vec{\nu}_f, \vec{\nu}_0)}(\vec{Q}, \vec{P}) T_b^{*(\vec{\nu'}_f, \vec{\nu'}_0)}(\vec{Q}', \vec{P}')
\end{aligned}
$$

$$
\Theta_t[\vec{Q}, \vec{P}, \vec{p}, \vec{q}] = \int_0^t d\tau \sum_{k=1}^{N_{osc}} \sum_{\alpha, \beta = 1}^{N_{st}} \sqrt{\frac{2}{M_k \Omega_k}} a^\dagger_{cl}(Q_k, P_k) \nabla_{Q_k} h_{\alpha, \beta}(\{Q_i\}) \frac{1}{2}(q_\alpha q_\beta + p_\alpha p_\beta - \delta_{\alpha, \beta})
$$

$$
\begin{aligned}
\langle n_f | \hat{\sigma}(t) | n'_f \rangle \propto \int & d\vec{q}_0 d\vec{p}_0 d\vec{q}'_0 d\vec{p}'_0 d\vec{Q}_0 d\vec{P}_0 d\vec{Q}'_0 d\vec{P}'_0 \\
& \times \mathcal{G}(\vec{q}_0, \vec{p}_0) \mathcal{G}(\vec{q}'_0, \vec{p}'_0) \mathcal{B}_\beta(\vec{Q}_0, \vec{P}_0, \vec{Q}'_0, \vec{P}'_0) e^{\frac{i}{2}\Phi_t[\vec{Q}, \vec{P}, \vec{Q}', \vec{P}', \vec{q}, \vec{p}, \vec{q}', \vec{p}']} \\
& \times \sum_{n_0, n'_0 = 1}^{N_{st}} \rho_s^{(n_0, n'_0)} T_s^{(n_f, n_0)}(q_{n_{f_t}}, p_{n_{f_t}}, q_{n_{0_0}}, p_{n_{0_0}}) T_s^{*(n'_f, n'_0)}(q'_{n'_{f_t}}, p'_{n'_{f_t}}, q'_{n'_{0_0}}, p'_{n'_{0_0}})
\end{aligned}
$$

High frequency harmonic vibrations treated with coherent state density matrix (CSDM) dynamics

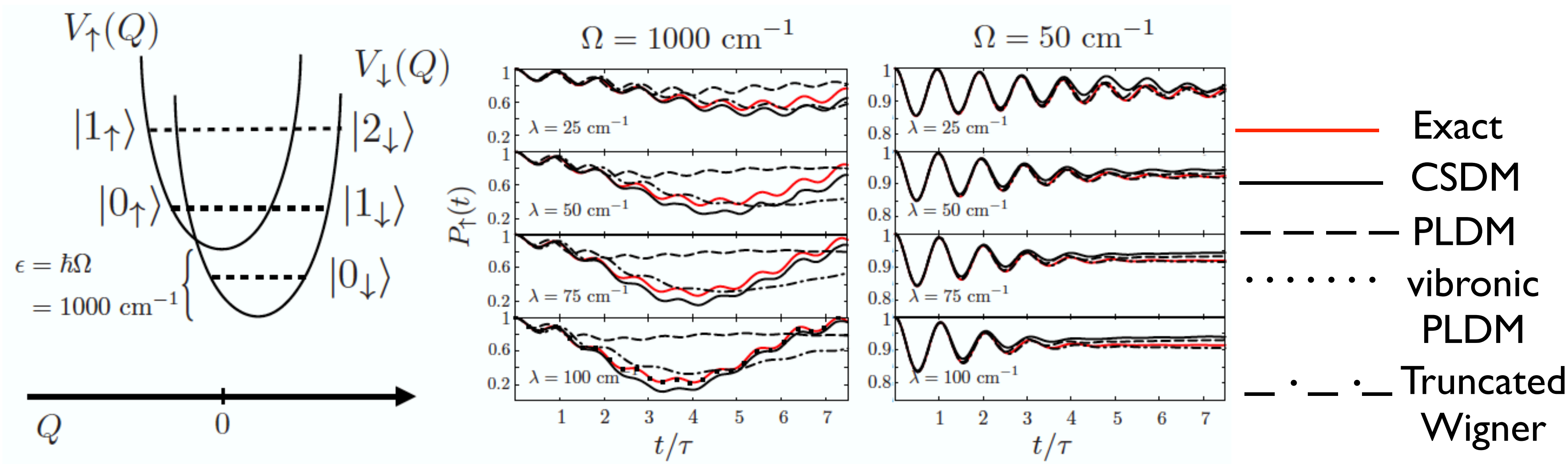

$$\hat{H} = \frac{\epsilon}{2}\,\hat{\sigma}_z + \Delta\,\hat{\sigma}_x + \frac{\hat{P}^2}{2M} + \frac{1}{2}M\Omega^2(\hat{Q} - \frac{c}{M\Omega^2}\,|\downarrow\rangle\langle\downarrow|)^2$$

$\epsilon = \Omega = 1000\ \mathrm{cm}^{-1}$, $\Delta = 200\ \mathrm{cm}^{-1}$, and $T = 77$ K

$$\hat{H}_{\mathrm{map}} = \sum_{k=1}^{N_Q}\left(\frac{\hat{P}_k^2}{2M_k} + \frac{1}{2}M_k\Omega_k^2\hat{Q}_k^2\right) + \sum_{k=1}^{N_R}\left(\frac{\hat{P}_{Rk}^{\;2}}{2M_{Rk}} + V_0(\{\hat{R}_j\})\right)$$

$$+\frac{1}{2\hbar}\sum_{\alpha,\beta=1}^{N_{st}} h_{\alpha,\beta}(\{\hat{Q}_i\},\{\hat{R}_j\})(\hat{q}_\alpha\hat{q}_\beta + \hat{p}_\alpha\hat{p}_\beta - \hbar\delta_{\alpha,\beta})$$

$$h_{\alpha,\beta}(\{\hat{Q}_i\},\{\hat{R}_j\}) = \left(\tilde{\epsilon}_\alpha - \sum_{k=1}^{N_Q} c_k^{(\alpha)}\hat{Q}_k + V_{\alpha,\beta}(\{\hat{R}_j\})\right)\delta_{\alpha,\beta} + \Delta(\{\hat{R}_j\})_{\alpha,\beta}(1-\delta_{\alpha,\beta})$$

$$\langle n_f|\hat{\sigma}(t)\,|n_f'\rangle \propto \int d\vec{q}_0 d\vec{p}_0 d\vec{q}_0' d\vec{p}_0' d\vec{Q}_0 d\vec{P}_0 d\vec{Q}_0' d\vec{P}_0' d\bar{R}_0$$

$$\times\, \mathcal{G}(\vec{q}_0,\vec{p}_0)\mathcal{G}(\vec{q}_0',\vec{p}_0')\mathcal{B}_\beta(\vec{Q}_0,\vec{P}_0,\vec{Q}_0',\vec{P}_0')e^{\frac{i}{2}\Phi_t[\vec{Q},\vec{P},\vec{Q}',\vec{P}',\vec{q},\vec{p},\vec{q}',\vec{p}']}$$

$$\times \sum_{n_0,n_0'=1}^{N_{st}} \rho_s^{(n_0,n_0')} T_s^{(n_f,n_0)}(q_{n_{f_t}},p_{n_{f_t}},q_{n_{0_0}},p_{n_{0_0}}) T_s^{*(n_f',n_0')}(q'_{n'_{f_t}},p'_{n'_{f_t}},q'_{n'_{0_0}},p'_{n'_{0_0}})$$

$$\times\left(\prod_{k=1}^{N-1}\int d\bar{R}_k\frac{d\bar{P}_{R_k}}{2\pi}\right)\rho_W^{n_0 n_0'}(\bar{R}_0,\bar{P}_{R_1})\prod_{k=1}^{N-1}\delta\left(\frac{\bar{P}_{R_{k+1}}-\bar{P}_{R_k}}{\epsilon} - F_k\right)\prod_{k=1}^{N}\delta\left(\frac{\bar{R}_k-\bar{R}_{k-1}}{\epsilon} - \frac{\bar{P}_{R_k}}{M_R}\right)$$

$$F_k = -\tfrac{1}{2}\nabla_{\bar{R}_k}(\tilde{H}(\{Q_i\},\{\bar{R}_j\},\vec{q},\vec{p}) + \tilde{H}(\{Q'_i\},\{\bar{R}_j\},\vec{q}',\vec{p}'))$$

$$\tilde{H} = H_{\mathrm{map}} + \tfrac{1}{2}\sum_{\alpha=1}^{N_{st}} h_{\alpha,\alpha}(\{Q_i\},\{R_j\})$$

Multi-Level
CSDM-PLDM

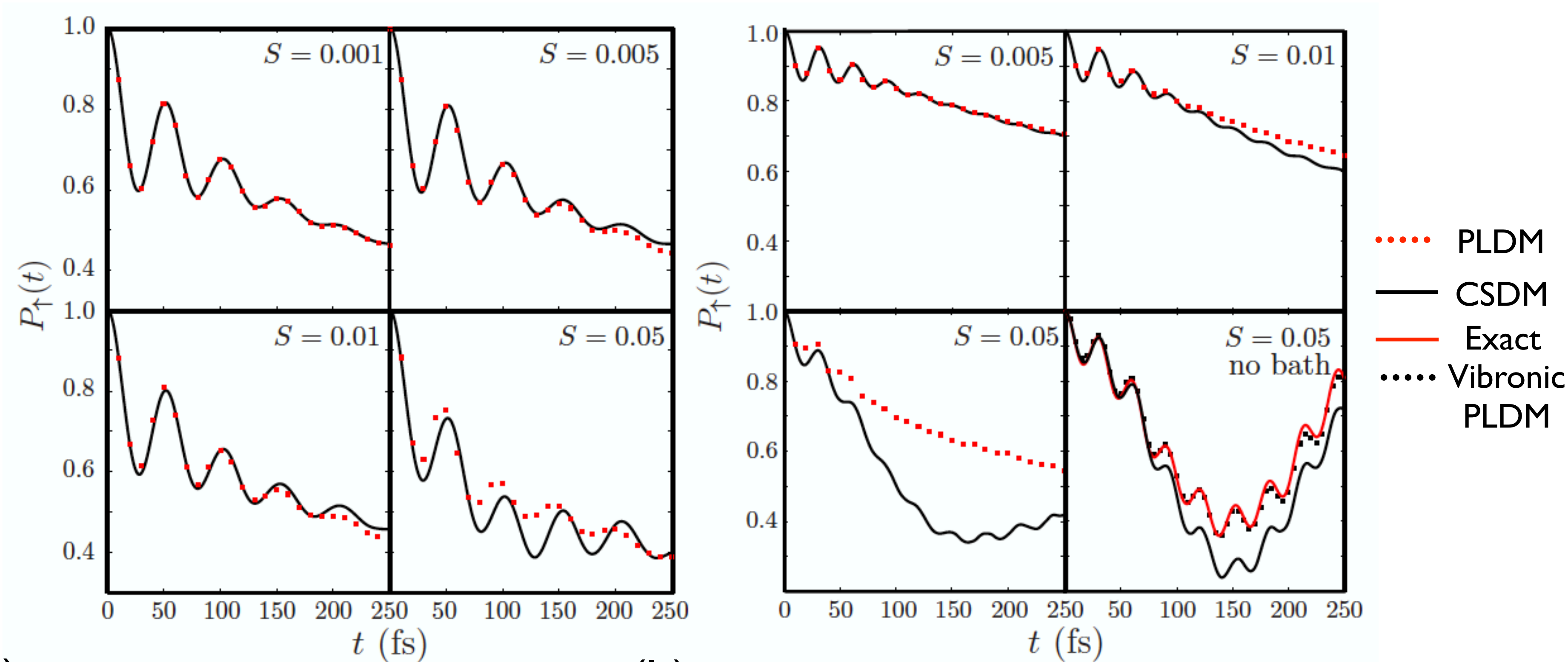

(a) $N_{\rm d} = 1$ where $\epsilon = \Omega_1 = 500$ cm^{-1}

(b) $N_{\rm d} = 2$ where $\epsilon = \Omega_1 = 1000$ cm^{-1} and $\Omega_2 = 500$ cm^{-1}

$$S = \frac{C_1^2}{2\hbar M_1 \Omega_1^3} = \frac{C_2^2}{2\hbar M_2 \Omega_2^3}$$

$$\hat{H} = \frac{\epsilon}{2}\,\hat{\sigma}_z + \Delta\,\hat{\sigma}_x + \sum_{K=1}^{N_{\rm d}} \frac{\hat{P}_K^2}{2M_K} + \frac{1}{2}M_K\Omega_K^2(\hat{Q}_K - \frac{C_K}{M_K\Omega_K^2}\left|\downarrow\right\rangle\left\langle\downarrow\right|)^2 +$$
$$\sum_{k_\downarrow=1}^{N_c} \frac{\hat{p}_{k_\downarrow}^2}{2m_{k_\downarrow}} + \frac{1}{2}m_{k_\downarrow}\omega_{k_\downarrow}^2(\hat{q}_{k_\downarrow} - \frac{c_{k_\downarrow}}{m_{k_\downarrow}\omega_{k_\downarrow}^2}\left|\downarrow\right\rangle\left\langle\downarrow\right|)^2 + \sum_{k_\uparrow=1}^{N_c} \frac{\hat{p}_{k_\uparrow}^2}{2m_{k_\uparrow}} + \frac{1}{2}m_{k_\uparrow}\omega_{k_\uparrow}^2(\hat{q}_{k_\uparrow} - \frac{c_{k_\uparrow}}{m_{k_\uparrow}\omega_{k_\uparrow}^2}\left|\uparrow\right\rangle\left\langle\uparrow\right|)^2$$

$N_c = 100$ $\quad J(\omega) = 2\lambda\frac{\omega/\omega_c}{1+(\omega/\omega_c)^2}$ with $\lambda = 50$ cm^{-1} and $\omega_c = 200$ cm^{-1}

CSDM-PLDM

$\Delta = 200$ cm^{-1} at $T = 77$ K

OUTLINE:

(1) Spectral Density Calculations
(2) Excitation Energy Calculations
(3) Dissipative Quantum Dynamics for General Regimes
(4) Issues with Linearized Dynamics of Higher Frequency Modes
(5) Spectra (PC645/HPC645) - Influence of Protonation and "Flickering" Pathways
(6) Quantum Dynamics and Nonlinear Spectroscopy
(7) Coherent State Density Matrix Dynamics (+PLDM)

Thank You!